NDOT Research Report

Report No. 224-14-803 TO 8

Resilient Modulus Prediction Models of Unbound Materials for Nevada

June 2018

Nevada Department of Transportation
1263 South Stewart Street
Carson City, NV 89712

Disclaimer

TECHNICAL REPORT DOCUMENTATION PAGE

1. Report No. P224-14-803	2. Government Accession No.	3. Recipient's Catalog No.
4. Title and Subtitle Resilient Modulus Prediction Models of Unbound Materials for Nevada		5. Report Date June 26, 2018 6. Performing Organization Code None
7. Author(s) Elie Y. Hajj, Jeyakaran Thavathurairaja, Sarah Stolte, Peter E. Sebaaly, Murugaiyah Piratheepan, and Ramin Motamed		8. Performing Organization Report No. WRSC-UNR-20180626
9. Performing Organization Name and Address Western Regional Superpave Center Pavement Engineering & Science Department of Civil and Environmental Engineering University of Nevada Reno, Nevada 89557		10. Work Unit No. 11. Contract or Grant No.
12. Sponsoring Agency Name and Address Nevada Department of Transportation 1263 South Stewart Street Carson City, NV 89712		13. Type of Report and Period Covered Final Report 14. Sponsoring Agency Code
15. Supplementary Notes		

16. Abstract

The American Association of State Highway and Transportation Officials (AASHTO) adopted the Mechanistic-Empirical Pavement Design Guide (MEPDG) as an interim pavement design standard in 2008. In 2015, the Nevada Department of Transportation (NDOT) implemented the MEPDG for the structural design of new and rehabilitated flexible pavements. The resilient modulus of the unbound materials remains an important parameter in pavement design. This parameter also used to characterize the unbound materials in the MEPDG. The MEPDG follows a hierarchical approach in defining the required engineering properties of the pavement structure. Three levels of input are specified in the AASHTOWare® Pavement ME design software. This includes direct measurement from the laboratory testing offering the highest level of accuracy (i.e., Level 1), estimated values using correlations with soil properties (i.e., Level 2), and typical values offering the lowest level of accuracy (i.e., Level 3). NDOT currently uses R-value to estimate the resilient modulus of unbound materials which is not originally developed for Nevada. The major objective of this study is to develop a new resilient modulus prediction model for use in pavement rehabilitation designs.

Unbound materials (i.e., base, borrow, and subgrade) were sampled from several locations throughout Nevada and various tests were conducted to determine unbound material properties and characteristics, including the classification of the evaluated material (i.e., soil classification), R-value, moisture-density relationships, and resilient modulus testing. The resilient modulus test was conducted according to AASHTO T307 procedure. Prediction models for all three unbound material types (i.e., base, borrow, and subgrade) correlating resilient modulus to R-value and other physical properties were developed for pavement rehabilitation designs. District 1 materials were used to develop these prediction models, and the District 2 and District 3 materials were used to verify the models. Additionally, it was concluded that the current available NDOT resilient model correlation equation overestimates the resilient modulus anticipated in an existing pavement structure, thus resulting in a likely under designed asphalt concrete layer thickness.

17. Key Words MEDPG, AASHTO 93, modulus, unbound materials, stress-dependent, flexible pavement, rehabilitation	18. Distribution Statement No restrictions. This document is available through the: National Technical Information Service Springfield, VA 22161		
19. Security Classif. (of this report) Unclassified	20. Security Classif. (of this page) Unclassified	21. No. of Pages 113	22. Price

Final Report
June 2018

RESILIENT MODULUS PREDICTION MODELS OF UNBOUND MATERIALS FOR NEVADA

SOLARIS Consortium, Tier 1 University Transportation Center
Center for Advanced Transportation Education and Research
Department of Civil and Environmental Engineering
University of Nevada, Reno
Reno, NV 89557

Elie Y. Hajj, PhD
Pavement Engineering & Science Program
Department of Civil and Environmental Engineering
University of Nevada, Reno
Reno, NV 89557

SI* (MODERN METRIC) CONVERSION FACTORS

APPROXIMATE CONVERSIONS TO SI UNITS

Symbol	When You Know	Multiply By	To Find	Symbol
		LENGTH		
in	inches	25.4	millimeters	mm
ft	feet	0.305	meters	m
yd	yards	0.914	meters	m
mi	miles	1.61	kilometers	km
		AREA		
in^2	square inches	645.2	square millimeters	mm^2
ft^2	square feet	0.093	square meters	m^2
yd^2	square yard	0.836	square meters	m^2
ac	acres	0.405	hectares	ha
mi^2	square miles	2.59	square kilometers	km^2
		VOLUME		
fl oz	fluid ounces	29.57	milliliters	mL
gal	gallons	3.785	liters	L
ft^3	cubic feet	0.028	cubic meters	m^3
yd^3	cubic yards	0.765	cubic meters	m^3
		NOTE: volumes greater than 1000 L shall be shown in m^3		
		MASS		
oz	ounces	28.35	grams	g
lb	pounds	0.454	kilograms	kg
T	short tons (2000 lb)	0.907	megagrams (or "metric ton")	Mg (or "t")
		TEMPERATURE (exact degrees)		
^oF	Fahrenheit	5 (F-32)/9 or (F-32)/1.8	Celsius	^oC
		ILLUMINATION		
fc	foot-candles	10.76	lux	lx
fl	foot-Lamberts	3.426	candela/m^2	cd/m^2
		FORCE and PRESSURE or STRESS		
lbf	poundforce	4.45	newtons	N
lbf/in^2	poundforce per square inch	6.89	kilopascals	kPa

APPROXIMATE CONVERSIONS FROM SI UNITS

Symbol	When You Know	Multiply By	To Find	Symbol
		LENGTH		
mm	millimeters	0.039	inches	in
m	meters	3.28	feet	ft
m	meters	1.09	yards	yd
km	kilometers	0.621	miles	mi
		AREA		
mm^2	square millimeters	0.0016	square inches	in^2
m^2	square meters	10.764	square feet	ft^2
m^2	square meters	1.195	square yards	yd^2
ha	hectares	2.47	acres	ac
km^2	square kilometers	0.386	square miles	mi^2
		VOLUME		
mL	milliliters	0.034	fluid ounces	fl oz
L	liters	0.264	gallons	gal
m^3	cubic meters	35.314	cubic feet	ft^3
m^3	cubic meters	1.307	cubic yards	yd^3
		MASS		
g	grams	0.035	ounces	oz
kg	kilograms	2.202	pounds	lb
Mg (or "t")	megagrams (or "metric ton")	1.103	short tons (2000 lb)	T
		TEMPERATURE (exact degrees)		
^oC	Celsius	1.8C+32	Fahrenheit	^oF
		ILLUMINATION		
lx	lux	0.0929	foot-candles	fc
cd/m^2	candela/m^2	0.2919	foot-Lamberts	fl
		FORCE and PRESSURE or STRESS		
N	newtons	0.225	poundforce	lbf
kPa	kilopascals	0.145	poundforce per square inch	lbf/in^2

TABLE OF CONTENTS

List of Tables

Table of Figures

ABSTRACT

The American Association of State Highway and Transportation Officials (AASHTO) adopted the Mechanistic-Empirical Pavement Design Guide (MEPDG) as an interim pavement design standard in 2008. In 2015, the Nevada Department of Transportation (NDOT) implemented the MEPDG for the structural design of new and rehabilitated flexible pavements. The resilient modulus of the unbound materials remains an important parameter in pavement design. This parameter also used to characterize the unbound materials in the MEPDG. The MEPDG follows a hierarchical approach in defining the required engineering properties of the pavement structure. Three levels of input are specified in the AASHTOWare® Pavement ME design software. This includes direct measurement from the laboratory testing offering the highest level of accuracy (i.e., Level 1), estimated values using correlations with soil properties (i.e., Level 2), and typical values offering the lowest level of accuracy (i.e., Level 3). NDOT currently uses R-value to estimate the resilient modulus of unbound materials which is not originally developed for Nevada. The major objective of this study is to develop a new resilient modulus prediction model for use in pavement rehabilitation designs.

Unbound materials (i.e., base, borrow, and subgrade) were sampled from several locations throughout Nevada and various tests were conducted to determine unbound material properties and characteristics, including the classification of the evaluated material (i.e., soil classification), R-value, moisture-density relationships, and resilient modulus testing. The resilient modulus test was conducted according to AASHTO T307 procedure. Prediction models for all three unbound material types (i.e., base, borrow, and subgrade) correlating resilient modulus to R-value and other physical properties were developed for pavement rehabilitation designs. District 1 materials were used to develop these prediction models, and the District 2 and District 3 materials were used to verify the models. Additionally, it was concluded that the current available NDOT resilient model correlation equation overestimates the resilient modulus anticipated in an existing pavement structure, thus resulting in a likely under designed asphalt concrete overlay thickness.

Keywords: MEDPG, AASHTO 93, modulus, unbound materials, stress-dependent, flexible pavement, rehabilitation.

EXECUTIVE SUMMARY

The primary goal of this project was to develop models correlating resilient modulus for pavement rehabilitation projects to R-value and other physical properties for Nevada's unbound materials. This was done by sampling base, borrow, and subgrade materials from each of the three Nevada Department of Transportation (NDOT) Districts. Twenty six materials were collected that included nine base materials, nine borrow materials, and eight subgrade materials. Laboratory testing was then conducted on the sampled materials, including tests for soil classification, R-value, moisture-density relationship, and resilient modulus (in accordance with AASHTO T307). Overall, the stress-dependent behavior of the resilient modulus for base material fitted the theta model, while the stress-dependent behavior of the resilient modulus for the subgrade material fitted the Uzan model.

To develop resilient modulus prediction models for pavement rehabilitation design, the ILLIPAVE 2005 software was used to find the deflection basins for different combinations of unbound materials and traffic loading conditions. Once these deflection basins were found, the backcalculation software MODULUS 6.1 was used to backcalculate the resilient moduli of the pavement structures' layers. These moduli were then used to correlate resilient modulus to R-value and other unbound material properties for pavement rehabilitation design.

The majority of the unbound materials were collected from District 1 (17 of the 26 materials collected). Out of the nine materials collected from District 2 and District 3, only six were able to be tested for resilient modulus. Therefore, the testing results for the District 1 materials were used to first develop the resilient modulus prediction models, then the results for the District 2 and District 3 materials were used to verify these models.

The developed prediction models for base, borrow, and subgrade materials were, in general, function of R-value, percent's passing 3/8 inch and No. 40 sieve, maximum dry density, optimum moisture content, plasticity index, and equivalent layer thickness. The maximum dry density and plasticity index were only considered in the case of subgrade material. On the other hand, the equivalent layer thickness accounts for pavement structure capacity and was only a statistically significant predictor variable for the case of base and borrow materials. The developed models resulted in lower predicted resilient moduli when compared to the current available NDOT correlation; thus influencing the structural design of pavement rehabilitation with a likelihood of underestimating the thickness of the asphalt concrete overlay when using current NDOT correlation.

In summary, it is recommended for NDOT and local agencies to implement the developed models in this study for predicting resilient modulus of unbound materials in their design of rehabilitated flexible pavements using AASHTO 93 or MEPDG (Level 2) approach.

CHAPTER 1 BACKGROUND

The American Association of State Highway and Transportation Officials (AASHTO) adopted the Mechanistic-Empirical Pavement Design Guide (MEPDG), as an interim pavement design standard in 2008 (1) . While numerous agencies have transitioned to this new method, some other agencies are in the process of evaluating the procedure, creating input libraries to tailor the AASHTO MEPDG procedure to their local conditions, soils, and materials. The Nevada Department of Transportation (NDOT) is within the latter category of agencies and has started the implementation of the MEPDG for the structural design of flexible and rigid pavements.

NDOT's goal is to implement the MEPDG through a phased approach, similar to many other agencies. This phased approach includes building material libraries and tying some of the inputs to their day to day practices to minimize deviations from current practice and maximize use of historical information and data. One of the input categories to the MEPDG is the characterization of all unbound layers and subgrades. The input parameters for the unbound layers include: resilient modulus, Poisson's ratio, dry density, water content, gradation, Atterberg limits, etc. The resilient modulus (M_r) is considered a key input parameter that has a significant impact on the structural responses of a pavement structure, and thus affects its performance and design.

Multiple sensitivity analyses have been completed to identify input parameters that significantly affect the calculation or prediction of different pavement distresses. Results from these sensitivity analyses are used to determine where the agency should focus its resources to facilitate the implementation process; in other words, "getting the biggest outcome for the funds invested." The review of published papers and reports indicate resilient modulus of unbound materials and soils has an impact on pavement performance. The following is a general summary of the impact levels of the subgrade resilient modulus on pavement performance indicators (3):

- Flexible Pavements.
    - Fatigue Longitudinal Cracking – Moderate to High Impact.
    - Fatigue Alligator Cracking – Low to Moderate Impact.
    - Transverse Cracking – None to Low Impact.
    - Rutting – Low to Moderate Impact.
    - International Roughness Index, IRI – Variable.
- Rigid Pavements.
    - Faulting – Low Impact.
    - Transverse Cracking – Moderate to High Impact.
    - IRI – None to Low Impact.

Recognizing the role of M_r of unbound materials on the design and performance of flexible and rigid pavements, some questions that are typically asked by an agency prior to the full implementation of the MEPDG include: a) what test method should be used to measure resilient modulus, b) how is the design resilient modulus determined, and c) what is the "best" correlation (form and accuracy) between M_r and other unbound materials properties or test results?

PURPOSE AND SCOPE

The purpose of this chapter is to compile information in specific areas related to the inputs to the MEPDG, including: a) the latest development and implementation of the MEPDG around the country, and b) summarize existing correlation equations to estimate the M_r from other physical properties of the unbound materials for base and subgrade layers. A similar literature review and summary was prepared by members of the research team for the Federal Highway Administration (FHWA) under a project recently completed (under publication) entitled; "Precision and Bias of the Resilient Modulus Test" (4). In addition, selected agencies actively running the resilient modulus test were contacted to obtain any results from recently completed and/or on-going studies relating the resilient modulus to other soil properties for use in design and in building the agency's materials library.

The background chapter is divided into several sections, including: 1) the hierarchical input structure of the MEPDG as related to unbound layers to facilitate implementation; 2) a review of laboratory M_r test methods; 3) reviewing M_r test data; 4) summarizing available correlations between M_r and other physical properties or tests.

HIERARCHICAL INPUT LEVELS OF THE MEPDG

Table 1 summarizes the input parameters and how they are determined as recommended in the MEPDG Manual of Practice. Most of the input parameters are well defined and commonly measured by the agency on a day-to-day basis for various reasons. Performing the repeated load resilient modulus test, however, is expensive and time consuming. In addition, the process of determining the design resilient modulus has been widely debated. As such, many agencies have expended resources to determine an appropriate procedure to estimate the design M_r for specific site features and design strategy.

The M_r is a required input for all unbound granular materials and subgrades. The M_r values are used in the structural response computation models and have a significant effect on the pavement responses and modulus of subgrade reaction (k-value) computed internally. The M_r can be measured directly from laboratory testing, or obtained through correlations with other material strength properties. There are three different levels of inputs for M_r and consist of the following:

- *Input Level 1 – Project Specific Measured Values.*
  The level 1 resilient modulus for unbound granular materials and subgrade are determined from cyclic triaxial tests. The test standards recommended for use are AASHTO T 307 and NCHRP 1-28A. The M_r is estimated using a generalized constitutive model (Equation 1). The *k* coefficients are determined by using linear or nonlinear regression analyses to fit the model to the laboratory test results. The

input level 1 procedure is applicable to new design, reconstruction and rehabilitation design (5).

$$M_r = k_1 p_a \left(\frac{\theta}{P_a}\right)^{k_2} \left(\frac{\tau_{oct}}{P_a} + 1\right)^{k_3} \quad (1)$$

where

M_r = resilient modulus (psi)
θ = bulk stress (psi)
τ_{oct} = octahedral shear stress (psi)
P_a = atmospheric pressure (psi)
k_1, k_2, k_3 = regression constants obtained by fitting M_r test data to equation

In earlier versions of AASHTOWare Pavement ME Design (6), the regression coefficients (k_1, k_2, k_3) could be entered directly into the software. The program used a finite element program for calculating pavement responses within the various unbound layers based on the nonlinear regression coefficient to determine the stress dependent resilient modulus appropriate for the in-place stress condition. Version 1.0 excluded the finite element response program, so a user could no longer enter the regression coefficients from a repeated load resilient modulus test. Thus, the design resilient modulus is entered directly in the program which is determined external to the software and only the linear response is considered in calculating the critical pavement responses. The in-place stress condition is determined by the user which should represent the value at the critical condition – higher damage rate.

- *Input Level 2 – Correlations with Other Material Properties or Tests.*
  While the repeated load resilient modulus test provides a fundamental approach to characterize the nonlinear stress dependent behavior of unbound materials, the test itself is time-consuming and costly. In light of these issues, most state highway agencies have elected to implement level 2 input for unbound materials. Many existing correlations can be used to estimate M_r, and the correlations can be direct or indirect. Table 2 summarizes the correlations included in the Pavement ME design software. For input level 2 design, the user can input a representative M_r or use the enhance integrated climatic model to adjust the M_r for seasonal effects or input a M_r for each month of the year.
- *Input Level 3 – Typical Values based on Soil Classification or Local Experience.*
  In level 3, typical M_r values are specified for different types of materials or soils. These typical values can represent the global defaults or represent local experience. The global values are built into the software, are dependent on soil classification, and represent the M_r at the optimum water content and maximum dry unit weight. These values should be used with caution as they represent approximate values. Level 1 or Level 2 input is recommended to achieve more representative materials behavior (5).

Table 1. Unbound Aggregate Base, Subbase, Embankment, and Subgrade Soil Input Parameters and Test Protocols for New and Existing Materials.

Design Type	Measured Property	Source of Data		Recommended Test Protocol and/or Data Source
		Test	Estimate	
New (lab samples) and existing (extracted materials)	Determine the average design resilient modulus for the expected in-place stress state from laboratory resilient modulus tests.	✓		The generalized model used in MEPDG design procedure – see equation 1; AASHTO T 307 or NCHRP 1-28A
	At-Rest earth pressure coefficient		✓	No national test standard; value used external to the software.
	Poisson's ratio		✓	No national test standard, use default values included in the MEPDG.
	Maximum dry density	✓		AASHTO T 180
	Optimum moisture content	✓		AASHTO T 180
	Gradation	✓		Gradation of the unbound aggregate or embankment soil measured in accordance with AASHTO T 88
	Atterberg Limits	✓		Liquid limit measured in accordance with AASHTO T 89, and plastic limit and plasticity index determined in accordance with AASHTO T 90.
	Specific gravity	✓		AASHTO T 100
	Saturated hydraulic conductivity	✓		AASHTO T 215
	Soil water characteristic curve parameters	✓		Pressure plate (AASHTO T 99), OR Filter paper (AASHTO T 180), OR Tempe cell (AASHTO T 100)
Existing material to be left in place	FWD backcalculated modulus	✓		AASHTO T 256 and ASTM D 5858
	Poisson's ratio		✓	No national test standard, use default values included in the MEPDG.

Table 2. Models Relating Material Index and Strength Properties to M_r (After Ref. 5).

Strength/Index Property	Model	Comments	Test Standard
CBR	$M_r = 2555(CBR)^{0.64}$ M_r in psi	CBR = California Bearing Ratio	AASHTO T193
R-value	$M_r = 1155+555R$ M_r in psi	R = R-value	AASHTO T190
AASHTO layer coefficient	$M_r = 30000(a_i/0.14)$ M_r in psi	a_i = AASHTO layer coefficient	AASHTO Guide for the Design of Pavement Structures
PI and gradation*	CBR = 75/[1+0.728(wPI)]	wPI = P200*PI P200 = percent passing No. 200 sieve size PI = plasticity index (percent)	AASHTO T27 AASHTO T90
DCP*	$CBR = 292/(DCP^{1.12})$	CBR = California Bearing Ratio DCP = dynamic cone penetrometer index (mm/blow)	ASTM D 6951

*Estimates of CBR are used to estimate M_r.

The following summarizes the values and data sources for characterizing the unbound layers or materials used by most agencies that have completed or are in the process of implementing the Pavement ME software. The default values used become important when completing the calibration and validation of the distress transfer functions to ensure consistency of use.

- <u>Design Resilient Modulus</u>: Many agencies have generated M_r databases for the aggregate base materials commonly specified by the agency and soils that are predominantly encountered within the agency's jurisdictions. Other agencies use correlations to California Bearing Ratio (CBR), R-value, materials physical properties, and dynamic cone penetrometer (DCP) test results.
- <u>Dry Density and Water Content</u>: The software asks for the maximum dry unit weight and optimum water content but the values depend on how the test specimens were prepared and/or the condition of the test specimens for the correlations that the agency is using to estimate the M_r. For example, some agencies use the CBR to estimate the design M_r. A few of these agencies have run soaked CBR tests and measured M_r at the dry density and water content from the soaked CBR test, while other agencies have measured M_r at the dry density and water content before the specimen is subjected to water soaking during the CBR test. How the correlation was developed defines the input values. It is important that the dry density and water content be entered to be consistent with the method used to define the correlation regardless of what other test is used.
- <u>Poisson's Ratio</u>: Poisson's ratio of is identified as an insignificant input parameter in terms of the predicted cracking and distortion type distresses, and is generally ignored. However, Poisson's ratio does have an impact on the selection of the design M_r of any unbound layer because it affects the vertical and horizontal stresses – this is called the Poisson's ratio effect.
- <u>At-Rest Lateral Earth Pressure Coefficient</u>: This input parameter is largely ignored because the selection of M_r is not part of the input level 1 in the current version of the Pavement ME Design software. However, the at-rest earth pressure coefficient is important in defining the design M_r. At-rest earth pressure coefficients can vary from 0.50 to well over 1.0 depending on the condition of the soil or aggregate base layers. The coefficient has an impact on the lateral stress condition, which in turn affects the design M_r.
- <u>Gradation and Atterberg Limits</u>: Most agencies define the average gradation, plasticity limit, and liquid limit for the commonly used aggregate base layers and predominant soils found within the agency's jurisdictions. The local default values are typically compared to the global default values included in the Pavement ME Design software to determine the difference between the default values. Sometimes differences in the physical properties will explain some of the differences between the global and local design M_r.
- <u>Soil-Water Characteristic Curve Parameters</u>: Just about all agencies have used the global default values which are soil classification dependent.
- <u>Specific Gravity</u>: All agencies have simply used the global default value of 2.7 included in the Pavement ME Design software for all soil classifications.

- Saturated Hydraulic Conductivity: All agencies have used the global default value in their implementation and local calibration studies, which are soil classification dependent.

OVERVIEW OF RESILIENT MODULUS TEST

The resilient modulus is similar to the elastic modulus of a material and is defined as a ratio of deviator stress to resilient or elastic strain experienced under repeated loading conditions that aims to simulate traffic loading. Figure 1 shows a representation of the resilient modulus. The main reason for using the resilient modulus as the parameter for unbound bases and subgrades is that it represents a basic material property and can be used in mechanistic analyses to calculate pavement responses used to predict different distresses (i.e., rutting, cracking, and roughness).

Prior to 1980, an attempt was made to standardize the testing procedure. A standard test was not reached due to different philosophies on specimen preparation, on versus off specimen deformation measurements, stress states (vertical stress and confinement), as well as type of load application (haversine versus square load pulses). Several studies were performed in the process in attempts to standardize testing methods. Many of these studies are summarized in the precision and bias report (4). Some other factors that were studied include, drained versus undrained conditions, load cell location, and the number of conditioning cycles required for stable results.

The NCHRP Synthesis 382 summarized M_r testing procedures and results from various sources. The summary is presented based on testing performed prior to 1986, between 1986 and 1996, and after 1996 (7). In summary, the research performed prior to 1986 mostly focused on three different criteria namely: (a) the development of test procedures and equipment modifications to test cohesive subgrades and granular base materials, (b) the development of appropriate models to represent the resilient behavior, and (c) the introduction of few correlations based on soil properties to predict resilient properties (7). The M_r research performed between 1986 and 1996 focused on the use of various laboratory and field equipment to determine the properties of both unbound bases and subgrades. Some studies were performed to develop a database of resilient properties which were then used to develop models to predict resilient properties of subgrades and aggregate bases. Considerable advances were made after 1996 which lead to the development of a large M_r database for better interpretation of resilient properties for mechanistic pavement design. One of these studies tested the M_r values for LTPP sections across the United States (7).

In other advancements, various studies determined parameters which affect the measurement of M_r. One such study determined that soil suction was an important factor in measuring the M_r. Soil suction is not measured as part of the AASHTO T-307 or NCHRP 1-28A testing procedures. Another study suggested that modifications should be made to the stress state conditions when measuring M_r on unsaturated unbound materials (4).

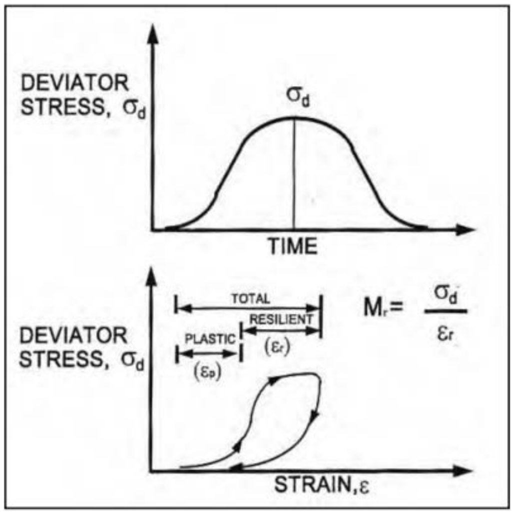

Figure 1. Definition of resilient modulus (7).

The M_r test using the repeated load triaxial (RLT) test simulates traffic wheel loading on in situ soils by applying repeated or cyclic loads on compacted soil specimens. The stress levels applied to the soil specimens are dependent on the location of the material within the pavement structure. A confining pressure is also applied to the specimen that represents the overburden lateral pressure at a specific location in the subgrade. The axial deviator stress consists of two components, the cyclic stress, and a constant stress. The constant stress is typically equivalent to 10% of the total axial deviator stress.

The test procedure requires a compacted soil specimen using impact compaction methods. The specimen is then transferred into the triaxial chamber and the confining pressure is applied. The test is initiated by applying various levels of deviator stresses. Multiple confining pressures and deviator stresses are used during the testing process. The M_r values are determined at each combination of confining pressure and deviator stress. The design M_r is established by determining the M_r value at the appropriate confining pressure and deviator stress level corresponding to the location of the materials within the pavement structure.

Various versions of the repeated load triaxial test have been used to measure M_r for ME based pavement design procedures, including: AASHTO T274, T292, T294, and T307. All of these test methods differ from each other in one or more of the following aspects: specimen preparation, conditioning, seating stress, testing sequences, and deformation measurements inside/outside of the triaxial cell.

Table 3 summarizes the chronology of the AASHTO resilient modulus test procedures. AASHTO adopted test procedure T-307 which is similar to the test procedure used in the Long-Term Pavement Performance (LTPP) program.

Table 3. Chronology of AASHTO Test Procedures for Mr Measurements (7).

Test Procedure	Details
AASHTO T-274-1982	Earliest AASHTO test procedure; No details on the sensitivities of displacement measurement devices were given; Criticisms on test procedure, test duration (5 hours long test) and probable failures of soil sample during conditioning phase; testing stresses are too severe.
AASHTO T-292-1991	AASHTO procedure introduced in 1991; Internal measurement systems are recommended; Testing sequence is criticized owing to the possibility of stiffening effects of cohesive soils.
AASHTO T-294-1992	AASHTO modified the T-292 procedure with different sets of confining and deviator stresses and their sequence; Internal measurement system is followed; 2-parameter regression models (bulk stress for granular and deviator stress model for cohesive soils) to analyze test results; Criticism on the analyses models.
Strategic Highway Research Program P-46-1996	Procedural steps of P-46 are similar to T-294 procedure of 1992; External measurement system was allowed for displacement measurement; Soil specimen preparation methods are different from those used in T-292.
AASHTO T-307-1999	T-307-1999 was evolved from P-46 procedure; recommends the use of external displacement measurement system. Different procedures are followed for both cohesive and granular soil specimen preparation.
NCHRP 1-28 A: Harmonized Method-2004 (RRD 285)	This recent method recommends a different set of stresses for testing. Also, a new 3-parameter model is recommended for analyzing the resilient properties. The use of internal measurement system is recommended in this method.

A recent review of 30 state DOTs and other agencies specifications indicated that 22 out the 30 are currently using AASHTO T307 test method for measuring M_r of unbound materials (4). Table 4 lists the M_r test procedures being used by different agencies, which was prepared by Von Quintus et al. from a review of more recent publications and specifications (4). The overall satisfaction of those agencies regarding use of resilient modulus for ME based pavement design was found to be low due to constant modification of the test procedures, measurement difficulties, and design-related issues.

The M_r test data generated from the triaxial test should undergo data anomaly checks to identify if issues with the data exist. It is essential to ensure that the good quality data without errors are used before making any assessment on the M_r results. Possible problems that could affect the M_r test data are listed below (8):

- Different condition sequences or different stress application sequences used in the test program.
- Leaks occurring in the membrane during the test.
- Different stress states used in the test program than required by the test protocol.
- Test specimens that begin to fail or exhibit disturbance at the higher stress states.
- Linear variable differential transformer (LVDT) clamps that begin to move or move suddenly because of vibrations during the loading sequence.
- LVDTs that begin to drift during the testing sequence or become restricted due to friction in the measurement system.
- Measured deformations that begin to exceed the linear ranges of the LVDTs.

Table 4. State DOT/Other Laboratories Conducting Resilient Modulus Testing.

State DOT/Other Laboratories	Test Protocol Followed
Alaska DOT	AASHTO T 307-99
Alabama DOT	AASHTO T 307-99
Arizona DOT/ASU Geotechnical Laboratory	NCHRP 1-28A
Cold Regions Research & Engineering Laboratory (CRREL)	AASHTO T 307-99
Colorado DOT	AASHTO T 307-99
Florida DOT	AASHTO T 307-99
Georgia DOT	AASHTO T 307-99
Iowa DOT	NCHRP 1-28A/ AASHTO T307-99
Idaho Transportation Department Laboratory	AASHTO T 307-99
Indiana DOT	AASHTO T 307-99
Kansas DOT	AASHTO T 307-99
Kentucky DOT/University of Kentucky Transportation Center	AASHTO T 307-99
Louisiana DOT/Louisiana Transportation Research Center (LTRC) Laboratory	AASHTO T 307-99
Manitoba Provence, Canada	NCHRP 1-28A
Michigan DOT	AASHTO T 307-99
Minnesota DOT	NCHRP 1-28A
Missouri DOT	AASHTO T 307-99
Mississippi DOT	AASHTO T 307-99
Montana DOT	AASHTO T 307-99
Nebraska DOT/University of Nebraska-Lincoln (UNL) Geomaterials Laboratory	AASHTO T 307-99
North Dakota DOT	NCHRP 1-28A
New Hampshire DOT	AASHTO TP46-94
New Jersey DOT/Rutgers University Asphalt/Pavement Laboratory (RAPL)	AASHTO TP46-94
Ohio DOT/ORITE Pavement Material Test Laboratory	AASHTO T-274
Oklahoma DOT	AASHTO T 307-99
Rhode Island DOT	AASHTO T 307-99
Tennessee DOT	AASHTO T 307-99
Texas DOT	AASHTO T 307-99
Virginia DOT	AASHTO T 307-99
Wisconsin DOT	AASHTO T 307-99

The following provides a summary of the more important findings relative to determining the precision and bias of the M_r test methods. These findings were extracted from the FHWA report on the precision and bias of the resilient modulus test (4).

- There are several test systems available on the market today. The so-called high-end equipment (MTS, Interlaken and Instron) is about double the cost of the lower-end equipment (GCTS, GeoComp and IBC). This statement does not imply the high-end equipment is twice as accurate as the lower-end equipment. Few studies have focused on determining if there is a bias between these different systems, as well as defining the precision of the test system.

- The end effects for off-specimen LVDTs were obvious and significantly increased the variability in the test results of triplicate samples, in comparison to on-specimen LVDTs. Different studies, however, have reported opposite results in comparing the resilient modulus values between on-specimen and off-specimen displacement measurements for calculating resilient modulus.
- It was found that all soils exhibited a decrease in M_r with an increase in saturation, but the magnitude of the decrease in resilient modulus was found to depend on the soil type. It was observed and reported a 3 to 5 percent increase in moisture content from optimum conditions can result in a 50 to 70 percent reduction in M_r. The drying of the test specimens can also result in a significant increase in resilient modulus, in some cases ten-fold. Thus, moisture content and dry density are important in measuring the resilient modulus.
- The studies reviewed indicated that the M_r values were impacted by moisture content, soil suction, Atterberg limits, gradation, source lithology, stress-strain levels, degree of saturation, seasonal variation, aggregate angularity, and surface texture.

CORRELATIONS FOR ESTIMATING RESILIENT MODULUS

Numerous M_r correlation equations have been developed over the years (9). Most of these correlations are regression-based equations developed by comparing M_r test results from the repeated load triaxial to the less expensive and more routine test results such as R-Value (R), CBR, unconfined compressive (UC) strength, dynamic cone penetrometer test, physical properties, etc. An extensive literature review was conducted and showed that most of the correlation equations were developed from relatively small sample sets and often for region-specific material types (10). Accordingly, it was recommended to further assess and verify the suitability and reliability of the regression analysis before the use of any of the correlation equations. Two different types of correlations have been developed, direct and indirect.

- Direct correlations consist of developing a relationship between M_r and various soil properties and in-situ related parameters. These correlations are usually developed by using some type of statistical regression between the test data and M_r. Two types of direct correlations are typically developed. The first method develops a direct correlation between M_r and various soil properties. The second correlates the moduli with in-situ parameters.
- The indirect method develops correlations by formulating an equation that accounts for confining or deviator or both stress forms. Usually these correlations contain model constant parameters. Some of these models can have two, three or four parameter correlations that account for the different stress states.

Puppala presented a detailed summary of the different types of correlations that have been developed (7). The summary details various correlation equations developed for both direct and indirect correlations. This literature review will continue to focus on the detailed correlations developed which directly affect the implementation of the Pavement-ME design software. The following lists some of the correlations that have been developed.

Yau and Von Quintus, 2001; Crushed Stone Materials, LTPP Material Code 303:

$$M_r = \left[0.7632 + 0.0084(P_{3/8}) + 0.0088(LL) - 0.0371(W_{opt}) - 0.0001(\gamma_{opt})\right]p_a * \left[\frac{\theta}{p_a}\right]^{\left(2.2159 - 0.0016P_{3/8} + 0.0008LL - 0.038W_{opt} - 0.0006\gamma_{opt} + 2.4x10^{-7}\left[\frac{\gamma_{opt}^2}{P_{40}}\right]\right)} * \left[\frac{\tau_{oct}}{p_a} + 1\right]^{(-1.1720 - 0.00822LL - 0.0014W_{opt} + 0.0005\gamma_{opt})} \quad (2)$$

where

LL = liquid limit
W_{opt} = optimum water content
γ_{opt} = maximum dry unit weight at optimum water content
$P_{3/8}$ = percent passing the 3/8 inch sieve (percent)
P_{40} = percent passing the #40 sieve (percent)
Number of points = 853
Mean squared error = 1699.6 psi
S_e = 41.23; S_y = 87.42; S_e/S_y = 0.4716

Yau and Von Quintus, 2001; Sand, LTPP Material Code 306:

$$M_r = \left[-0.2786 + 0.0097(P_{3/8}) + 0.0219(LL) - 0.0737(PI) + 1.8x10^{-7}\left(\frac{\gamma_{opt}^2}{P_{40}}\right)\right]p_a * \left[\frac{\theta}{p_a}\right]^{\left(1.1148 - 0.0053P_{3/8} - 0.0095LL + 0.0325PI + 7.2x10^{-7}\left[\frac{\gamma_{opt}^2}{P_{40}}\right]\right)} * \left[\frac{\tau_{oct}}{p_a} + 1\right]^{(-0.4508 + 0.0029P_{3/8} - 0.0185LL + 0.0798PI)} \quad (3)$$

where

PI = Plasticity Index
Number of Points = 2,323
Mean squared error = 1883.9
S_e = 43.40; S_y = 80.19; S_e/S_y = 0.5413

Yau and Von Quintus, 2001; Coarse-Grained Gravelly Soils:

$$M_r = \left[1.3429 - 0.0051\left(P_{3/8}\right) + 0.0124(\%Clay) + 0.0053(LL) - 0.0231(W_s)\right]p_a *$$
$$\left[\frac{\theta}{p_a}\right]^{\left(0.3311+0.0010P_{3/8}-0.0019(\%Clay)-0.0050LL-0.0072PI+0.0093W_s\right)} *$$
$$\left[\frac{\tau_{oct}}{p_a}+1\right]^{\left(1.5167-0.0302P_{3/8}+0.0435(\%Clay)+0.0626LL-0.2353W_s\right)} \quad (4)$$

where

W_s = water content of test specimen
%Clay = percentage clay or material passing the No. 200 sieve
Number of Points = 957
Mean squared error = 301.3
S_e = 17.36; S_y = 26.81; S_e/S_y = 0.6474

Yau and Von Quintus, 2001; Fine-Grained Silty Soils:

$$M_r = \left[1.0480 + 0.0177(\%Clay) + 0.0279(PI) - 0.37(W_s)\right]p_a *$$
$$\left[\frac{\theta}{p_a}\right]^{(0.5097-0.0286PI)} * \left[\frac{\tau_{oct}}{p_a}+1\right]^{\left(-0.2218+0.0047(\%Silt)+0.0849PI-0.1399W_s\right)} \quad (5)$$

where

%Silt = percentage of silt fines
Number of Points = 464
Mean squared error = 193.0
S_e = 13.89; S_y = 24.71; S_e/S_y = 0.5622

Yau and Von Quintus, 2001; Fine-Grained Clayey Soils:

$$M_r = \left[1.3577 + 0.0106(\%Clay) - 0.0437(W_s)\right]p_a *$$
$$\left[\frac{\theta}{p_a}\right]^{\left(0.5193-0.0073P_4+0.0095P_{40}-0.0027P_{200}-0.0030LL-0.0049W_{opt}\right)} *$$
$$\left[\frac{\tau_{oct}}{p_a}+1\right]^{\left(1.4258-0.0288P_4+0.0303P_{200}+0.0251(\%Silt)+0.0535LL-0.0672W_{opt}-0.0026\gamma_{opt}+0.0025\gamma_s-0.6055\left(\frac{W_s}{W_{opt}}\right)\right)} \quad (6)$$

where
P_4 = percentage of material passing the No. 4 sieve
P_{200} = percentage of material passing the No. 200 sieve

γ_s = dry unit weight of test specimen.
Number of Points = 1,484
Mean squared error = 557.9
S_e = 23.62; S_y = 29.22; S_e/S_y = 0.8082

Drum, et al., 2008:

$$M_r = 45.8 + 0.00052\left(\frac{1}{a}\right) + 0.188(UC) + 0.45(PI) + 0.216(\gamma_s) - 0.25(S) - 0.15(P_{200}) \tag{7}$$

where

a = initial tangent modulus (psi)
UC = unconfined compressive strength (psi)
S = degree of saturation (percent)
Coefficient of Determination, R^2 = 0.83

Lee, et al., 1997:

$$M_r = 695.4(S_{@1\%}) - 5.93(S_{@1\%})^2 \tag{8}$$

where

$S_{@1\%}$ = stress at 1.0 percent strain in the unconfined compressive strength test
Coefficient of Determination, R^2 = 0.97

Hossain and Kim, 2014, Static Compaction:

$$M_r = 6082 + 142(UC) \tag{9}$$

Coefficient of Determination, R^2 = 0.64

$$M_r = 7884.2 + 99.7(UC) + 193.1(PI) - 47.9((P_{200}) \tag{10}$$

Coefficient of Determination, R^2 = 0.86

Hossain and Kim, 2014, Impact Compaction (Proctor Hammer):

$$M_r = 4283 + 143(UC) \tag{11}$$

Coefficient of Determination, R^2 = 0.73

$$M_r = 6113 + 95.1(UC) + 173.7(PI) - 27.8((P_{200}) \tag{12}$$

Coefficient of Determination, R^2 = 0.91

$$M_r = 657(S_{@1\%}) - 6.75(S_{@1\%})^2 \quad (13)$$

Coefficient of Determination, $R^2 = 0.97$

IMPLEMENTATION AND USE OF RESILIENT MODULUS

Several State Agencies have implemented or are in the process of implementing the MEPDG. This section will focus on the efforts related to developing M_r input databases for each State. Table 5 summarizes the outcome from selected agencies regarding resilient modulus and other properties of unbound layers. The important observation from Table 5 and from the design manual of selected agencies is that almost no agency performs repeated load resilient modulus tests for measuring M_r. The M_r is predominantly estimated using a library of values and/or through a regression equation related to other properties or test results.

Table 5. Methods used to Estimate Design Resilient Modulus for Selected Agencies.

State DOT	Test Procedure	Mr Correlated with and/or Determined by
Arizona	NCHRP 1-28A	R-value and a library of Mr values.
Colorado	AASHTO T 307-99	R-value and a library of Mr values.
Florida	AASHTO T 307-99	LBR-value, backcalculated from deflection basins, and a library of Mr Values.
Georgia	AASHTO T 307-99	Soil Support, Physical properties, and a library of Mr values.
Idaho	AASHTO T 307-99	R-value and a library of Mr values.
Michigan	AASHTO T 307-99	Library of Mr values and backcalculated from deflection basins.
Missouri	AASHTO T 307-99	Regression equations to calculate k_1, k_2, and k_3 from soil physical properties; similar to FHWA regression equations.
Mississippi	AASHTO T 307-99	CBR and a library of Mr values.
Montana	AASHTO T 307-99	Library of Mr values and backcalculated from deflection basins.
Pennsylvania	AASHTO T 307-99	Unconfined compressive strength and a library of values
Tennessee	AASHTO T 307-99	Index of soil properties.
Texas	AASHTO T 307-99	Texas Triaxial Classification Value
Virginia	AASHTO T 307-99	Unconfined compressive strength
Wisconsin	AASHTO T 307-99	Regression equations to calculate k_1, k_2, and k_3 from soil physical properties; similar to FHWA regression equations.
Wyoming	AASHTO T 307-99	R-value and a library of Mr values.

Most agencies east of the Mississippi River use CBR for estimating the design M_r, while agencies west of the Mississippi use R-value. The regression equations for estimating Mr from the R-value vary by agency, but only two regression equations are typically used for estimating M_r from CBR. The R-value regression equations are listed by agency in the following section, while the two regression equations based on CBR are; Mr =1500*CBR and $M_r = 2555(CBR)^{0.64}$.

CHAPTER 2 RESEARCH APPROACH

This chapter describes the tests that were conducted on the sampled base, borrow, and subgrade materials from NDOT Districts 1, 2, and 3. These tests included gradation, Atterberg Limits, maximum dry unit weight and optimum water content, R-value, and M_r testing. Additionally, the procedure followed for the collection of the unbound materials are discussed.

MATERIAL COLLECTION

The materials tested in this project included base, borrow, and subgrade materials from all three NDOT districts. A total of eight base material types were collected – five from District 1, one from District 2, and two from District 3. Nine borrow material types were collected – six from District 1, three from District 2, and one from District 3. Eight subgrade types were collected – six from District 1 and two from District 2. In total, 26 types of materials were sampled and tested.

Base and borrow materials were collected together whenever possible. Recent NDOT pavement construction projects were identified, and base and borrow materials were sampled from the pits used for these projects. Table 6 summarizes the base and borrow materials sampled from all three NDOT Districts. Figure 2 and Figure 3 show the sampling locations for District 2 and District 3 base and borrow materials, respectively.

Table 6. Sampled Base and Borrow Materials.

ID	District	County	Pit	Borrow (No. of Buckets)	Type 1 Class B Base (No. of Buckets)
3605	1	Clark	Sloan Commercial Pit	–	20
3607	1	Esmeralda	Pit ES 03-08	10	20
3546	1	Clark	Apex Pit	10	20
3597	1	Clark	Lhoist Pit	10	20
3613	1	Clark	Material Pit 69-01	10	20
3583	1	Clark	LVP Lone Mountain Pit	10	20
Lockwood	2	Washoe	Lockwood Facility	15	15
SNC	2	Washoe	Sierra Nevada Construction Mustang Pit	30	–
Elko	3	Elko	Staker-Parson Pit	15	15
Hunnewill	3	Humboldt	Hunnewill Pit	–	15

–Material not collected.

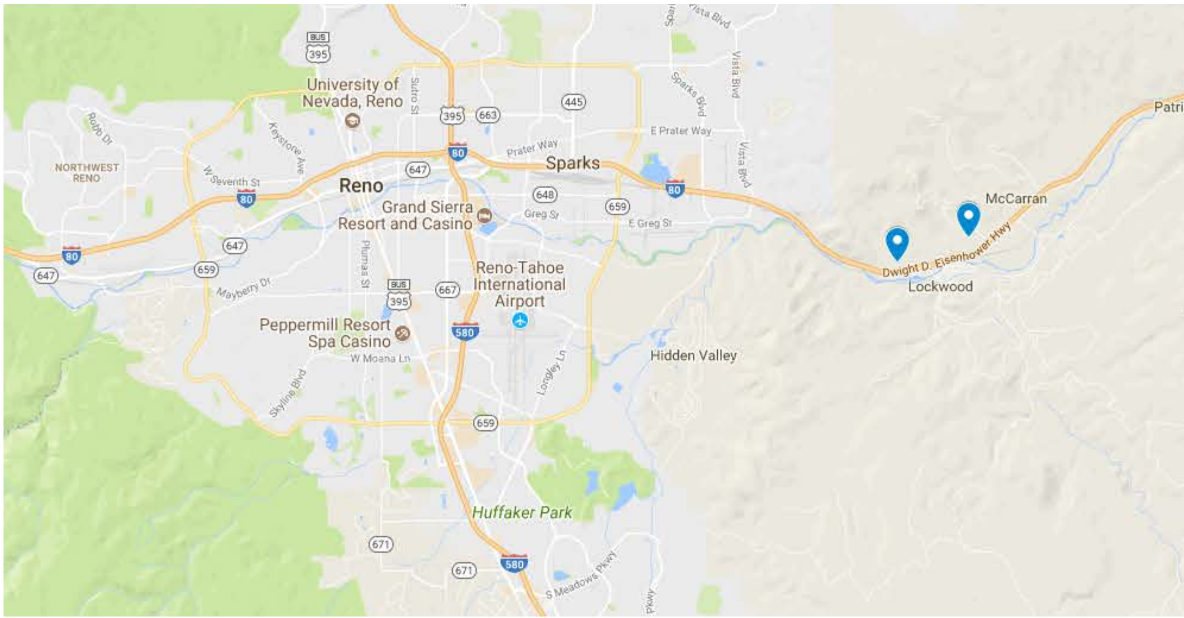

Figure 2. District 2 base and borrow sampling locations.

Figure 3. District 3 sampling locations.

Using the ASU Soil Map, several types of subgrade materials were identified. Twelve locations throughout District 1 were identified. These proposed locations are shown in Figure 4 and Table 7. Using the ASU Soil Map, the soil type as a function of depth was determined. The AASHTO Soil Classifications A-1-a, A-1-b, A-2-4 and A-4 were found to be the most prominent soil types in District 1. Of the twelve proposed locations, six locations were sampled from. While the goal was to sample a wide variety of soil types, each of the subgrade types sampled from District 1 fell into AASHTO Soil Classification A-1-b or A-2-4; therefore, rather than naming each of the subgrade samples by their classification, for this report, they are labeled as “Sample 1,” “Sample 2,” etc.

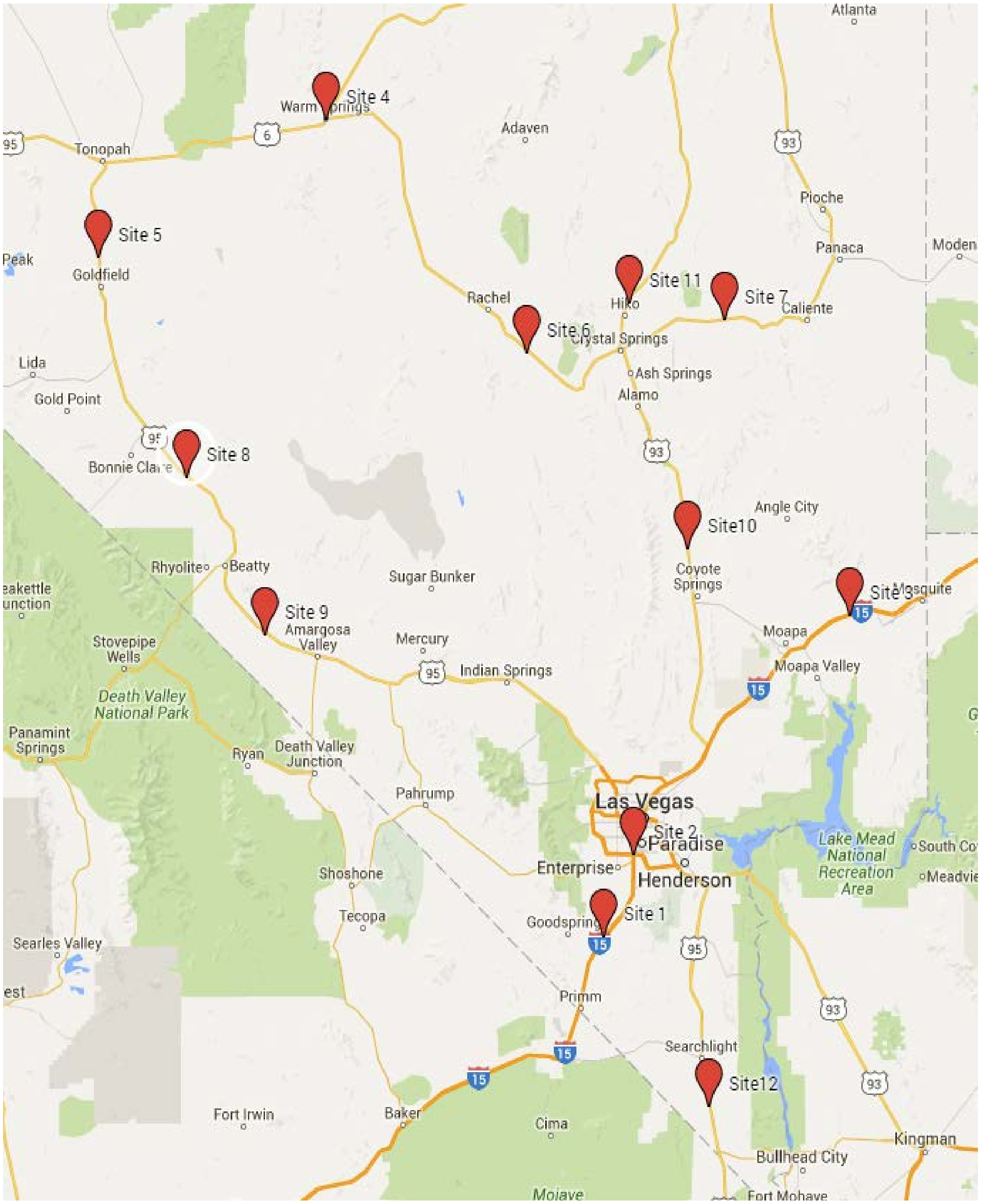

Figure 4. Proposed District 1 subgrade sampling location.

Table 7. Proposed District 1 Subgrade.

Site	Thickness (inch)	Soil Classification	Latitude (°)	Longitude (°)
1	2	A-4	35.8256	115.2970
	5.9	A-4		
2	9.1	A-2-4	36.0657	115.1806
3	2	A-2-4	36.7653	114.3457
	16.1	A-4		
	7.9	A-2-4		
4	1.2	A-4	38.1917	116.3685
	19.7	A-6		
	20.1	A-2-6		
	18.9	A-1-a		
5	5.1	A-1-a	37.7967	117.2461
	54.7	A-1-a		
6	9.1	A-2-4	37.4604	115.5078
7	2	A-4	37.6185	114.8291
	18.1	A-4		
8	5.9	A-1-b	37.1625	116.9055
	53.9	A-1-b		
9	7.9	A-1-a	36.7103	116.6061
	52	A-1-a		
10	2	A-4	36.9587	114.9719
	5.1	A-2-4		
11	3.9	A-1-b	37.6653	115.1998
	7.1	A-1-b		
	26.8	A-1-b		
12	7.9	A-5	35.3294	114.8962
	18.1	A-2-4		
	33.9	A-1-b		

Two locations in District 2 were identified for sampling. These locations were outside the Scrugham Engineering and Mines building (SEM) at UNR, where one subgrade was sampled, and Jacks Valley Road in Douglas County, where one subgrade was sampled. Figure 5, Figure 6, and Table 8 summarize the locations from where the materials were collected. Surface material outside of SEM at UNR was discarded, and the subgrade material was collected at a depth of two feet below the surface, as shown in Figure 7.

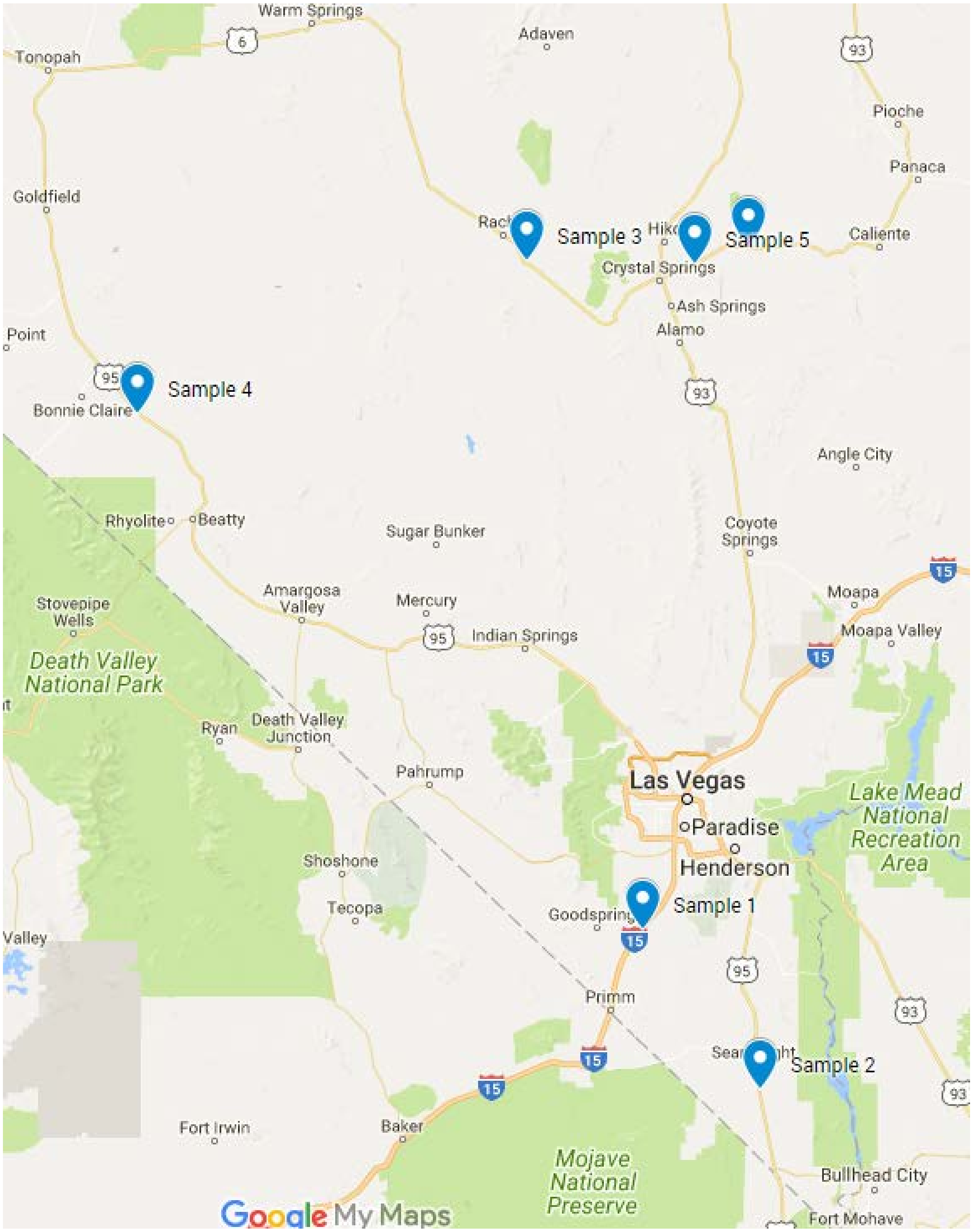

Figure 5. District 1 sampled subgrade locations.

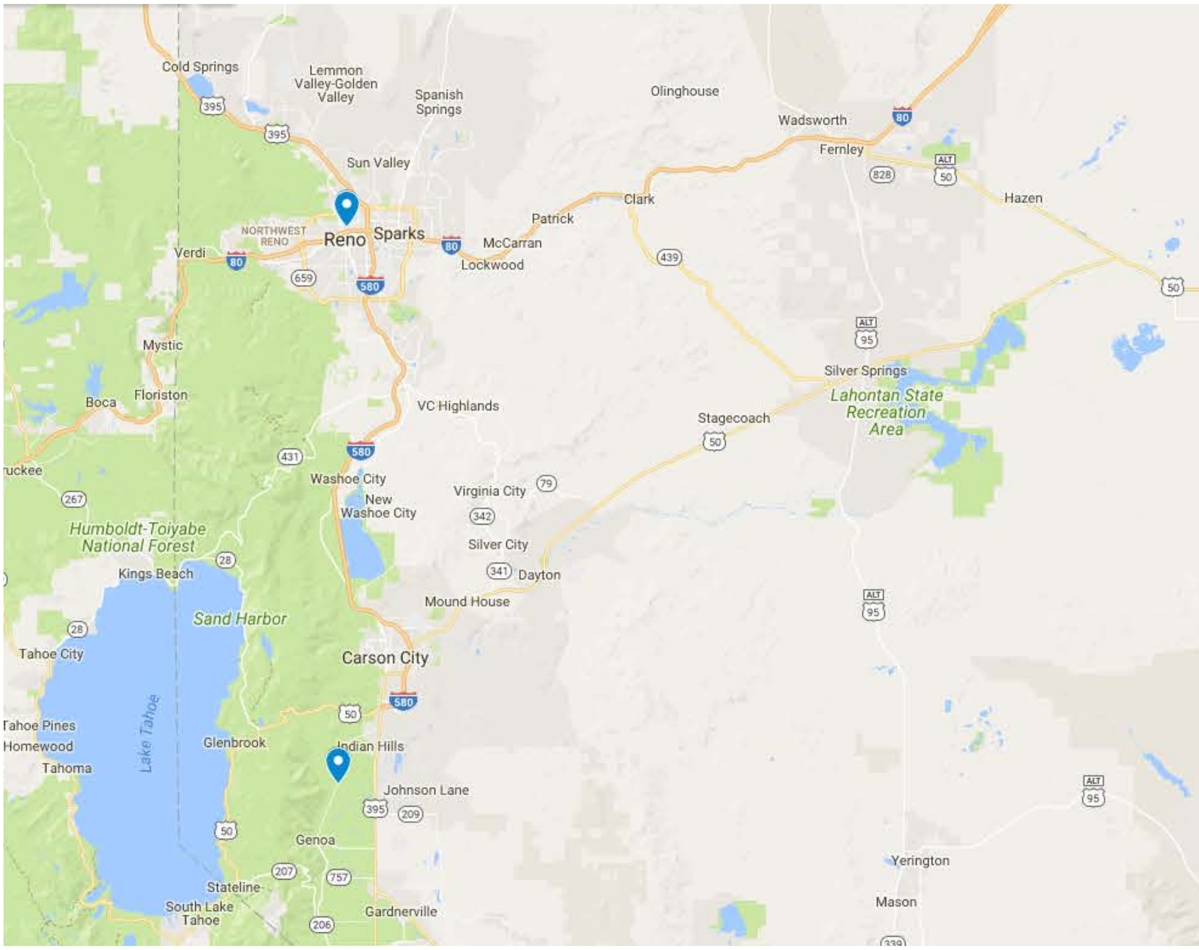

Figure 6 District 2 Base and Borrow Sampling Locations.

Table 8. Sampled Subgrade Materials.

Subgrade Source	**District**	**Location**	**Quantity (No. of Buckets)**
Sample 1	1	I-15/Goodsprings	10
Sample 2	1	US-95/Searchlight	10
Sample 3	1	NV-375/Rachel	10
Sample 4	1	US-95/Bonnie Claire	10
Sample 5	1	US-93/Crystal Spring MP62	10
Sample 6	1	US-93/Crystal Spring MP67	10
Jacks Valley	2	Douglas County	10
SEM Soil	2	SEM Building at UNR	15

Figure 7. Sampling of SEM soil at a depth of two feet.

One type of drain rock material was sampled from District 2 at the Lockwood Facility as well; however, this material could not be tested. While gradation and coarse aggregate specific gravity testing could be conducted on the drain rock, all other testing including Atterberg Limits, fine aggregate specific gravity, R-value, and M_r testing could not be conducted. The drain rock is comprised of all coarse material, which is material retained on the No. 4 sieve that is too coarse of an aggregate blend to be able to conduct these tests.

LABORATORY EVALUATION

This section presents the laboratory testing program of the base, borrow, and subgrade materials that were sampled in this study. The materials were subjected to five groups of laboratory testing: Soil Classification, Moisture-density Relationship, Repeated Load Triaxial Resilient Modulus, and Resistance Value "R-Value." The following sections briefly describe the test methods and presents the data generated from each testing group.

Soil Classification Testing

The selected materials were classified using particle size analysis and Atterberg limits following both AASHTO and USCS systems which are widely used in practice. The particle size analysis for the aggregate and soil materials was conducted in accordance with NDOT test method Nev. T206 and ASTM D 421 and D 422, respectively. NDOT test methods Nev. T210I, T211I, and T212I were used to determine the Liquid Limit (LL), Plastic Limit (PL), and Plasticity Index (PI) of the selected materials, respectively.

Particle Size Analysis

Aggregate from base and borrow materials were split into the sample size around 3000g and dried until to a constant weight at a temperature not exceeding 110°C. The dry aggregate was washed over sieve No. 10 and sieve No. 200. Retained materials on sieve No. 10, sieve No. 200, and washing vessel were transferred into a pan, dried at 110°C, and sieved through a set of sieves in a mechanical sieve shaker.

Materials from subgrade samples were split into the required sample size and dried at 60˚C. The dry material was pulverized by using a rubber head hammer. Washing was performed on sieve No. 10 and poured through sieve No. 200 until clear water appears. Retained materials on sieve No. 10 and sieve No. 200 were carefully transferred into a pan and dried at a temperature of 60°C. The dry material was pulverized again and sieve analysis was done in a mechanical sieve shaker.

Atterberg Limits

Liquid limit and plastic limit are often referred to as “Atterberg Limits.” Based on its moisture content, soil can be in the state of; liquid, plastic, semi-solid, or solid. Liquid limit is the moisture content at which the soil transforms from plastic to liquid. Plastic limit is the moisture content at which the soil transforms from semi-solid to plastic. Liquid limit and plastic limit tests were conducted according to Nev. T210I and T211I, respectively.

A representative sample with minimum weight of 150g was obtained from passing sieve No. 40. Moisture was added and mixed until a uniform color is achieved. For the liquid limit test, the Casagrande apparatus was used to determine the number of blows to close the 13mm groove. The moisture content was changed in order to obtain three sets of number of blows in the range of; 25-35, 20-30, and 15-25. Around 8g of soil from the 25-35 was used for the plastic limit test. The sample was divided into 1.5-2g portion and rolled on a glass plate until it forms a 3mm thread. This process was continued until the thread crumbles at which the moisture content was obtained.

Figure 8 shows the apparatus and tools used for the liquid limit and plastic limit tests. The moisture content of the sample that gives 25 blows to close the groove by 13 mm is considered as the liquid limit.

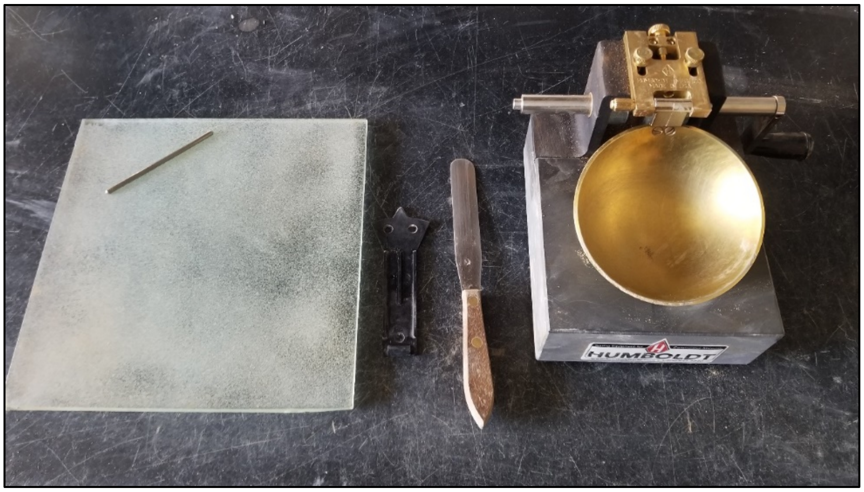

Figure 8. Atterberg Limits testing equipment.

Moisture Density Relationship

Compaction is the densification process of the material by applying mechanical energy. As the moisture content increases, water particles fill the air voids and increase the density of the material. This densification process occurs up to a certain moisture content, after which any additional water will displace the solid particles leading to reduction in the density. The corresponding moisture content at the maximum density is labeled as the optimum moisture content (OMC).

The moisture-density relationships for the various selected materials were established and OMC values corresponding to the maximum dry unit weight were identified in accordance with NDOT test method Nev. T108B. For method A, a 4-inch diameter sample was compacted in 5 equal lifts with 25 blows in each lift. For method B, a 6-inch diameter mold was compacted in 5 equal lifts with 54 blows in each lift. Both compaction methods used a 10 lb rammer with an 18 inch drop. Top lift was compacted with an extension collar and sample was trimmed to the mold surface level. Two moisture content samples were taken; one near top and one near bottom of compacted sample.

Resilient Modulus

Resilient modulus, M_r, is an important parameter in the pavement design which represents the stress-dependent stiffness of the base, borrow, and subgrade materials under a certain pattern of repeated loading and confinement stress level using a triaxial set-up. AASHTO T307 is the most commonly used test for M_r of unbound materials (i.e., 22 out of 30 agencies/DOTs). Therefore, AASHTO T307 standard procedure was followed for determining the Mr of the sampled materials. The loading pattern for the M_r test consists of a repeated axial cyclic stress of fixed amplitude with a loading duration of 0.1 second followed by a rest period of 0.9 second. The AASHTO standard stipulates detailed testing procedures for unbound materials which include loading sequences, confining pressures, maximum axial stresses, cyclic stresses, constant stresses, and the number of loading applications. Overall, base materials are subjected to higher stresses during the testing than the subgrade soils despite the similarities in the testing sequences. The loading sequence for the base and borrow materials is presented in Table 9 and the loading sequence for the subgrade materials is summarized in Table 10.

Table 9. Testing Sequence for Base and Subbase Materials.

Sequence No.	Confining Pressure (psi)	Max. Axial Stress (psi)	Cyclic Stress (psi)	Contact Stress (psi)	No. of Load Application
0	6	4	3.6	0.4	500-1,000
1	6	2	1.8	0.2	100
2	6	4	3.6	0.4	100
3	6	6	5.4	0.6	100
4	6	8	7.2	0.8	100
5	6	10	9.0	1.0	100
6	4	2	1.8	0.2	100
7	4	4	3.6	0.4	100
8	4	6	5.4	0.6	100
9	4	8	7.2	0.8	100
10	4	10	9.0	1.0	100
11	2	2	1.8	0.2	100
12	2	4	3.6	0.4	100
13	2	6	5.4	0.6	100
14	2	8	7.2	0.8	100
15	2	10	9.0	1.0	100

Table 10. Testing Sequence for Subgrade Materials.

Sequence No.	Confining Pressure (psi)	Max. Axial Stress (psi)	Cyclic Stress (psi)	Contact Stress (psi)	No. of Load Application
0	15	15	13.5	1.5	500-1,000
1	3	3	2.7	0.3	100
2	3	6	5.4	0.6	100
3	3	9	8.1	0.9	100
4	5	5	4.5	0.5	100
5	5	10	9.0	1.0	100
6	5	15	13.5	1.5	100
7	10	10	9.0	1.0	100
8	10	20	18.0	2.0	100
9	10	30	27.0	3.0	100
10	15	10	9.0	1.0	100
11	15	15	13.5	1.5	100
12	15	30	27.0	3.0	100
13	20	15	13.5	1.5	100
14	20	20	18.0	2.0	100
15	20	40	36.0	4.0	100

Sample Preparation

According to AASTHO T307, the minimum diameter of the sample must be five times the maximum particle size. In this study, a 4-inch dimeter by 8-inch height mold was used and particles exceeding the limit were scalped. All samples were prepared at optimum moisture content and 90% of the maximum dry unit weight. The required amount of material was calculated based on the volume of the mold and dry density. OMC was added to the material and kept in the sealed plastic bag for 16-48 hours. A vibratory compactor was used for the compaction as shown in Figure 9. The specimens were compacted in six lifts of equal mass. After compaction, the sample was extruded and a membrane was installed immediately. Figure 10 shows the sample after extrusion and Figure 11 shows the membrane installed on the sample. Porous stones with filter papers were placed at top and bottom of the sample. Finally, the sample with membrane and porous stones was sealed very carefully using an ‘O’ ring (Figure 11).

Figure 9. Vibratory compactor and sample mold.

Figure 10. Extruded compacted sample.

Figure 11. Compacted sample with membrane, porous stones, and O-rings.

Sample Testing

The prepared sample was carefully installed inside the triaxial chamber. The drainage valves were connected to the top and bottom of the sample. A vacuum pressure was applied through the drainage valves to make sure there was no leakage. Figure 12 shows the sample inside the chamber after vacuum was applied. LVDT's were mounted in the outside of the chamber and connected to the load cell to measure the axial deformation of the sample as shown in Figure 13. The loading protocol for the base, borrow and subgrade materials was controlled by the software. Frequent manual checks were made to confirm that the machine was applying the correct cyclic stress, confinement, and contact stress.

Figure 12. Sample inside the triaxial chamber.

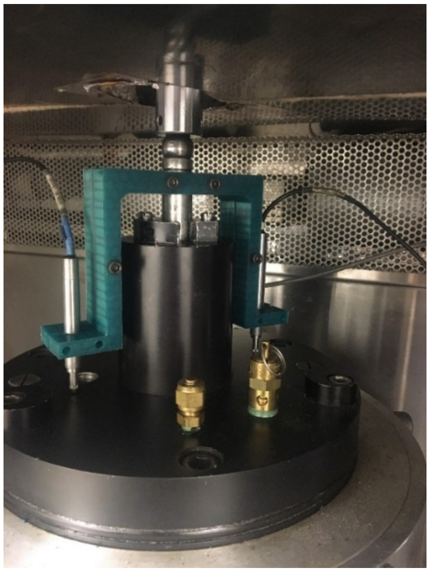

Figure 13. LVDT's connected on the outside of the triaxial chamber.

Resistance R-Value

The R-value testing is an empirical measure of unbound materials strength and expansion potential which has been used in designing flexible pavements in Nevada. The R-value of the collected base, borrow, and subgrade materials were determined in accordance with NDOT test method Nev. T115D. Sample was split in to the required size and based on the gradation, four 1200g samples were batched for the R-value test. The initial moisture content was measured and different amount of water was added to get different moisture content. Steel mold with the diameter of 4 inch and height of 5 inch was used to prepare the sample. The mechanical kneading compactor was used to compact the sample as shown Figure 14. For the compaction 100 tamps were applied to the specimen (using 200 psi foot pressure).

Figure 14. Kneading compactor.

The mold was placed on the exudation device as shown in Figure 15 after the compaction. A uniformly increasing load at a rate of 2,000 lb per minute was applied until exudation was achieved. The exudation pressure was calculated by taking the exudation load and dividing it by the area of the specimen. Then the sample was kept undisturbed for 16-20 hours with the addition of approximately 200 mL of water to calculate the expansion pressure as shown in Figure 16. After the specimen is tested for expansion, it was forced into stabilometer as shown in Figure 17. Horizontal pressure and displacement were obtained at vertical pressure of 160 psi.

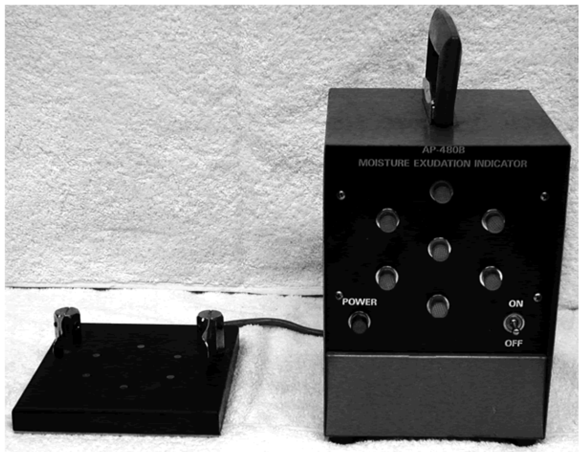

Figure 15. Exudation-indicator device.

Figure 16. Expansion pressure device.

Figure 17. R-value testing equipment.

The R-value was calculated from the Equation 14. The R-value is plotted against the exudation pressure. The final R-value was determined from the graph for the 300 psi exudation pressure.

$$R = 100 - \frac{100}{\left[\frac{2.5*(Pv-1)}{D*Ph}+1\right]} \qquad (14)$$

where

R = R-value
Pv = vertical pressure equal to 160 psi
D = turns displacement reading
Ph = Horizontal pressure (Stabilometer gauge reading for 160 psi vertical pressure)

ESTIMATION OF DESIGN RESILIENT MODULUS

This study focused on the development of representative resilient moduli of unbound materials for the pavement design of rehabilitation projects (i.e., asphalt concrete (AC) overlay), which are the most common type of projects in Nevada. The effort examined correlations between the M_r of unbound materials and corresponding R-value and other physical properties. A stepwise mechanistic analysis approach for determining a representative M_r value for existing base, borrow, and subgrade layers was applied. The ILLI-PAVE 2005 finite element (FE) pavement analysis program (11) was employed as an advanced structural model for computing stresses as well as deflection basins in typical flexible pavement structures under standard traffic loading.

The main unique features of ILLI-PAVE in comparison with other pavement analysis software are:

- Inclusion of constitutive models (a total of six different models are readily available) allowing for the characterization of the non-linear "stress-dependent" resilient behavior of granular materials and fine-grained soils under repetitive loading which is unavailable in Linear Elastic Programs (LEP).
- Implementation of Mohr-Coulomb failure criteria (c and ϕ) for unbound materials.
- Substantially lower computational effort because of the use of axi-symmetric FE formulation.
- Ability to handle a flexible pavement structure with up to ten different layers.

It should be noted that the ILLI-PAVE allows the use of the constitutive M_r equations developed from the AASHTO T307 tests.

Stepwise Procedure

The stepwise mechanistic approach using ILLI-PAVE implemented for the determination of M_r values for pavement rehabilitation designs is summarized as follows:

- *Step 1-Select Representative Pavement Structures.* The analysis is initiated by establishing representative NDOT's flexible pavement structures.
- *Step 2-Pavement Layer Properties*.
    - <u>Asphalt Concrete (AC)</u>: in order to incorporate the viscoelastic behavior of the AC mixture in the ILLI-PAVE model, the AC layer was divided into sublayers and the dynamic modulus master curve for the asphalt mixture commonly used in NDOT was utilized to properly assign an elastic modulus for each of the sublayers using the appropriate loading frequency and temperature.
    - <u>Crushed Aggregate Base (CAB), Borrow, and Subgrade (SG)</u>: The constitutive stress-dependent models developed from the AASHTO T307 M_r tests as well as the laboratory determined Mohr-Coulomb failure criteria (c and ϕ) were used in the ILLI-PAVE model.
- *Step 3-Pavement Responses*. When considering the non-linearity of the unbound materials, the M_r property varies at different locations within the respective layer. In other words, the state of stresses at each point in the layer results in a different M_r value caused by the stress-dependency of the unbound material. Hence, calculating the M_r from a determined state of stresses at a specific location within the layer under the center of load and assigning the M_r value to the entire layer might be questionable. In this study, surface deflection basins (i.e., vertical deflection at various radial distances from the applied load) were generated through the ILLI-PAVE model for the representative pavement structures under the allowable maximum tire load in Nevada on a circular plate. The generated surface deflection basins obtained are then employed in a backcalculation analysis to identify the M_r of each pavement layer including the base, borrow, and subgrade.

- *Step 4-Establish the Mr Correlation Equations*. Using the backcalculated moduli for various types of unbound materials and pavement structures, correlations between M_r and R-value were developed and examined for their effectiveness.

CHAPTER 3 FINDINGS AND APPLICATIONS

This chapter presents and summarizes the test results and findings from: (a) laboratory evaluation program, and (b) determination of representative resilient modulus for pavement rehabilitation design. The chapter also presents the newly developed prediction model for M_r to be used in the design of rehabilitated pavements in Nevada as a function of empirical and physical properties for the unbound materials.

LABORATORY EVALUATION

This section presents and discusses the results from the laboratory evaluation that was conducted on Nevada's unbound materials. Conformance with NDOT specifications is also discussed in this section.

Soil Classification Testing

Gradation and Atterberg Limits testing results are presented. Using these results, the material could be classified according to AASHTO and USCS soil classification systems.

Gradation

The gradation results for District 1 to District 3 base materials are shown in Table 11 and Table 12. The respective gradation curves for base materials are shown in Figure 18 to Figure 20. All the base materials collected are classified as Type 1 Class B base material, which is the most common base material used by NDOT. Each of the gradation tables contains a column listing the specification limits that the percent passing for that sieve must satisfy. The base materials collected for this study all meet the specification limits required for Type 1 Class B material in Nevada.

Table 11. District 1 Base Material Gradation.

Size (mm/inch)	Percent Passing						
	Specifi-cation	Contract No.					
		3546	3583	3597	3605	3613	3607
25.0 mm (1”)	80-100	100	100	100	100	100	99.3
19.0 mm (3/4”)	–	96.8	98.1	97.7	90.2	88.9	92.7
12.5 mm (1/2”)	–	76.4	86.7	83.9	66.3	67.8	68.7
9.5 mm (3/8”)	–	62.3	76.3	69.4	54.1	57.6	56.1
4.75 mm (No. 4)	30-65	40.8	45.6	43.4	35.3	38.6	45.4
2.36 mm (No. 8)	–	27.5	31.2	27.2	25.1	27.9	32.1
2.00 mm (No. 10)	–	25.2	29.1	24.7	23.3	26.1	28.9
1.18 mm (No. 16)	15-40	19.5	24.4	18.8	19.0	21.6	22.8
0.6 mm (No. 30)	–	14.9	20.4	14.1	15.0	18.3	17.8
0.425 mm (No. 40)	–	13.3	19.3	12.6	13.5	17.2	16.0
0.3 mm (No. 50)	–	12.0	17.0	11.4	12.1	15.8	14.5
0.15 mm (No. 100)	–	10.3	12.4	9.7	9.9	10.4	12.4
0.075 mm (No. 200)	2-12	8.8	8.7	8.3	7.7	5.3	10.0

–No specification.

Table 12. District 2 and District 3 Base Material Gradation.

Size (mm/inch)	Percent Passing			
	Specification	District 2 Lockwood	District 3 Elko	District 3 Hunnewill
25.0 mm (1”)	80-100	100	100	100
19.0 mm (3/4”)	–	96.7	99.7	98.1
12.5 mm (1/2”)	–	79.2	92.5	91.7
9.5 mm (3/8”)	–	68.5	83.1	81.0
4.75 mm (No. 4)	30-65	46.6	59.0	57.7
2.36 mm (No. 8)	–	33.6	43.3	43.7
2.00 mm (No. 10)	–	31.3	39.8	40.2
1.18 mm (No. 16)	15-40	25.2	31.6	31.6
0.6 mm (No. 30)	–	19.6	22.0	23.0
0.425 mm (No. 40)	–	16.6	17.7	19.4
0.3 mm (No. 50)	–	13.7	13.8	16.6
0.15 mm (No. 100)	–	10	9.7	12.9
0.075 mm (No. 200)	2-12	7.8	7.5	9.7

–No specification.

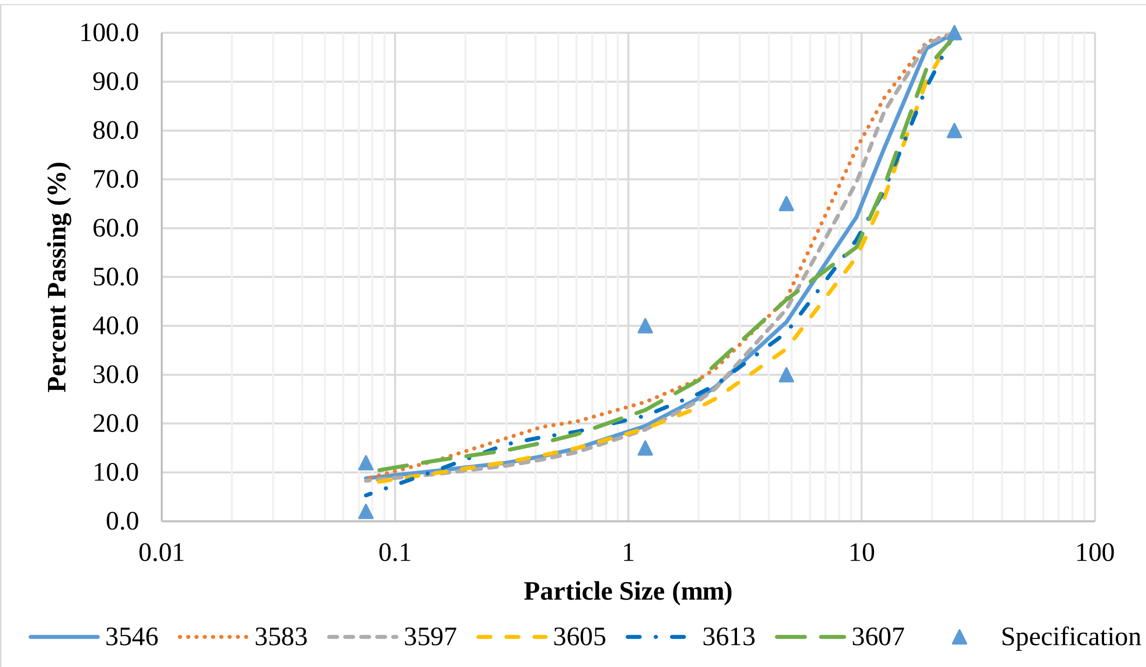

Figure 18. District 1 base material gradations.

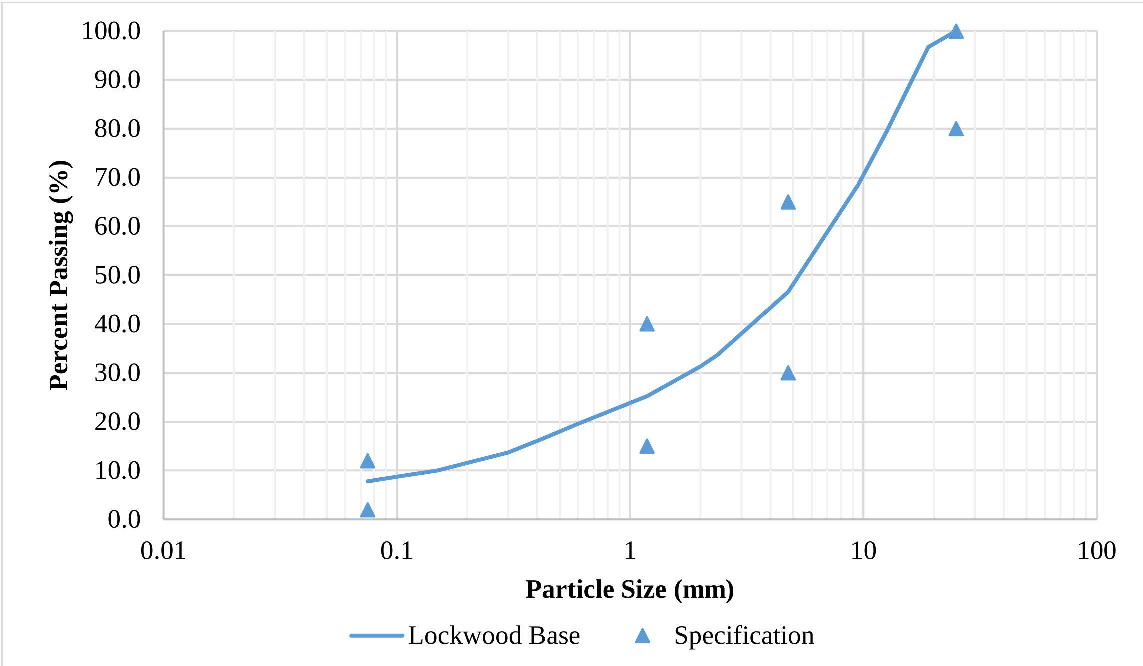

Figure 19. District 2 base material gradation.

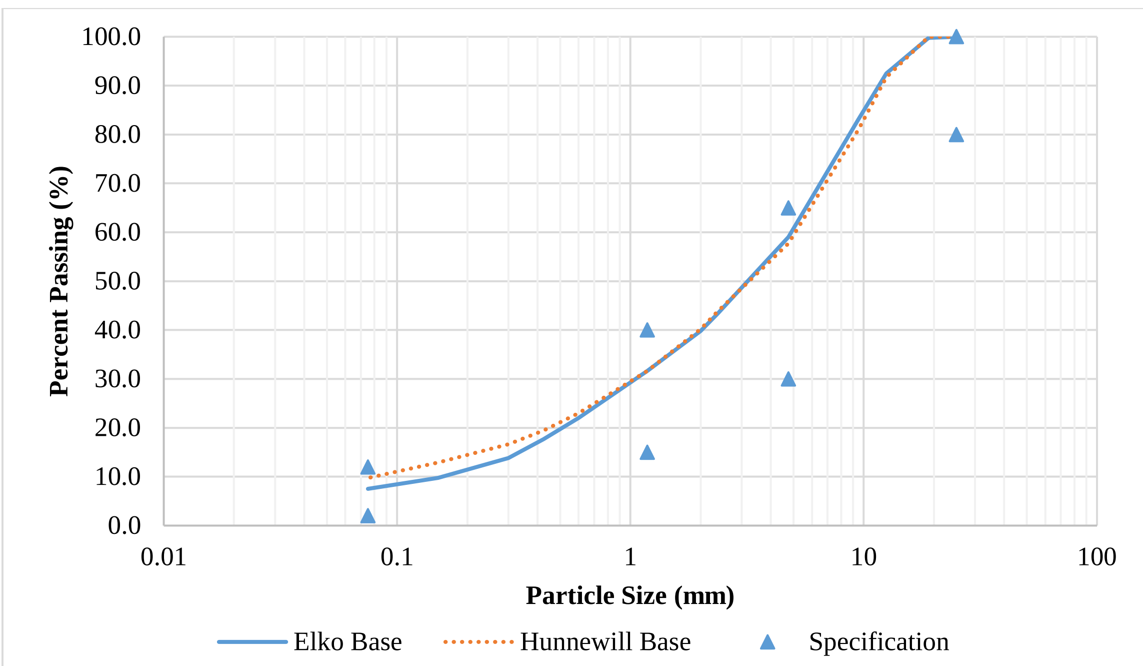

Figure 20 District 3 base material gradations.

The gradation results for Districts 1, 2, and 3 borrow materials are shown in Table 13 and Table 14. The gradation curves are shown in Figure 21 to Figure 23. According to NDOT specifications, the only criteria that borrow material gradations must meet is that 100% of the material must pass the 3-inch sieve. All the sampled borrow materials for this project satisfy this criterion. However, the gradations were highly variable, as evident in each of the gradation curve plots.

Table 13. District 1 Borrow Material Gradation.

Size (mm/inch)	Percent Passing					
	Specification	Contract No.				
		3546	3583	3597	3613	3607
75 mm (3")	100	100	100	100	100	100
50 mm (2")	–	100	100	100	100	100
37.5 mm (1.5")	–	100	100	100	97.4	100
25.0 mm (1")	–	100	99.1	97.7	89.9	98.0
19.0 mm (3/4")	–	100	95.5	96.0	85.3	94.5
12.5 mm (1/2")	–	100	92.9	90.2	76.8	89.9
9.5 mm (3/8")	–	99.9	91.1	85.6	69.8	86.2
4.75 mm (No. 4)	–	79.9	88.1	71.7	53.3	75.9
2.36 mm (No. 8)	–	48.6	86.7	56.7	40.8	65.3
2.00 mm (No. 10)	–	43.0	86.4	53.3	38.1	62.6
1.18 mm (No. 16)	–	28.6	85.6	42.1	32.4	54.0
0.6 mm (No. 30)	–	18.4	84.6	32.4	27.9	43.0
0.425 mm (No. 40)	–	15.4	84.2	28.7	26.3	37.6
0.3 mm (No. 50)	–	13.3	83.5	25.7	24.0	32.0
0.15 mm (No. 100)	–	11.4	80.6	20.9	14.3	23.7
0.075 mm (No. 200)	–	10.5	66.9	16.4	7.3	16.4

–No specification.

Table 14. District 2 and District 3 Borrow Material Gradation.

Size (mm/inch)	% Passing				
	Specification	District 2	District 2	District 2	District 3
		Lockwood Borrow	SNC Primary	SNC Secondary	Elko Borrow
75 mm (3")	100	100	100	100	100
50 mm (2")	–	100	100	100	100
37.5 mm (1.5")	–	100	100	100	100
25.0 mm (1")	–	100	100	100	87.3
19.0 mm (3/4")	–	98.8	100	100	82.0
12.5 mm (1/2")	–	91.5	97.5	100	74.6
9.5 mm (3/8")	–	82.9	91.7	100	68.9
4.75 mm (No. 4)	–	62.7	70.1	98.7	53.4
2.36 mm (No. 8)	–	48.1	54.1	69.9	40.9
2.00 mm (No. 10)	–	45.1	50.7	61.5	37.4
1.18 mm (No. 16)	–	37.5	41.8	40.7	29.3
0.6 mm (No. 30)	–	31.5	33.3	25.2	18.8
0.425 mm (No. 40)	–	29.1	30.1	20.6	13.8
0.3 mm (No. 50)	–	26.8	27.5	17.9	10.0
0.15 mm (No. 100)	–	22.6	23.6	14.6	6.5
0.075 mm (No. 200)	–	17.9	18.5	12.3	4.9

–No specification.

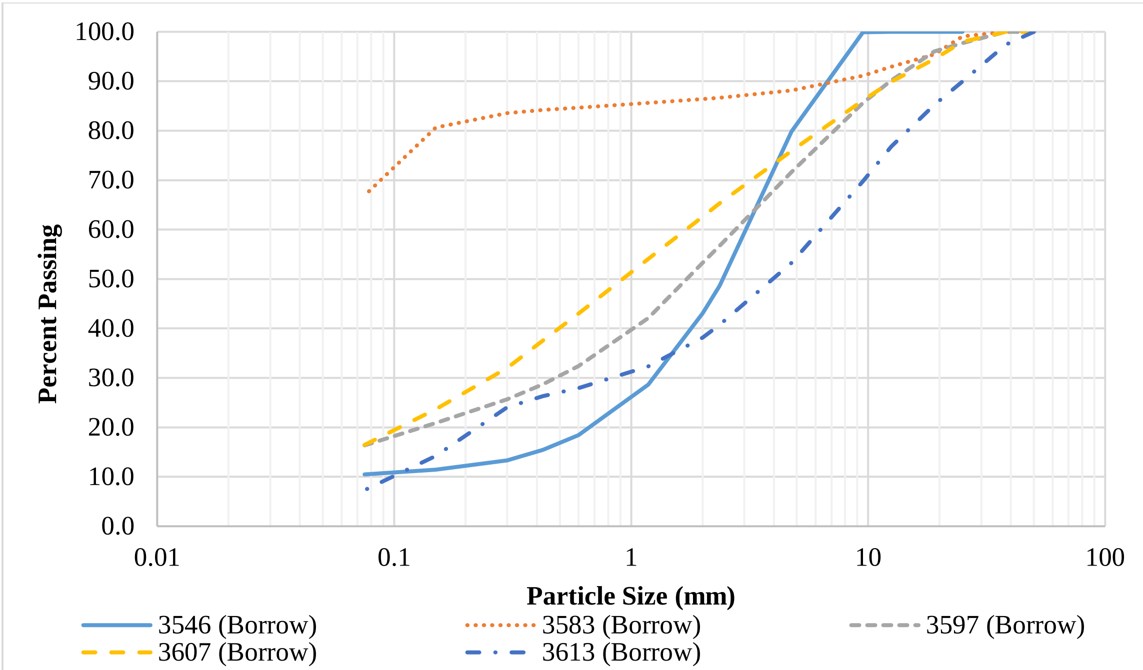

Figure 21. District 1 borrow material gradations.

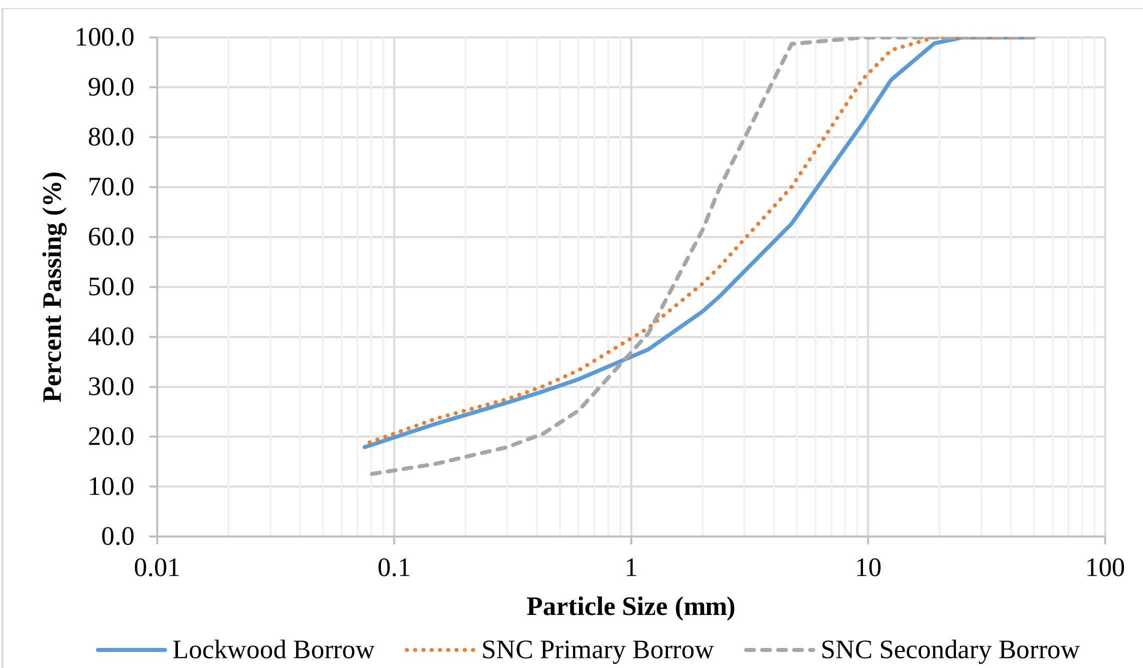

Figure 22. District 2 borrow material gradation.

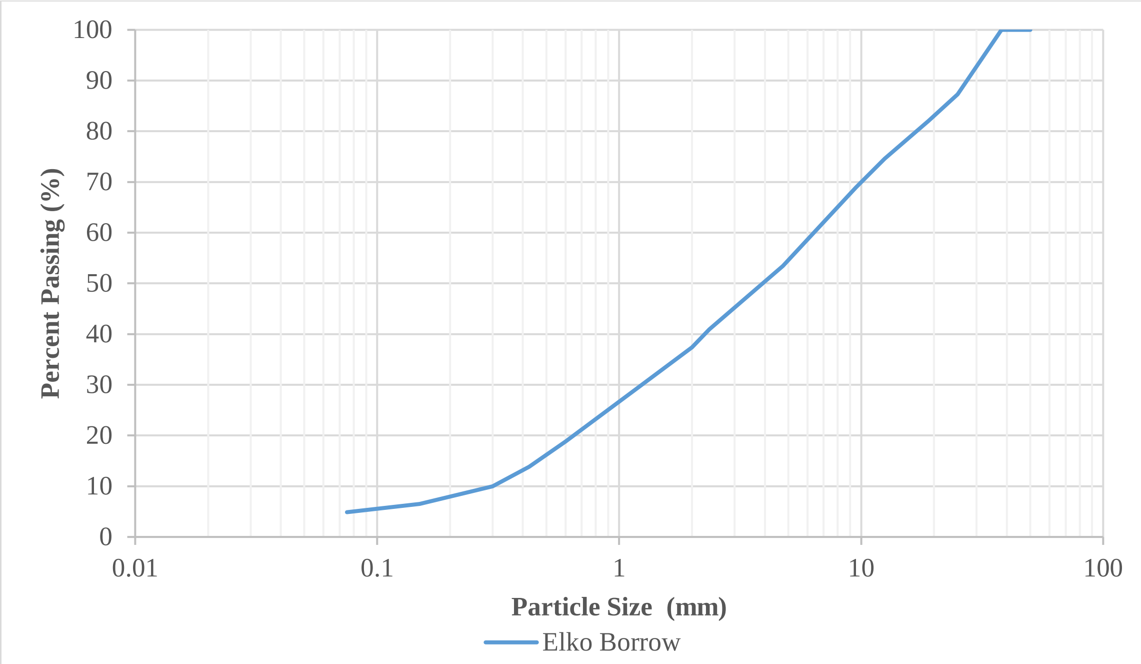

Figure 23. District 3 borrow material gradation.

The results for gradation of the subgrade materials are shown in Table 15 and Table 16. The curves are shown in Figure 24 and Figure 25. Subgrade material is the native material found at the project location.

Table 15. District 1 Subgrade Gradation.

Size (mm/inch)	Percent Passing					
	I-15/ Goodspring	US-95/ Search-light	NV-375/ Rachel	US-95/ Bonnie Claire	US-93/ Crystal Spring MP62	US-93/ Crystal Spring MP67
50.0 mm (2")	97.5	100	100	100	100	100
25.0 mm (1")	83.5	96.7	87.5	98.8	100	100
9.5 mm (3/8")	57.2	92.7	52.2	95.4	99.3	97.2
4.75 mm (No. 4)	43.4	87.8	33.5	92	95.6	89.3
2.00 mm (No. 10)	34.4	68.7	23.2	84.3	81.4	77.2
0.425 mm (No. 40)	28	43.9	15.2	37.6	44.5	52.6
0.3 mm (No. 50)	26.6	39.3	13.4	25.2	37.1	46.7
0.15 mm (No. 100)	22.6	31.5	9.6	11.7	25.5	35.7
0.075 mm (No. 200)	14.6	23.9	5.4	5.5	18.1	26

Table 16. District 2 Subgrade Gradation.

Size (mm/inch)	Percent Passing	
	Jacks Valley	UNR Soil at SEM
37.5 mm (1.5")	100	100
25.0 mm (1")	100	93.4
19.0 mm (3/4")	100	87.7
12.5 mm (1/2")	100	78.7
9.5 mm (3/8")	100	74.8
4.75 mm (No. 4)	99.7	66.4
2.36 mm (No. 8)	97.8	59.6
2.00 mm (No. 10)	96.8	57.4
1.18 mm (No. 16)	93	49.6
0.6 mm (No. 30)	81.8	36.9
0.425 mm (No. 40)	72.3	31.4
0.3 mm (No. 50)	61	27.2
0.15 mm (No. 100)	42.3	21.4
0.075 mm (No. 200)	26.1	16.2

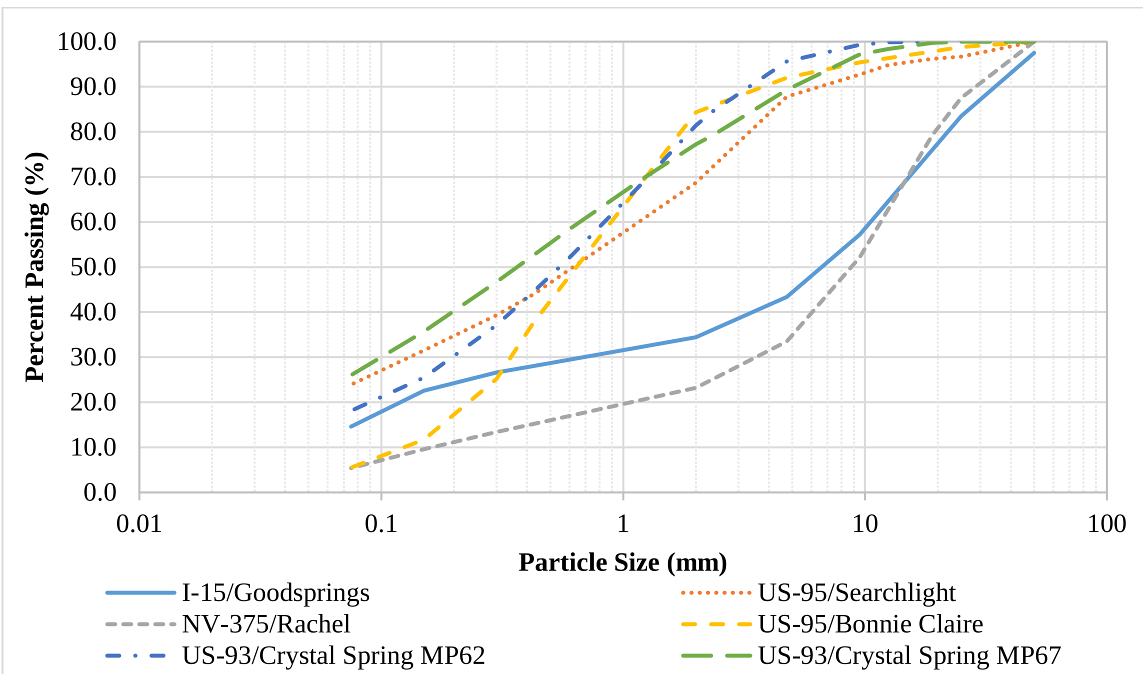

Figure 24. District 1 subgrade gradations.

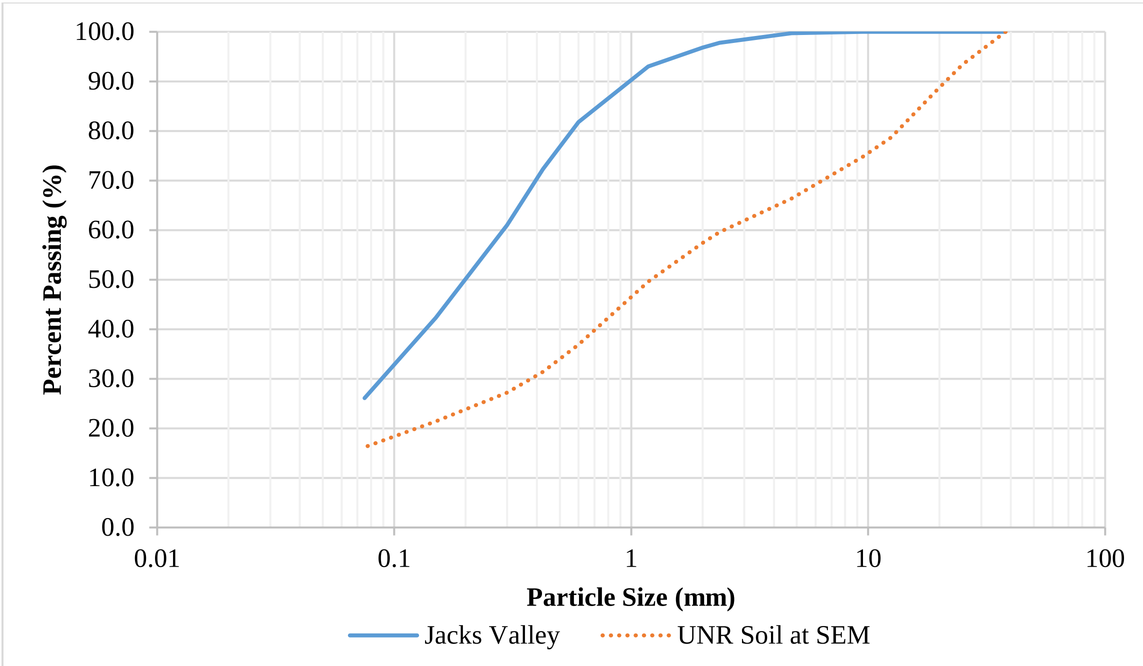

Figure 25. District 2 subgrade material gradations.

Atterberg Limits

All of the base materials from all three districts resulted as being non-plastic. The results of the Atterberg Limits testing for all borrow and subgrade materials are shown in Table 17 and Table 18, respectively. In some cases, non-plastic materials had issues being tested for resilient modulus, as there were not enough fine contents to hold the samples together for testing. This will be discussed further in the respective section.

Based on the data presented in Table 17 and Table 18, the following observations can be made:

- In the case of borrow materials, three of the evaluated materials were non-plastic (PI = 0), four of the materials were slightly plastic (PI < 7), and two of the materials were medium plastic (7 ≤ PI ≤ 17).
- In the case of subgrade, all evaluated materials were either non-plastic (PI = 0) or slightly plastic (PI < 7).

Table 17. Borrow Material Atterberg Limits.

Source	Liquid Limit, LL	Plastic Limit, PL	Plasticity Index, PI
3546	16.5	14.5	2.0
3583	23.5	18.8	4.7
3597	22.2	18.9	3.3
3607	23.2	23.1	0.1
3613	N/A[1]	NP[2]	0.0
Lockwood Borrow	45.9	31.9	14.0
SNC Primary	39.1	24	15.1
SNC Secondary	N/A[1]	NP[2]	0.0
Elko Borrow	N/A[1]	NP[2]	0.0

[1]Not Applicable.
[2]Non-plastic.

Table 18. Subgrade Material Atterberg Limits.

Material	Liquid Limit, LL	Plastic Limit, PL	Plasticity Index, PI
I-15/Goodsprings	18.4	16.9	1.5
US-95/Searchlight	N/A[1]	NP[2]	0.0
NV-375/Rachel	30.9	26.6	4.3
US-95/Bonnie Claire	21.1	20.1	1.0
US-93/Crystal Spring MP62	19.6	17.7	1.9
US-93/Crystal Spring MP67	22.2	17.8	4.5
Jacks Valley	22.9	20.5	2.4
UNR Soil at SEM	24.0	20.4	3.6

[1]Not Applicable.
[2]Non-plastic.

Soil Classification

After conducting sieve analysis and Atterberg Limits testing, the soil classification for each of the subgrade materials was determined. The most used classification systems are: AASHTO soil classification, and Unified Soil Classification System (USCS). The AASHTO soil classification system is used mostly by highway agencies and is based on particle size distribution and soil plasticity. On the other hand, USCS is widely used by geotechnical engineers and is based on particle size distribution, liquid limit, soil plasticity, and organic matter concentrations.

Table 19 summarizes the AASHTO soil classification and USCS of all evaluated subgrade materials. The evaluated materials were mostly silt and clay-type materials with a general rating according to AASHTO M145 of excellent to good.

Table 19. Subgrade Material Soil Classifications.

Material	AASHTO Soil Classification (AASHTO M145)	USCS (ASTM D 2487)	
		Group Symbol	Group Name
I-15/Goodsprings	A-1-a	GM	Silty gravel
US-95/Searchlight	A-1-b	SM	Silty sand
NV-375/Rachel	A-1-a	GP-GM	Poorly graded gravel with silt
US-95/Bonnie Claire	A-1-b	SW-SM	Well-graded sand with silt
US-93/Crystal Spring MP62	A-1-b	SM	Silty sand
US-93/Crystal Spring MP67	A-2-4	SC	Clayey sand
Jacks Valley	A-2-4	SM-SC	Silty, clayey sand
UNR Soil at SEM	A-1-b	SM-SC	Silty, clayey sand

Moisture-Density Relationship

The results of the base, borrow, and subgrade material moisture density testing are shown in Table 20 to Table 22, respectively. If Method A was used, and if there was more than 5% material retained on the No. 4 sieve (from gradation), then a correction needed to be applied to the maximum dry density and the optimum water content. If Method D was used, and there was more than 5% material retained on the ¾ inch sieve, then a correction needed to be applied to the maximum dry unit weight and the optimum water content.

The base material exhibited the highest maximum dry density values, with an average of 143.5 pcf. It also had the lowest optimum moisture content values, with an average of 5.3%. In comparison, the borrow material had an overall average maximum dry density of 134.9 pcf and an average optimum moisture content of 7.4%. The subgrade material had an average maximum dry density lower than that of borrow material and equal to 129.9 pcf. It also had an average optimum moisture content higher than that of borrow material and equal to 8.2%. Figure 26 is a graphical representation of this information, showing the optimum moisture content and the maximum dry density for the three material types.

Table 20. Base Material Moisture Density Results.

Sample	Max Dry Density (pcf)	OMC (%)	Corrected Max Dry Density (pcf)	Corrected OMC (%)
3546	144.7	5.0	–	–
3583	147.3	5.6	–	–
3597	143.0	3.9	–	–
3605	147.5	5.0	149.7	4.7
3607	135.8	6.7	137.8	6.4
3613	141.6	3.5	144.4	3.3
Lockwood Base	138.2	8.0	–	–
Elko Base	129.7	8.4	141.1	5.8
Hunnewill base	132.8	7.2	145.5	5.0

–No correction.

Table 21. Borrow Material Moisture Density Results.

Sample	Max Dry Density (pcf)	OMC (%)	Corrected Max Dry Density (pcf)	Corrected OMC (%)
3546	136.9	7.2	144.8	5.7
3583	119.4	10.7	123.3	9.7
3597	133.8	6.2	142.9	5.0
3607	125.6	11.3	132.9	9.1
3613	143.2	5.4	–	–
Lockwood Borrow	125.4	9.3	137.0	6.6
SNC Primary	124.4	10.6	133.8	8.0
SNC Secondary	136.1	9.6	–	–
Elko Borrow	124.9	9.5	139.7	6.0

–No correction.

Table 22. Subgrade Material Moisture Density Results.

Sample	Max Dry Density (pcf)	OMC (%)
I-15/Goodsprings	134.9	6.3
US-95/Searchlight	133.3	6.6
NV-375/Rachel	139.2	6.1
US-95/Bonnie Claire	126.9	9.4
US-93/Crystal Spring MP62	122.4	9.8
US-93/Crystal Spring MP67	123.8	9.3
Jacks Valley	125.5	9.4
UNR Soil at SEM	132.8	8.5

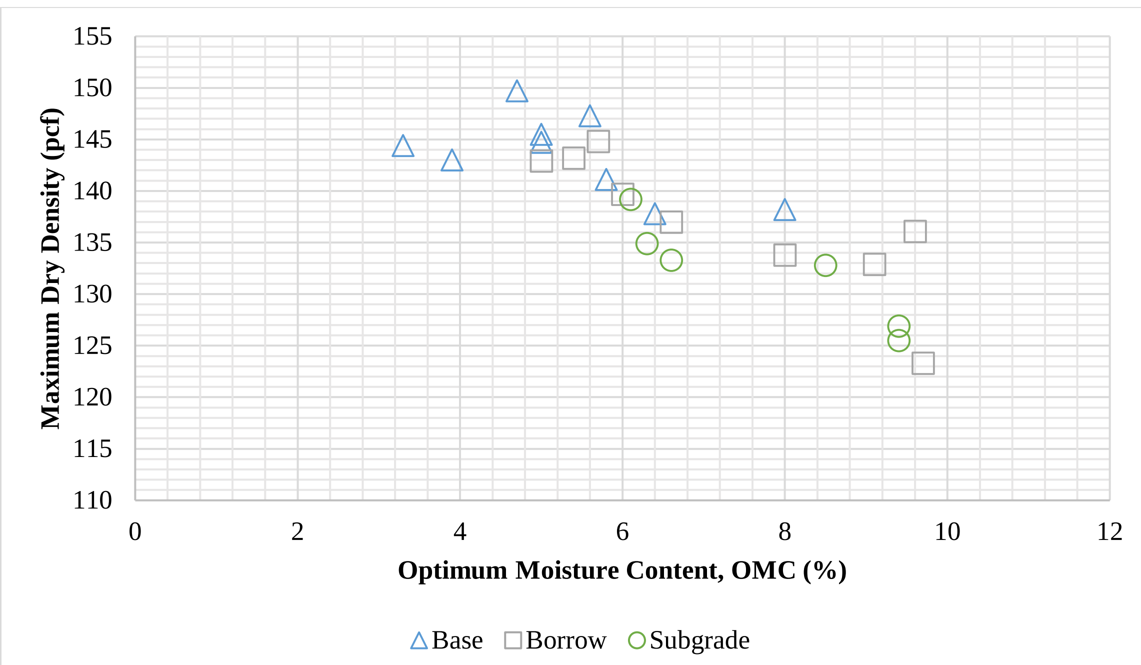

Figure 26. Moisture density summary of base, borrow and subgrade materials.

Resilient Modulus

The results from the triaxial testing of the base, borrow, and subgrade materials were used to develop the non-linear models that relate the M_r to the stress conditions. For the base and borrow materials, the Theta model (Equation 15) was used to represent the stress-hardening behavior. For the subgrade material the Uzan and the Universal model (Equation 16 and Equation 17) were used. The constitutive model equations are given below.

Theta Model:

$$M_R = K\theta^n \quad (15)$$

where

K, and n = regression coefficients
θ = bulk stress (psi)

Uzan Model:

$$M_R = K\theta^n\sigma_d^m \quad (16)$$

where

K, and m = regression coefficients
σ_d = deviator stress (psi)

Universal Model

$$M_r = k_1 P_a \left(\frac{\theta}{P_a}\right)^{k_2} \left(\frac{\tau_{oct}}{P_a} + 1\right)^{k_3} \quad (17)$$

where

k_1, k_2, k_3 = regression coefficients
P_a = atmospheric pressure (psi)
τ_{oct} = octahedral shear stress (psi)

Resilient modulus value was obtained from the average value of the last five cycles for each sequence. The method of least squares in Microsoft Excel was used to develop the regression coefficients in the constitutive models. Table 23 presents typical data from the testing of a base sample and the necessary input parameters for the regression analysis. The Theta model showed good correlation for base and borrow materials as exemplified in Figure 27 and Figure 28. Both the Universal and Uzan models showed good correlations for the subgrade materials as shown in Figure 29 and Figure 30, respectively.

Table 23. Example of M_r Test Results for Base Material from Contract 3546.

Sequence	Cyclic Axial Stress (psi)	Contact Stress (psi)	Confinement Stress (psi)	Axial Resilient Modulus (psi)	Deviator Stress, σ_d (psi)	Major Principal Stress, σ_1 (psi)	Minor Principal Stress, σ_3 (psi)	Bulk Stress, θ (psi)	Octahedral Shear Stress (psi)
1	13.5	1.5	14.8	46,385	15.0	29.8	14.8	59.5	7.1
2	2.7	0.3	2.8	22,854	3.0	5.8	2.8	11.4	1.4
3	5.3	0.6	2.8	23,661	5.9	8.8	2.8	14.4	2.8
4	8.1	0.9	2.8	25,371	9.0	11.8	2.8	17.5	4.2
5	4.5	0.5	4.8	25,231	5.0	9.9	4.8	19.5	2.4
6	9.0	1.0	4.8	28,698	10.0	14.8	4.8	24.4	4.7
7	13.5	1.5	4.8	30,357	15.0	19.9	4.8	29.5	7.1
8	9.0	1.0	9.8	35,372	10.0	19.8	9.8	39.4	4.7
9	18.0	2.0	9.8	41,542	20.0	29.8	9.8	49.5	9.4
10	26.8	3.0	9.8	43,812	29.8	39.7	9.8	59.3	14.1
11	9.0	1.0	14.8	39,750	10.0	24.8	14.8	54.5	4.7
12	13.5	1.5	14.8	43,625	15.0	29.8	14.8	59.4	7.1
13	26.8	3.0	14.8	49,674	29.8	44.6	14.8	74.3	14.0
14	13.7	1.5	19.8	49,374	15.2	35.0	19.8	74.6	7.1
15	18.1	2.0	19.8	53,101	20.1	39.9	19.8	79.6	9.5
16	34.6	4.0	19.8	59,304	38.6	58.4	19.8	98.0	18.2

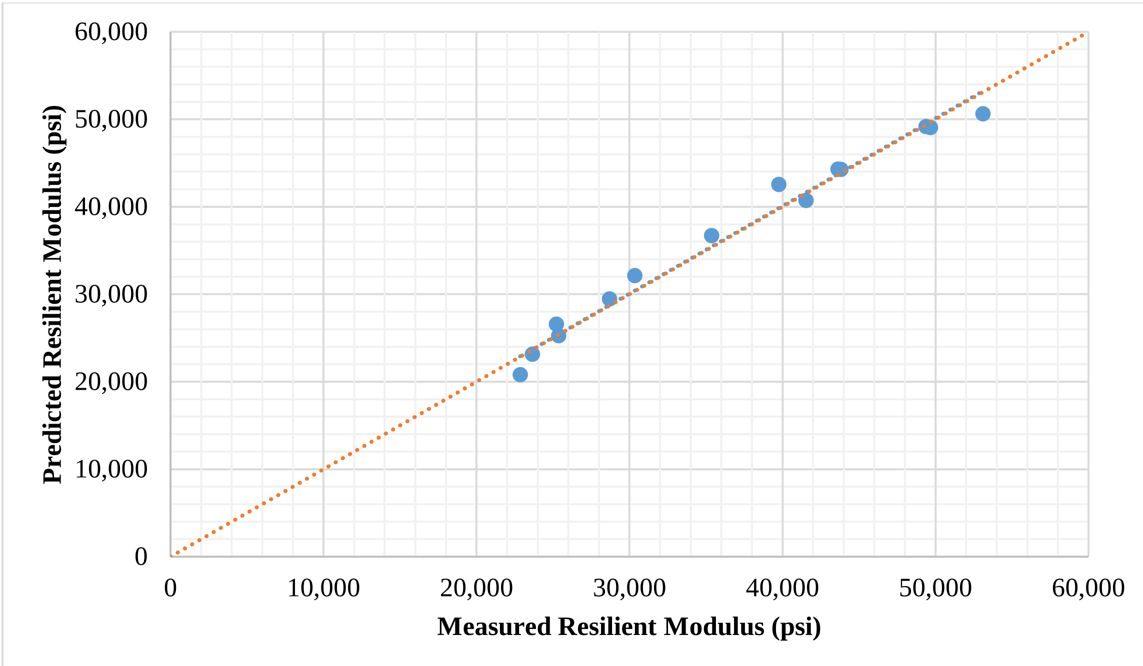

Figure 27. Example for measured versus predicted M_r using theta model: contract 3546 base material.

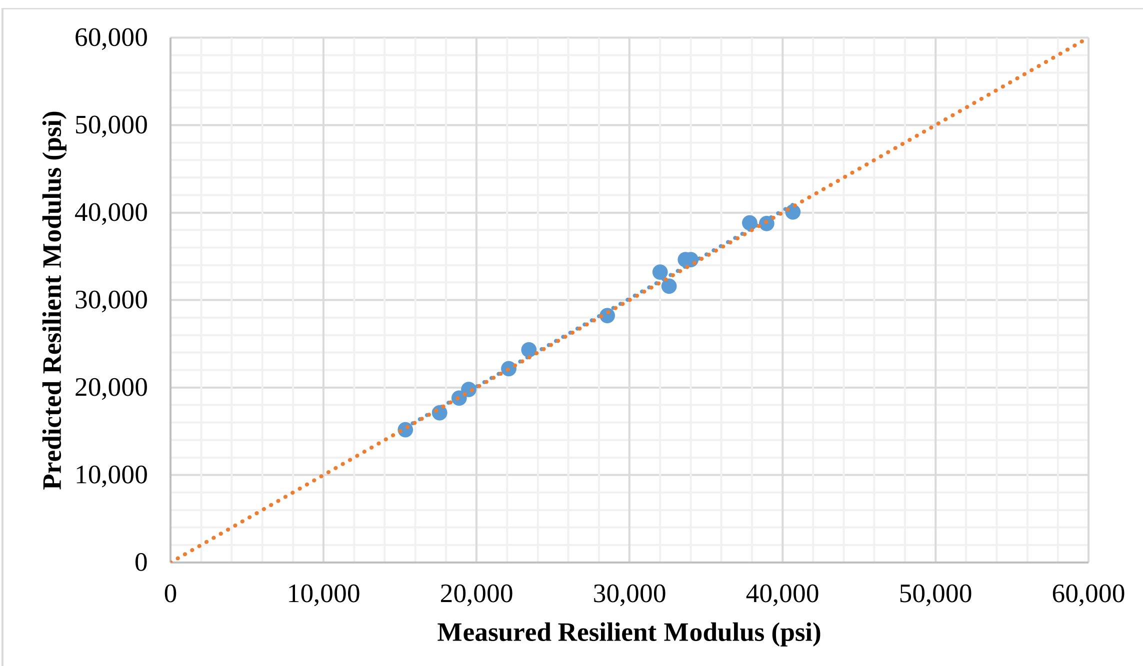

Figure 28. Example for measured versus predicted M_r using theta model: contract 3546 borrow material.

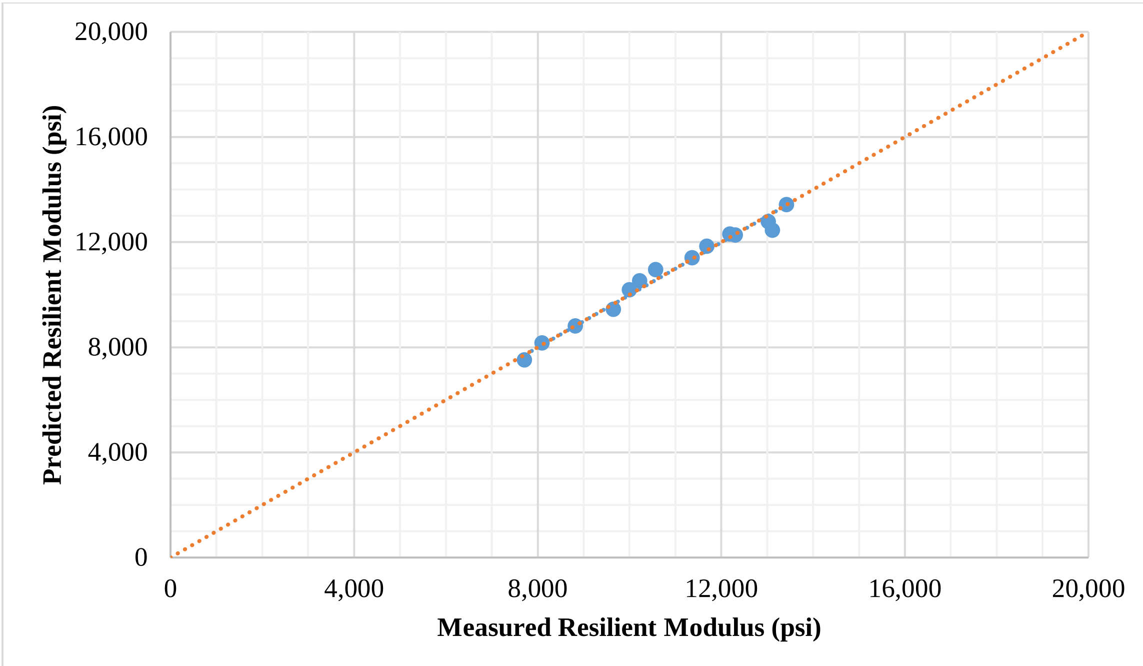

Figure 29. Example for measured versus predicted M_r using Uzan model: US-93/Crystal Spring MP62 subgrade material.

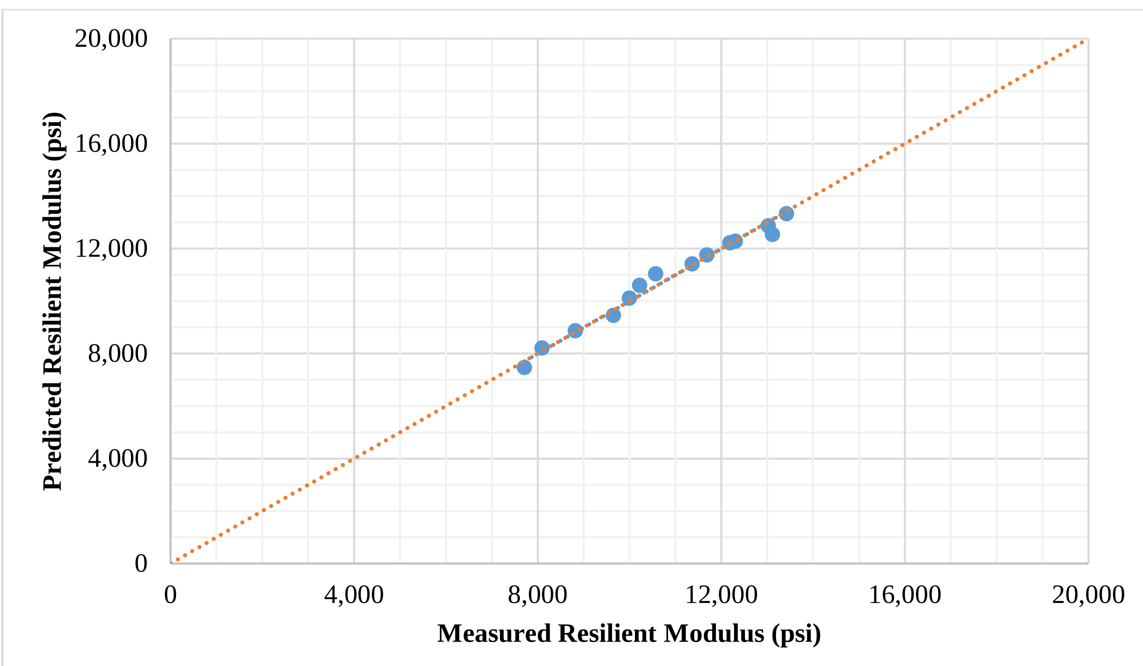

Figure 30. Example for measured versus predicted M_r using Universal model: US-93/Crystal Spring MP62 subgrade material.

The regression parameters of the various constitutive models for District 1 base, borrow and subgrade materials are summarized in Table 24 to Table 26, respectively. The variation in M_r with different state of stresses for the District 1 base, borrow and subgrade materials are presented in Figure 31 to Figure 33, respectively.

Table 24. Regression Coefficients for M_r Model of District 1 Base Materials.

Model	Regression Coefficients	Contract Number					
		3546	3583	3605	3607	3613	3597
Theta	*K*	6808	5806	3818	3497	5257	5806
	n	0.4585	0.4423	0.5492	0.5770	0.4722	0.4782

Table 25. Regression Coefficients for M_r Model of District 1 Borrow Materials.

Model	Regression Coefficients	Contract Number		
		3546	3613	3597
Theta	*K*	4514	4610	5534
	n	0.4990	0.4980	0.4379

Table 26. Regression Coefficients for M_r Model of District 1 Subgrade Materials.

Soil Source	Universal Model			Uzan Model		
	k_1	k_2	k_3	k	n	m
I-15/Goodsprings	1126	0.4538	-0.2688	4938	0.4547	-0.0356
US-95/Searchlight	971	0.4322	-0.5369	4797	0.4147	-0.0695
NV-375/Rachel	1041	0.5011	-0.2569	4030	0.5023	-0.0364
US-95/Bonnie Claire	748	0.3842	-0.2786	3949	0.3863	-0.0382
US-93/Crystal Spring MP62	742	0.5087	-0.4097	2837	0.5087	-0.055
US-93/Crystal Spring MP67	989	0.4009	-0.7937	5136	0.397	-0.1085
3583 Borrow	811	0.4418	-0.8092	4377	0.5278	-0.3195

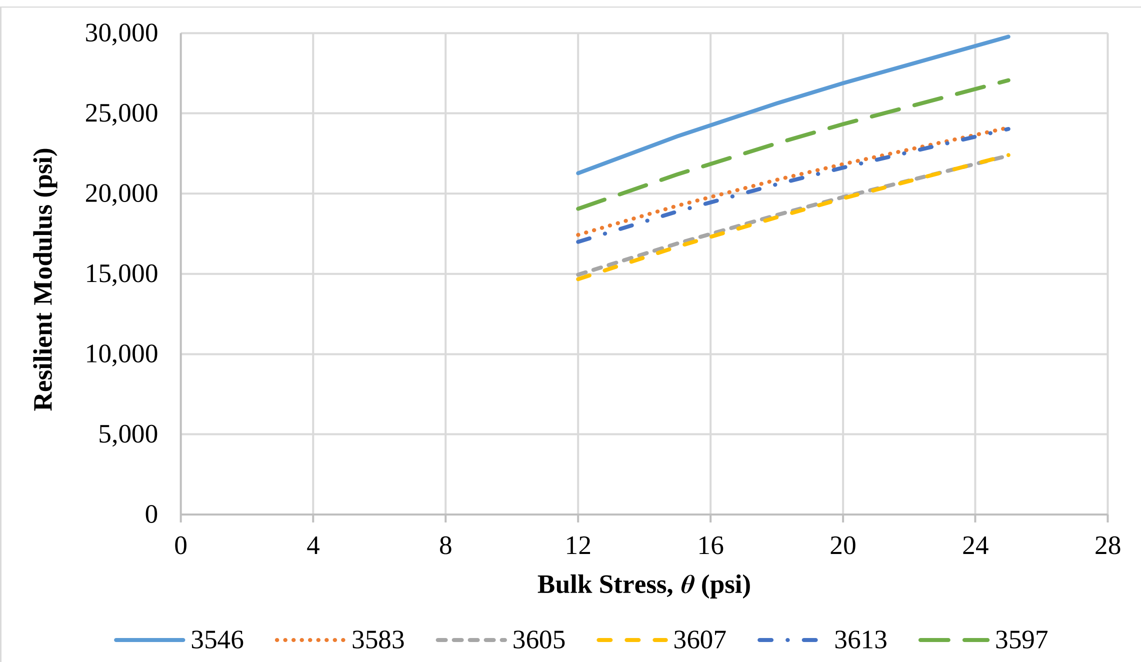

Figure 31. Variation of District 1 base materials M_r with bulk stress.

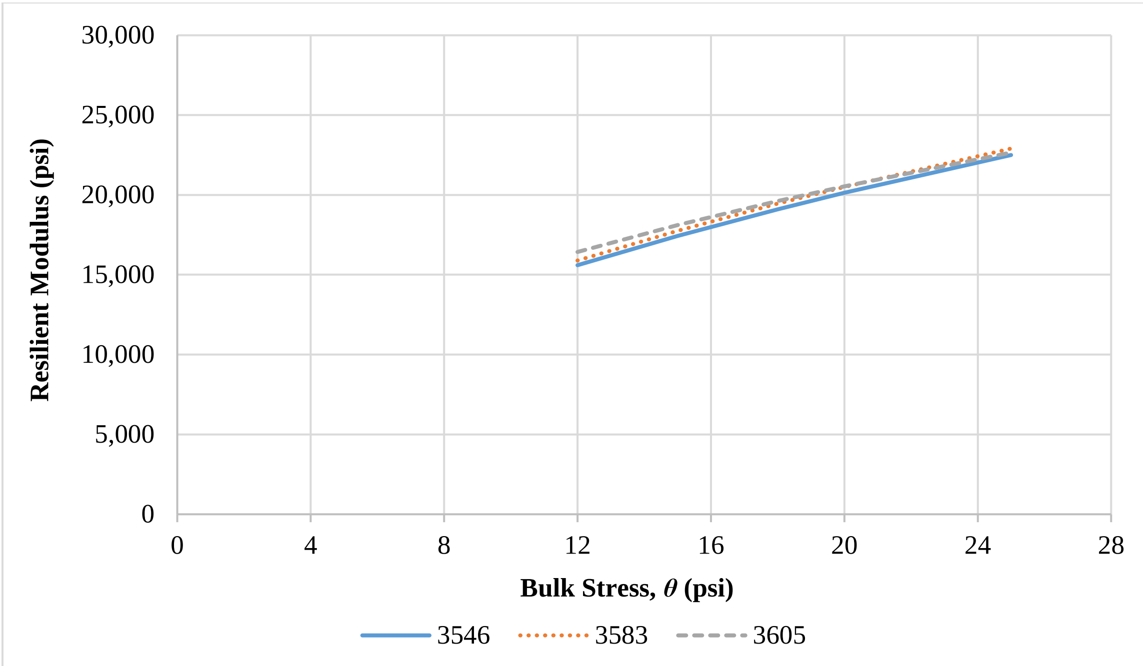

Figure 32. Variation of District 1 borrow materials M_r with bulk stress.

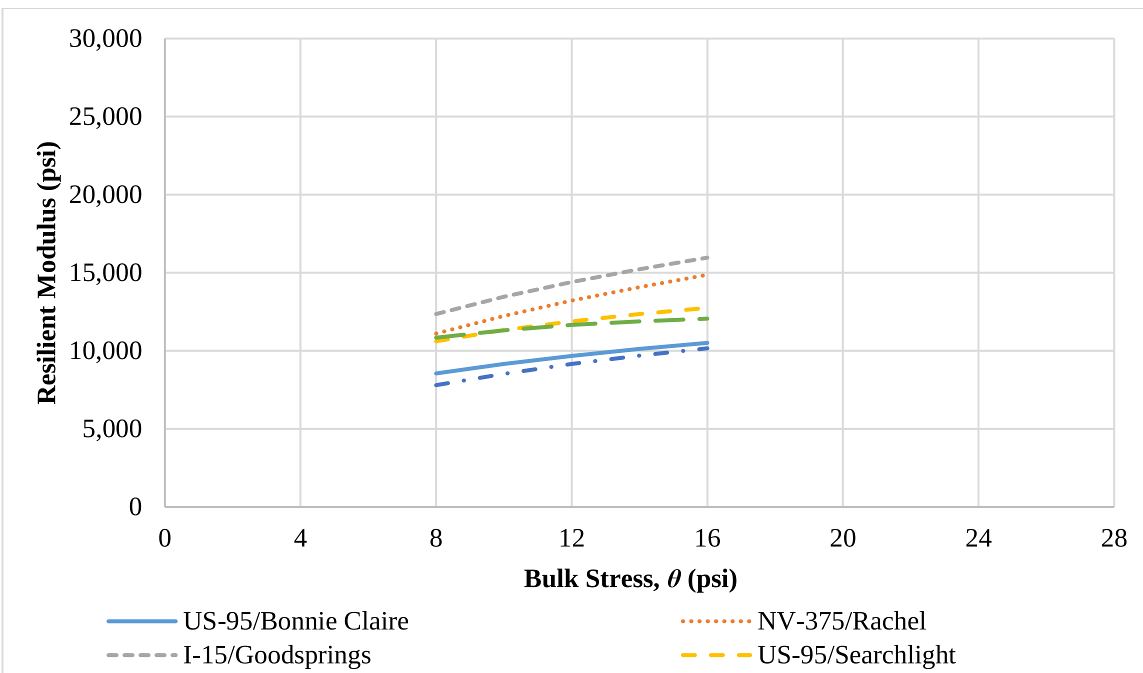

Figure 33. Variation of District 1 subgrade materials M_r with bulk stress.

The constitutive model regression parameters for the Districts 2 and 3 base, borrow, and subgrade materials are summarized in Table 27 to Table 29, respectively. The variation in M_r with different state of stresses are presented in Figure 34 to Figure 36. Nine unbound materials were sampled from District 2 and District 3; however, only six could be tested. The Lockwood Base, Elko Borrow, and SNC Secondary Borrow materials could not be tested for M_r, as these materials did not contain enough fines to hold the samples together for testing. Thus, the results presented below represent M_r testing for six materials total between District 2 and District 3.

Table 27. Regression Coefficients for M_r Model of Districts 2 and 3 Base Materials.

Model	Regression Coefficients	Base Source	
		Elko	Hunnewill
Theta	*K*	2659	2321
	n	0.5273	0.5371

Table 28. Regression Coefficients for M_r Model of Districts 2 and 3 Borrow Materials.

Model	Regression Coefficients	Borrow Source	
		Lockwood	SNC Primary
Theta	*K*	2956	3497
	n	0.4827	0.5770

Table 29. Regression Coefficients for M_r Model of District 2 Subgrade Materials.

Soil Source	Universal Model			Uzan Model		
	k_1	k_2	k_3	*k*	*n*	*m*
Jacks Valley Subgrade	702	0.2398	-1.015	5706	0.2404	-0.139
SEM Soil	806	0.5422	-0.9640	2865	0.5397	-0.1280

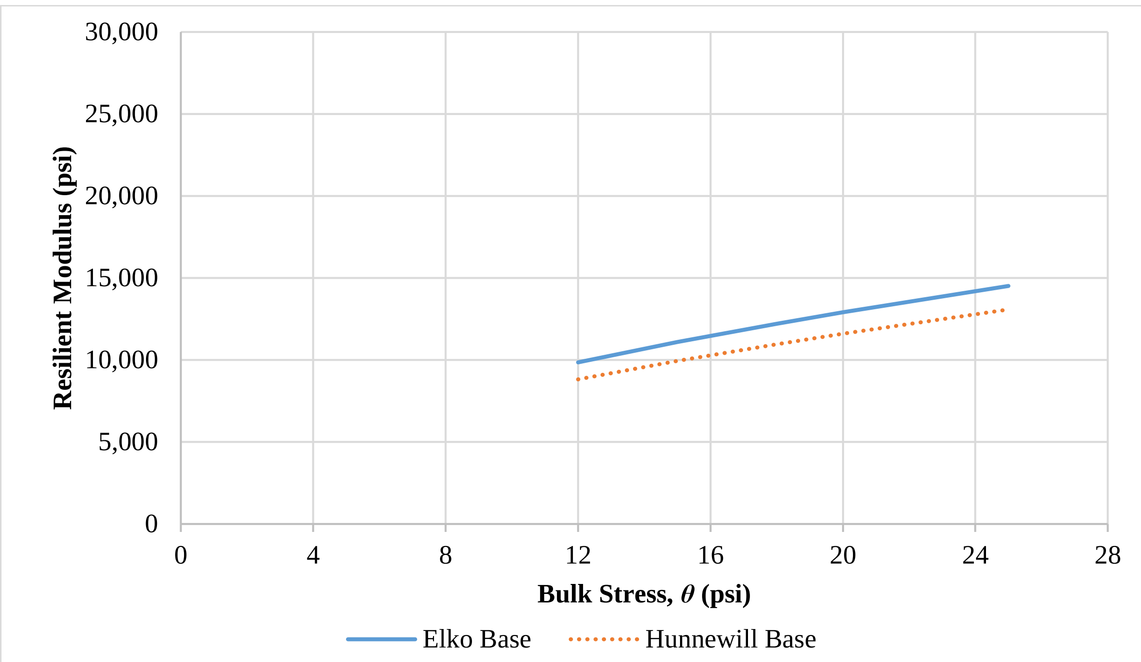

Figure 34. Variation of District 2 and District 3 base materials M_r with bulk stress.

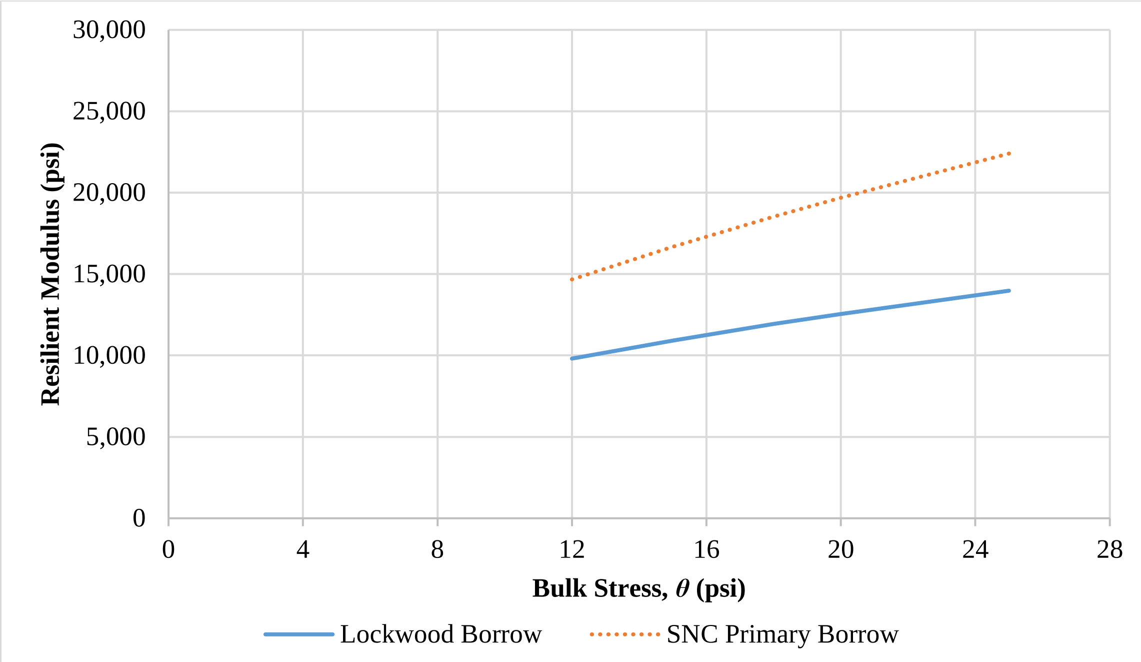

Figure 35 Variation of District 2 and District 3 borrow materials *M_r* with bulk stress.

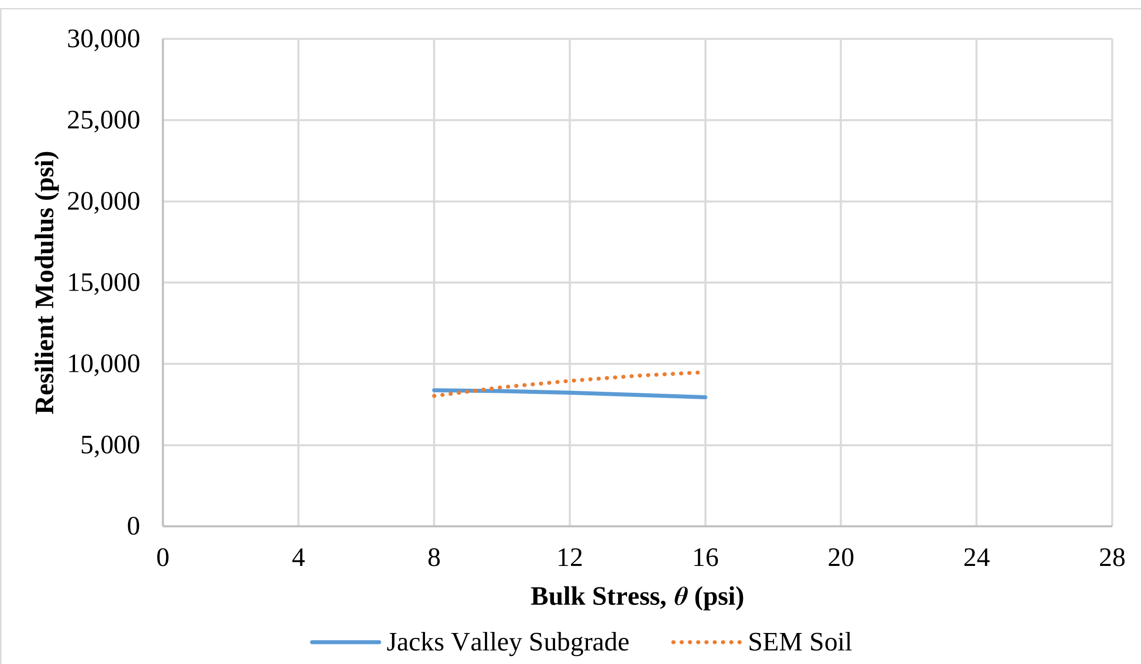

Figure 36 Variation of District 2 subgrade materials M_r with bulk stress.

Resistance R-value

A summary of the R-value testing results for the evaluated materials are shown in Table 30 to Table 32. According to NDOT specifications, Type 1 Class B Base Materials must have a R-value of at least 70. All of the tested base materials meet this minimum specification. Borrow materials must have a R-value of 45. All of the tested borrow materials meet this minimum specification, except for Contract 3583 borrow from District 1.

Table 30. Resistance R-value Test Results for Base Materials (All Districts).

Material	Sam-ple No.	Density (pcf)	Moisture Content (%)	Exudation Pressure (psi)	R-value	R-value Corr.	R-value @300 psi Exudation Pressure
3583 (Base)	1	138.9	6.8	100	79	78	80
	2	138.1	5.8	333	81	80	
	3	140.2	5.5	518	83	82	
3597 (Base)	1	121.0	3.9	608	82	82	71
	2	125.6	4.5	478	77	75	
	3	127.3	4.8	204	73	71	
3605 (Base)	1	132.4	5.4	354	83	81	78
	2	135.3	5.2	540	86	86	
	3	134.0	6.0	275	77	77	
3607 (Base)	1	125.7	6.6	530	85	85	85
	2	124.3	7.6	298	85	85	
	3	122.9	7.2	175	84	84	
3613 (Base)	1	135.0	5.0	699	87	87	83
	2	138.7	5.9	204	84	82	
	3	136.3	5.5	388	85	84	
Lockwood Base	1	124.1	7.8	541	84	84	84
	2	130.2	8.4	340	86	84	
	3	129.2	8.9	228	83	83	
Elko Base	1	129.9	6.6	755	86	86	78
	2	128.6	7.5	444	79	79	
	3	125.2	8.2	100	76	76	
Hunnewill Base	1	129.0	6.8	723	82	82	73
	2	127.9	7.7	340	75	75	
	3	129.4	9.0	107	65	65	

Table 31. Resistance R-value Test Results for Borrow Materials (All Districts).

Material	Sam-ple No.	Density (pcf)	Moisture Content (%)	Exudation Pressure (psi)	R-value	R-value Corr.	R-value @300 psi Exudation Pressure
3546 (Borrow)	1	123.8	5.0	727	84	84	78
	2	123.4	6.5	441	82	82	
	3	124.2	6.9	287	79	78	
3583 (Borrow)	1	116.8	13.5	125	32	32	44
	2	119.0	11.8	734	70	70	
	3	118.6	12.6	355	47	47	
3597 (Borrow)	1	136.1	8.1	149	74	71	78
	2	134.4	7.2	731	85	85	
	3	137.0	7.8	411	83	82	
3607 (Borrow)	1	119.7	13.0	100	57	57	78
	2	119.3	12.2	271	76	76	
	3	120.1	11.1	587	81	81	
3613 (Borrow)	1	138.3	5.9	361	85	85	84
	2	139.6	6.7	227	83	83	
	3	141.5	5.5	566	85	85	
Lockwood (Borrow)	1	119.8	13.8	0.7	66	64	69
	2	117.5	15.4	0.45	53	53	
	3	119.1	13.3	1.88	80	79	
Elko (borrow)	1	–	–	–	–	–	74
	2	121.0	8.4	405	76	76	
	3	120.8	9.1	103	64	64	
SNC Primary Borrow	1	129.4	10.5	176	47	50	71
	2	128.2	9.2	639	84	84	
	3	127.6	10.0	340	77	77	
SNC Secondary Borrow	1	125.2	8.6	643	86	86	76
	2	123.2	9.4	406	76	76	
	3	128.7	10.4	124	81	81	

–No Data.

Table 32. Resistance R-value Test Results for Borrow Materials (All Districts).

Material	Sam-ple No.	Density (pcf)	Moisture Content (%)	Exudation Pressure (psi)	R-value	R-value Corr.	R-value @300 psi Exudation Pressure
I-15/Goodsprings	1	131.9	7.9	188	78	78	82
	2	129.5	7.2	468	82	82	
	3	130.8	7.5	268	81	81	
US-95/Searchlight	1	130.9	8.4	148	71	69	75
	2	130.1	7.9	682	80	80	
	3	130.7	8.2	254	74	74	
NV-375/Rachel	1	129.5	8.8	302	80	81	80
	2	130.7	9.5	171	76	76	
	3	130.3	8.1	663	85	85	
US-95/Bonnie Claire	1	121.8	11.4	172	72	71	74
	2	121.1	10.2	719	74	74	
	3	120.9	10.6	391	75	75	
US-93/Crystal Spring MP62	1	119.2	10.5	404	80	81	74
	2	119.8	10.9	225	66	68	
	3	119.5	9.9	694	78	78	
US-93/Crystal Spring MP67	1	120.5	11.3	231	51	51	71
	2	120.8	10.8	323	77	77	
	3	119.6	10.1	628	78	78	
Jacks Valley Subgrade	1	121.2	11.4	727	78	78	60
	2	121.3	13.6	366	68	68	
	3	115.6	14.4	172	40	40	
UNR Soil at SEM	1	132.2	9.0	365	77	75	65
	2	131.7	8.4	529	82	81	
	3	132.3	9.9	219	47	47	

ESTIMATION OF DESIGN RESILIENT MODULUS

An estimation of the resilient moduli of the existing unbound layers is needed for the rehabilitation design of flexible pavements. The stepwise mechanistic analysis procedure described in Chapter 2 was implemented for determining representative M_r values and for establishing the M_r correlation equations. The measured properties of the evaluated unbound materials from District 1 were used throughout this process. The measured properties for District 2 and District 3 materials were then used in the verification process of the developed M_r correlation equations.

Step 1-Select Representative Pavement Structures

Typical pavement sections were designed using PaveXpress software which is based on the AASHTO 1993 design procedure. Two different traffic levels were considered for the pavement design. The NDOT *Pavement Structural Design Manual* was used as a reference for the input parameters as shown in Table 33. Structural coefficients for the AC layer, base layer, and borrow layer were selected in accordance with the NDOT manual to be 0.35, 0.10, and 0.07, respectively. Two different levels of subgrade resilient modulus were considered for the design; strong at 14,000 psi and weak at 8,000 psi.

Resilient modulus of the base layer was kept constant at 26,000 psi. Table 34 summarizes the designed pavement structures for the two traffic levels (i.e., low and medium).

For pavements on weak subgrade, borrow material was used as a subbase. For this case, the resilient modulus for the base, borrow, and subgrade were assumed to be 26,000, 11,250, and 6,800 psi, respectively. The designed pavement structure with borrow material is shown in Table 35. Only medium traffic is considered in this case

Table 33. Major Inputs for Flexible Pavement Designs.

Traffic Level	Design Traffic in Million ESALs (MESALs)	Reliability Level (%)	Initial Serviceability index, p_i	Terminal serviceability index, p_t	Overall Standard Deviation, S_o
Low	5	85	4.2	2	0.45
Medium	15	90	4.2	2.5	0.45

Table 34. Design Pavement Structures for Different Traffic Levels.

Traffic Level	Subgrade M_r (psi)	Thickness (inch)	
		AC Layer	Base Layer
Low	14,000	5	16
	8,000	7	16
Medium	14,000	7	18
	8,000	9.5	18

Table 35. Design Pavement Structures with Borrow Materials.

Traffic Level	Subgrade M_r (psi)	Thickness (inch)		
		AC Layer	Base Layer	Borrow Layer
Medium	6,800	7	18	10

Step 2-Pavement Layer Properties

AC Layer

in order to incorporate the viscoelastic behavior of the AC mixture in the ILLI-PAVE model, the AC layer was divided into sublayers and a representative damaged dynamic modulus master curve for the asphalt mixture was utilized to properly assign an elastic modulus for each of the sublayers using the appropriate loading frequency and temperature. A damaged dynamic modulus master curve was used in order to simulate the in-situ property of the AC layer of the flexible pavement in need for rehabilitation design. The following steps were completed to develop the damaged dynamic modulus master curve:

1. Use the dynamic shear modulus (G*) and phase angle properties for a typical District 1 asphalt binder of PG76-22NV (as shown in Table 36) to estimate the viscosity of the binder at different temperatures.

2. Use the dynamic modulus, E*, properties for a typical District 1 asphalt mixture (as shown in Table 37) to determine the regression parameters for the E* master curve shown in equation 18 and illustrated in Figure 37.
3. Determine the damage factor for the AC layer, d_{AC}, in Equation 19 based on the condition of the AC layer as follows: a) excellent condition, d_{AC} between 0.00 and 0.20, b) good condition, d_{AC} between 0.20 and 0.40, c) fair condition, d_{AC} between 0.40 and 0.80, d) poor condition, d_{AC} between 0.80 and 1.20, and e) very poor condition, d_{AC} greater than 1.20. In this research, a Fair condition was assumed for the existing AC layer and a damage value of 0.6 was selected for use in Equation 19.
4. Using Equation 19, determine the damaged dynamic modulus of the AC layer, E^*_{dam} for different frequencies and temperatures as shown in Table 38.

Table 36. Representative Mean G* and Phase Angle Values for PG76-22NV.

Temperature (°F)	Binder Shear Modulus, G* (Pa)	Phase Angle (°)
147.2	7,355	58.9
158.0	4,638	58.4
168.8	2,873	60.0

Table 37. Representative Mean E* Values in psi for PG76-22NV Mixture.

Frequency (Hz)	Temperature (°F)				
	14	40	70	100	130
0.1	2,437,149	1,142,867	231,733	49,451	22,928
0.5	2,796,769	1,566,757	371,867	79,212	29,081
1	2,929,984	1,786,152	459,860	99,621	38,053
5	3,189,069	2,208,295	700,905	174,052	65,800
10	3,280,392	2,398,327	841,850	225,042	77,131
25	3,384,391	2,819,783	1,041,907	335,073	107,196

$$\log(E^*) = \delta + \frac{\alpha}{1+e^{\beta+\gamma\log(t_r)}} \tag{18}$$

where

E^* = Asphalt concrete modulus (psi)
δ = regression parameter
t_r = Reduced time
α, β and γ = Regression parameters

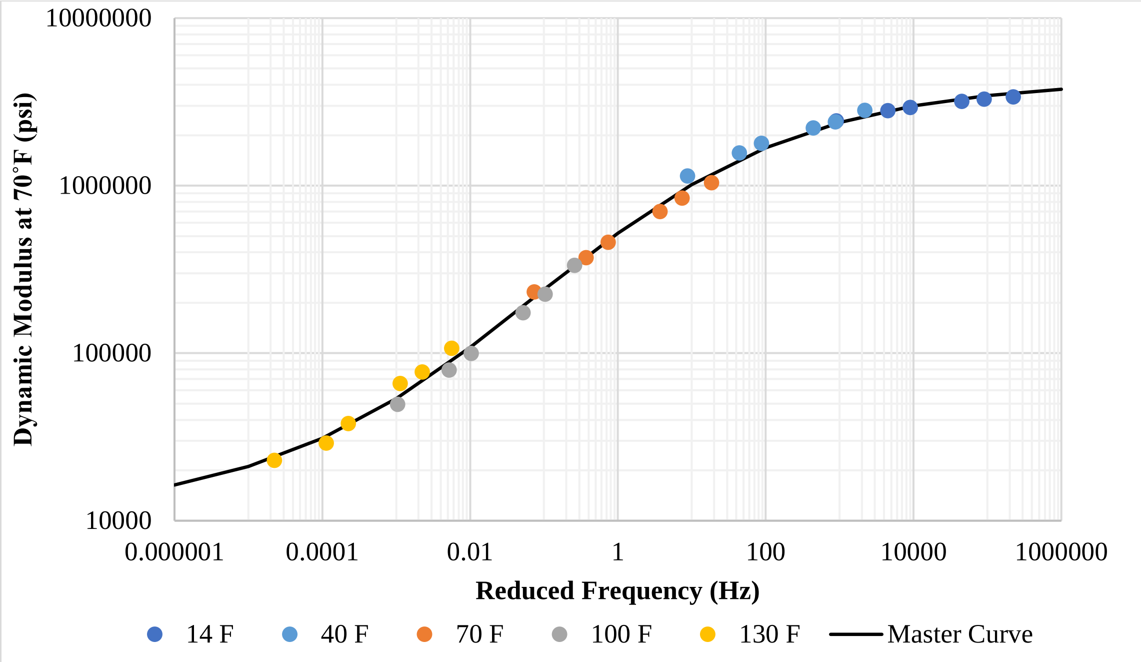

Figure 37. Dynamic modulus master curve for PG76-22NV mixture.

$$E^*_{dam} = 10^{\delta} + \frac{E^* - 10^{\delta}}{1 + e^{-0.3 + 5 * \log(d_{AC})}} \tag{19}$$

Table 38. Damaged E* Values in psi at Different Temperatures and Frequencies.

Frequency (Hz)	Temperature (°F)				
	14	**40**	**70**	**100**	**130**
0.1	1,997,842	828,806	172,699	44,108	20,482
0.5	2,301,555	1,181,348	299,833	70,823	27,379
1	2,414,573	1,342,907	376,385	88,597	31,821
5	2,635,369	1,716,813	611,987	153,256	47,935
10	2,713,571	1,870,344	738,021	194,959	58,616
25	2,802,917	2,061,039	924,129	267,061	77,985

Figure 38 presents the master curves for the undamaged and damaged dynamic moduli of the AC layer for a typical District 1 asphalt binder of PG76-22NV. It should be noted that the scales in Figure 38 are logarithmic, therefore, any small changes in the master curves can represent large differences in the actual values of the dynamic modulus.

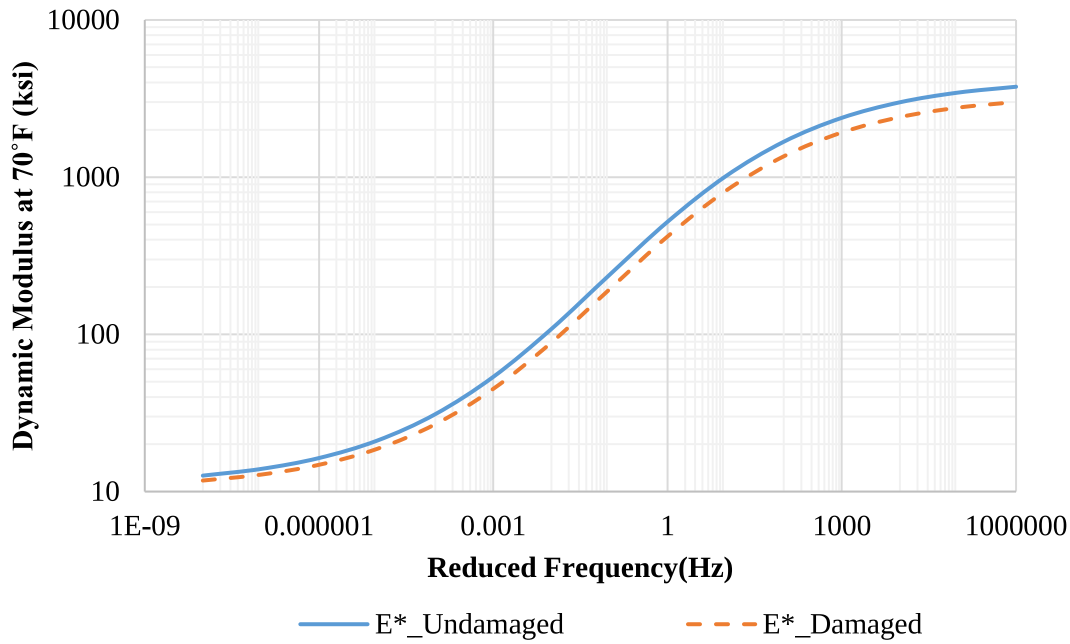

Figure 38. Damaged and undamaged dynamic modulus master curve.

The AC layer was divided into sublayers and each sublayer was assigned an appropriate damaged modulus value using the damaged modulus master curve. The thicknesses of the AC sublayers were transformed into equivalent thicknesses by using the method of equivalent thickness (MET) as shown in Figure 39. The pulse time was calculated from the effective length and an assumed vehicle speed of 45 mph following the MEPDG procedure. The frequency for each sublayer was then obtained from the estimated pulse time. The damaged dynamic modulus master curve was used to calculate the dynamic modulus for the corresponding frequencies for each sublayer.

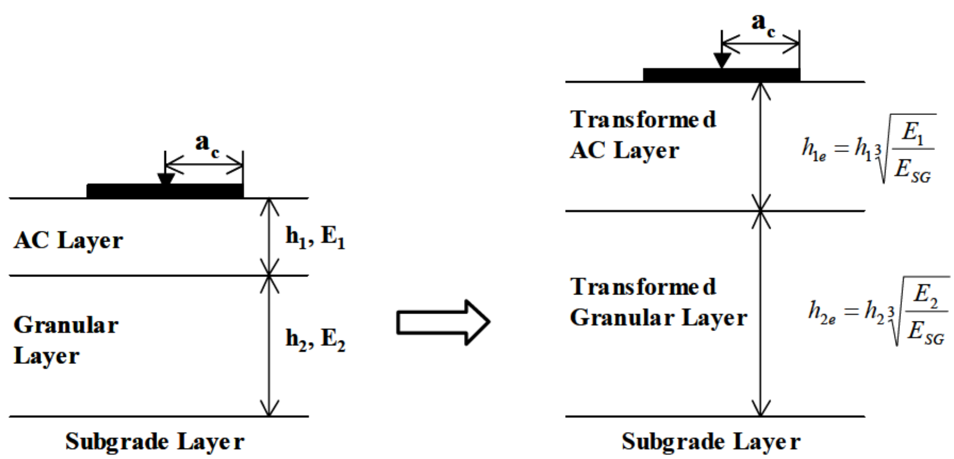

Figure 39. Equivalent thickness transformation using MET.

Crushed Aggregate Base (CAB), Borrow, and Subgrade (SG)

The constitutive stress-dependent models developed from the AASHTO T307 M_r tests as well as the laboratory determined Mohr-Coulomb failure criteria (c and ϕ) were used in the ILLI-PAVE model.

For the base and borrow materials, the theta model was used as an input to the ILLIPAVE software (Table 24 and Table 25) whereas for the subgrade, the Uzan model was used (Table 26). The Falling Weight Deflectometer (FWD) test was simulated in the ILLIPAVE model by applying a circular load of 9,000 lbs with a radius of 5.9 inch. The cohesion and friction angle properties for one base and one subgrade material were determined in the laboratory while the properties for the reaming materials were estimated based on their corresponding USCS classifications. The laboratory measured values as shown in Table 39 were close to the ones estimated based on the USCS classifications.

Table 39. Cohesion and Friction Angle from the Laboratory Testing.

Material	Cohesion (psi)	Friction angle (°)
Base (Contract 3583)	4.1	48.9
Subgrade (I-15/Goodsprings)	8.2	33.8

Step 3-Pavement Responses

The computer software, MODULUS 6.1, was used to backcalculate the modulus values of the various layers using the deflection basins obtained from the ILLIPAVE analysis. An apparent rigid layer was introduced in the MODULUS 6.1 software to capture the nonlinearity of the unbound materials. The backcalculation process was considered complete when the deflection basins calculated by MODULUS 6.1 model closely matched the deflections generated by the ILLIPAVE model. At this stage, the identified moduli were assigned to the corresponding layers.

A sample calculation for a flexible pavement structure with 5.0 inch AC and 16.0 inch base material from contract 3546 on top of the subgrade material from the US-95/Bonnie Claire location is presented in this section. The forward calculation of the surface deflections by the ILLIPAVE model are summarized in Table 40. These deflections were used as input in the MODULUS 6.1 model and the resulted backcalculated surface deflections are also summarized in Table 40. Figure 40 presents the comparison between forward calculated and backcalculated surface deflections. The backcalculated moduli of the various layers were: 195,400 psi for the AC layer, 22,900 psi for the CAB layer, and 8,400 psi for the SG layer. The absolute error was 0.97 and E4/stiffness ratio was 5.5.

A similar analysis was conducted for all the designed pavement structures. A summary of the results from this analysis are presented in Table 41 through Table 43 for the different pavement structures.

Table 40. Surface Deflections at Various Radial Distances.

Radial Distance (inch)	Vertical Surface Defection (mils)	
	ILLIPAVE Model	MODULUS 6.1 (Backcalculation)
0	23.08	23.14
8	16.39	16.29
12	12.68	12.65
18	8.73	–
24	6.28	6.43
36	3.63	3.55
48	1.99	1.99
60	1.04	1.13
72	0.55	–

–No Data.

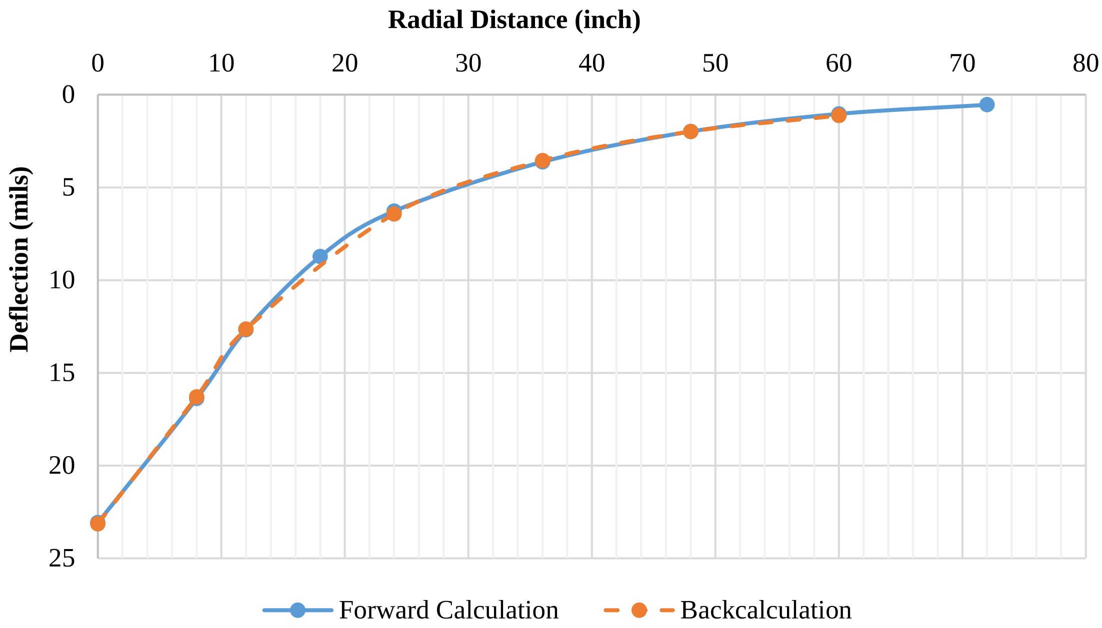

Figure 40. Forward calculated and backcalculated surface deflections.

Table 41. Backcalculated Moduli of Pavement Structures on Weak Subgrade (District 1).

Material		Traffic Level / SG Strength					
		Low/Low 7 inch AC & 16 inch CAB			Medium/Low 9.5 inch AC & 18 inch CAB		
		Backcalculated Moduli (psi)			Backcalculated Moduli (psi)		
CAB	**SG**	**CAB**	**SG**	**AC**	**CAB**	**SG**	**AC**
3546	US-95/Bonnie Claire	20,500	6,600	170,300	19,800	6,800	158,000
3546	US-95/Searchlight	22,800	7,300	165,200	21,000	7,700	158,000
3546	US-93/Crystal Spring MP62	20,600	5,700	167,700	19,000	6,400	158,600
3546	US-93/Crystal Spring MP67	22,800	7,300	166,100	21,100	7,800	157,600
3546	Borrow 3583	22,300	6,900	164,600	20,500	7,500	158,100
3583	US-95/Bonnie Claire	17,900	6,600	167,900	17,400	6,500	157,100
3583	US-95/Searchlight	19,300	7,600	164,800	18,300	7,500	157,000
3583	US-93/Crystal Spring MP62	17,600	6,000	167,500	17,200	6,000	156,400
3583	US-93/Crystal Spring MP67	19,400	7,600	164,300	18,400	7,500	156,600
3583	Borrow 3583	18,900	7,100	164,300	18,100	7,200	156,500
3597	US-95/Bonnie Claire	18,500	6,700	170,800	18,200	6,600	157,500
3597	US-95/Searchlight	20,100	7,600	167,700	19,100	7,600	158,000
3597	US-93/Crystal Spring MP62	18,400	6,000	168,100	17,500	6,200	158,200
3597	US-93/Crystal Spring MP67	20,200	7,600	167,400	19,500	7,500	156,300
3597	Borrow 3583	19,800	7,200	165,700	19,100	7,200	155,900
3605	US-95/Bonnie Claire	16,100	6,000	165,000	15,100	6,100	156,700
3605	US-95/Searchlight	16,900	7,200	164,600	16,000	7,000	155,600
3605	US-93/Crystal Spring MP62	15,300	5,700	167,600	14,500	5,800	156,900
3605	US-93/Crystal Spring MP67	17,000	7,100	164,800	16,000	7,000	156,200
3605	Borrow 3583	16,700	6,700	162,900	15,600	6,700	155,900
3607	US-95/Bonnie Claire	15,600	5,900	166,200	14,800	5,900	155,300
3607	US-95/Searchlight	16,500	7,000	165,300	15,600	6,900	155,600
3607	US-93/Crystal Spring MP62	14,800	5,500	168,400	14,000	5,700	157,400
3607	US-93/Crystal Spring MP67	16,900	6,800	164,000	15,600	6,800	155,700
3607	Borrow 3583	16,200	6,600	164,000	15,300	6,500	155,200
3613	US-95/Bonnie Claire	17,400	6,500	166,700	17,000	6,400	155,900
3613	US-95/Searchlight	18,900	7,400	164,100	17,800	7,400	156,500
3613	US-93/Crystal Spring MP62	17,100	5,800	166,500	16,300	6,100	157,300
3613	US-93/Crystal Spring MP67	19,000	7,200	168,800	17,900	7,300	156,100
3613	Borrow 3583	18,400	7,000	164,000	17,500	7,000	155,900

Table 42. Backcalculated Moduli of Pavement Structures on Strong Subgrade (District 1).

Material		Traffic Level / SG Strength					
		Low/High 5 inch AC & 16 inch CAB			Medium/High 7 inch AC & 18 inch CAB		
		Backcalculated Moduli (psi)			Backcalculated Moduli (psi)		
CAB	**SG**	**SG**	**CAB**	**AC**	**SG**	**CAB**	**AC**
3546	I-15/Goodsprings	8,400	22,900	195,400	8,200	22,300	176,700
3546	NV-375/Rachel	7,700	22,400	197,200	7,700	21,600	178,400
3586	I-15/Goodsprings	8,400	19,800	187,900	8,100	19,300	173,200
3583	NV-375/Rachel	7,600	19,700	185,900	7,400	19,100	172,800
3597	I-15/Goodsprings	8,200	21,300	191,700	8,000	20,600	174,700
3597	NV-375/Rachel	7,400	20,800	193,000	7,500	19,900	176,600
3605	I-15/Goodsprings	7,600	17,900	187,500	7,300	17,000	173,900
3605	NV-375/Rachel	6,900	17,600	187,800	6,900	16,700	173,100
3607	I-15/Goodsprings	7,200	17,800	186,700	7,200	16,500	174,700
3607	NV-375/Rachel	6,800	17,200	189,900	6,800	16,100	175,000
3613	I-15/Goodsprings	8,000	19,700	186,400	7,700	19,000	172,800
3613	NV-375/Rachel	7,500	19,100	187,800	7,300	18,500	172,500

Table 43. Backcalculated Moduli of Pavement Structures with Borrow Layer (District 1).

Material			Medium Traffic/Low SG Strength			
			7 inch AC, 18 inch CAB, & 10 inch Borrow			
			Backcalculated Moduli (psi)			
CAB	**Borrow**	**Subgrade**	**SG**	**Borrow**	**CAB**	**AC**
3546	3546	US-95/Bonnie Claire	5,400	11,900	16,500	191,000
3546	3546	US-95/Searchlight	6,300	13,300	16,800	189,400
3546	3596	US-93/Crystal Spring MP62	5,400	13,900	16,300	192,900
3546	3596	US-93/Crystal Spring MP67	6,300	15,500	16,500	192,800
3546	3613	Borrow 3583	5,600	10,700	17,100	186,300
3583	3613	US-95/Bonnie Claire	7,000	10,600	17,700	183,500

Correlation equations relating M_r to R-value were developed from testing and analysis of the unbound materials from District 1. However, M_r testing results for the District 2 and District 3 unbound materials were used to help verify these correlation equations. Therefore, the backcalculation procedure was completed for District 2 and District 3 materials as well. Both the Jacks Valley and SEM Soil subgrade materials were classified as weak subgrades, so a pavement design using borrow material was analyzed which consisted of a 7 inch AC, 18 inch CAB, and 10 inch borrow material. The surface deflections were then found using ILLI-PAVE. The moduli for each layer were backcalculated using MODULUS 6.1. This was an iterative process, where the moduli were recalculated until the error was less than one percent. Table 44 shows the resulting backcalculated moduli for each layer.

Table 44. Backcalculated Moduli of Pavement Structures with Borrow Layer (Districts 2 and 3).

Material			Medium Traffic/Low SG Strength 7 inch AC, 18 inch CAB, & 10 inch Borrow Backcalculated Moduli (psi)			
CAB	**Borrow**	**Subgrade**	**SG**	**Borrow**	**CAB**	**AC**
Elko	Lockwood	Jacks Valley	5,300	5,300	15,200	192,900
Elko	Lockwood	SEM Soil	5,500	5,700	14,800	195,300
Elko	SNC Primary	Jacks Valley	5,700	5,400	15,900	193,500
Elko	SNC Primary	SEM Soil	5,700	6,200	15,500	193,400
Hunnewill	Lockwood	Jacks Valley	5,100	5,100	14,300	193,000
Hunnewill	Lockwood	SEM Soil	5,300	5,100	14,100	194,900
Hunnewill	SNC Primary	Jacks Valley	5,300	5,600	14,800	192,600
Hunnewill	SNC Primary	SEM Soil	5,500	6,000	14,500	193,900

Step 4-Establish the Mr Correlation Equations

The goal of this analysis is to develop a prediction model for M_r value to be used in the design of rehabilitated pavements as function of empirical and physical properties for the unbound materials. The properties considered in the development of the prediction model, included; R-value, materials passing sieves No. 200, No. 40, 3/8 inch, maximum dry density, optimum moisture content, and plasticity index. In addition, the pavement equivalent thickness in terms of the base, borrow, or the subgrade layer were identified as critical parameters in the determination of the design M_r for unbound layers. The layer thicknesses above the base, borrow, and subgrade used for the state of stress calculations were transformed into equivalent thickness of base, borrow, or subgrade using MET as presented in Equation 20 through Equation 22.

$$H_{eq,\,CAB} = h_{AC}\left(\frac{E_{AC}*(1-\nu_{SG}^2)}{E_{SG}*(1-\nu_{AC}^2)}\right)^{(1/3)} + \frac{h_{CAB}}{4}*\left(\frac{E_{CAB}*(1-\nu_{SG}^2)}{E_{SG}*(1-\nu_{CAB}^2)}\right)^{(1/3)} \quad (20)$$

$$H_{eq,\,BOR} = h_{AC}\left(\frac{E_{AC}*(1-\nu_{SG}^2)}{E_{SG}*(1-\nu_{AC}^2)}\right)^{\left(\frac{1}{3}\right)} + h_{CAB}*\left(\frac{E_{CAB}*(1-\nu_{SG}^2)}{E_{SG}*(1-\nu_{SG}^2)}\right)^{\left(\frac{1}{3}\right)} + \frac{h_{BOR}}{4}*\left(\frac{E_{BOR}*(1-\nu_{SG}^2)}{E_{SG}*(1-\nu_{BOR}^2)}\right)^{(1/3)} \quad (21)$$

$$H_{eq,\,SG} = h_{AC}\left(\frac{E_{AC}*(1-\nu_{SG}^2)}{E_{SG}*(1-\nu_{AC}^2)}\right)^{\left(\frac{1}{3}\right)} + h_{CAB}*\left(\frac{E_{CAB}*(1-\nu_{SG}^2)}{E_{SG}*(1-\nu_{SG}^2)}\right)^{\left(\frac{1}{3}\right)} + 18 \quad (22)$$

where

$H_{eq,\,CAB}$ = equivalent thickness of the base layer (inch)
$H_{eq,\,BOR}$ = equivalent thickness of the borrow layer (inch)
$H_{eq,\,SG}$ = equivalent thickness of the subgrade layer (inch)

E_{AC} = modulus of AC layer (psi)
E_{CAB}= resilient modulus of base layer (psi)
E_{CAB}= resilient modulus of borrow layer (psi)
E_{SG} = resilient modulus of subgrade layer (psi)
ν_{AC} = Poisson's ratio of AC layer
ν_{CAB} = Poisson's ratio of base layer
ν_{BOR} = Poisson's ratio of borrow layer
ν_{SG} = Poisson's ratio of subgrade layer

Multi linear regression analysis was conducted using R software (12). The following assumptions were checked for each model:

- If errors are following a normal distribution.
- Multi-collinearity.

Anderson-Darling normality test (13) and variance inflation factors (14) were used to check the normality and multi-collinearity respectively. A backward elimination method was used to identify the best fit model. First, all of the identified variables were included in the analysis and tested for statistical significance. Next, the non-significant variables (for a p-value greater than 0.05) were removed and the analysis was repeated until all the significant variables were identified.

Based on the analysis results, it was observed that the variation in the design M_r of the subgrade is minimal with the evaluated pavement structures. However, the design M_r of base and borrow materials changed significantly with the pavement structure. Accordingly, the development of the corresponding prediction models for base, borrow, and subgrade were done separately. However, the borrow material data were very few. Therefore, it was decided to combine the base data with the borrow one to develop the model for the borrow materials. For the future, the borrow material analysis can be done separately when enough data are available. The ranges of data that were used for the model development are shown in Table 45.

Table 45. Range of Variables for the M_r Model Development.

Parameter	Range of Data					
	Subgrade		Base		Borrow	
	Min	Max	Min	Max	Min	Max
R-value	44	82	71	85	78	83
P200 (%)	5.4	66.9	5.3	10	7.3	16.4
P40 (%)	15.2	84.2	12.6	19.3	15.4	28.7
P3/8 (%)	52.2	99.3	54.1	76.3	69.8	99.9
Maximum Dry Density (pcf)	119.4	139.2	135.8	147.5	133.8	143.2
Optimum Moisture Content (%)	6.1	10.7	3.5	6.7	5.4	7.2
PI	1	4.7	0	0	0	3.3
H_{eq} (inch)	48.5	80.8	17.1	35.3	38.3	54.4
M_r (rehabilitation)	5,400	8,400	14,000	22,900	10,600	15,500

The statistical analysis (i.e., backward elimination method) was launched including all the variables and parameters except R-value. This process was done separately for the base, subgrade, and borrow materials. The summary of the developed models for pavement rehabilitation design are presented in Table 46. The typical residual plot and normality plot from the R software are shown in Figure 41 and Figure 42. The residual plot should look random, in other words, there should not be any pattern. The normality plot has to be linear in order to satisfy the linear regression assumption.

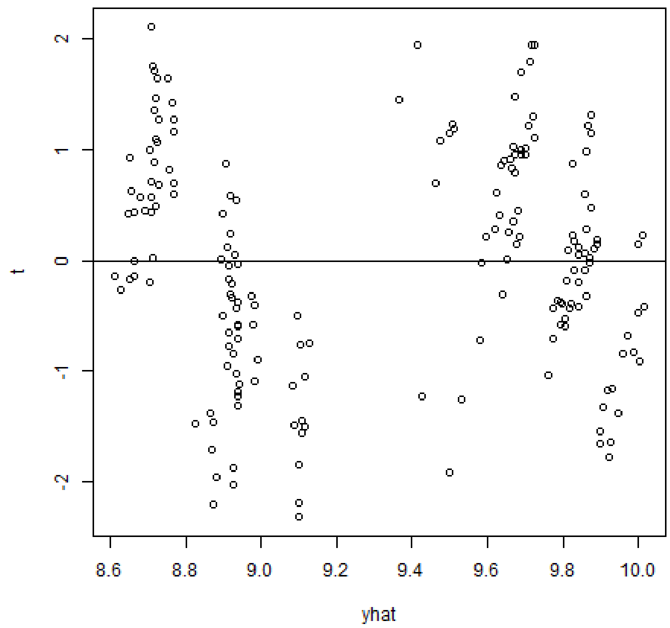

Figure 41. Example of residual error plot for prediction model.

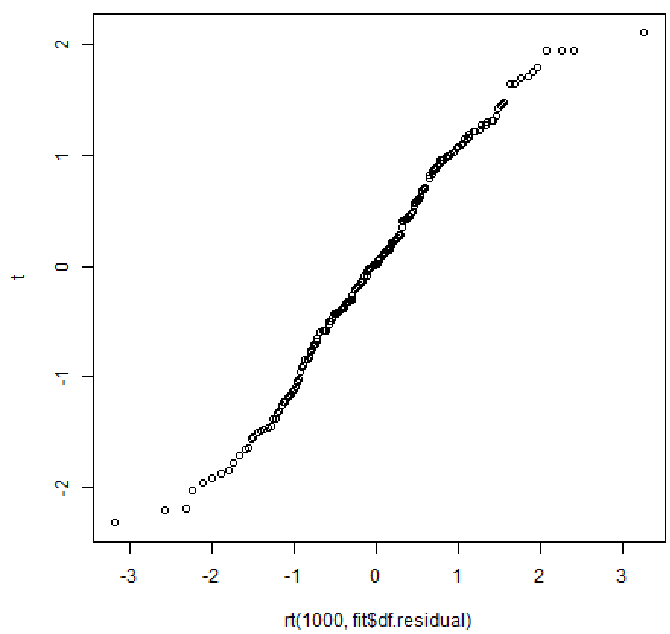

Figure 42. Example normality plot for prediction model.

Table 46. Established M_r Correlation Equations for Pavement Rehabilitation Design.

Response Variable	Regression Coefficients		
	Predictor Variable: Ln(M_{r-SG})	**Predictor Variable: Ln(M_{r-CAB})**	**Predictor Variable: Ln($M_{r-Borrow}$)**
Intercept (constant)	5.3982	8.014	9.2304
R-value	0.0134	0.0261	0.0136
Percent Passing No. 40 Sieve, P40 (%)	0.0125	-0.0485	-0.0229
Percent Passing 3/8 inch, P3/8 (%)	-0.0032	0.0161	0.0079
Maximum Dry Density, γ_{d-max} (pcf)	0.0168	–	–
Optimum Moisture Content, OMC (%)	–	-0.0659	-0.0661
Plasticity Index, PI	0.0177	–	–
Equivalent Thickness, H_{eq} (inch)	–	-0.0089	-0.0127
Statistical Checks			
Normality	Pass	Fail	Fail
Multi Collinearity	Fail	Pass	Pass
R-square	0.7065	0.8542	0.6594

–Regression coefficient equal to zero.

From the different comparisons established above, the resilient modulus of the base, borrow, and subgrade can be estimated from the R-value and other physical properties. The estimation of design M_r for CAB and Borrow layers requires H_{eq} as an input value. Based on the analysis of the data generated from this study, a correlation was found possible between the equivalent thickness and depth from pavement surface to the critical location in the base or borrow layer (D). The critical depth location was defined in the MEPDG procedure for aggregate base layer and embankment at quarter depth. Therefore, based on existing pavement structure (i.e., existing pavement layers), the critical depth can be determined for each unbound layer and used to calculate the equivalent thickness in terms of the layer being analyzed using Equation 23 and Equation 24 expressed below. Once the equivalent thickness is computed, the M_r of the layer being analyzed can be estimated from the model presented in Table 46.

$$H_{eqReh-CAB} = 2.399 * D - 1.7468 \quad (23)$$

$$H_{eqReh-BOR} = 1.543 * D + 8.044 \quad (24)$$

where

$H_{eqReh\text{-}CAB}$ = equivalent thickness of base layer (inch)
$H_{eqReh\text{-}BOR}$ = equivalent thickness of borrow layer (inch)
D = depth of critical location in base or borrow layer (inch)

As an example, for a rehabilitation design of an existing pavement structure with 5 inch of AC layer, on top of 10 inch of CAB layer, on top of SG, H_{eq} can be calculated as follows:

- Depth of interest for the CAB layer is at its quarter depth, D = 5 + 10/4 = 7.5 inch.
- Using Equation 23 and a D of 7.5 inch, the equivalent thickness is: $H_{eqReh-CAB}$ = 2.399*7.5 – 1.7468 = 16.25 inch. This value is then used in to estimate M_r from the model presented in Table 46 for CAB.

By examining the regression coefficients shown in Table 46, the following observations can be made:

- An increase in respective R-value can result in an increase in predicted M_r of the base, borrow, and subgrade material.
- An increase in percent passing No. 40 sieve (i.e., finer on the fine side) can result in an increase in predicted M_r of subgrade material and a decrease in predicted M_r of base and borrow materials.
- An increase in percent passing 3/8 inch (i.e., finer on the coarse side) can result in a decrease in predicted M_r of subgrade material and an increase in predicted M_r of base and borrow materials.
- An increase in maximum dry density or plasticity index can result in an increase in predicted M_r of subgrade material.
- An increase in optimum moisture content can result in a decrease in predicted M_r of base and borrow materials.
- An increase in equivalent thickness (e.g., unbound layers are at a deeper location in the pavement structure) can result in a decrease in predicted M_r of base and borrow materials.

COMPARISON AND VERIFICATION

A comparison between predicted M_r from the current NDOT correlation equation and that from the model developed in this study is presented in Figure 43 for the base, borrow, and subgrade materials from District 1. It can be seen that the current NDOT resilient modulus equation in terms of R-value consistently overestimates the design resilient modulus.

Only six of the nine materials sampled from District 2 and District 3 were able to be tested for resilient modulus. Therefore, rather than using the resilient modulus testing results from District 2 and District 3 in the development of the models, instead they were used to verify the validity of the prediction models recommended in this study. The predicted M_r values using the developed models in this study as well as the current available NDOT correlation equation were compared against the backcalculated moduli determined in “Step 3-Pavement Responses” above for District 2 and District 3 materials (refer to Table 44).

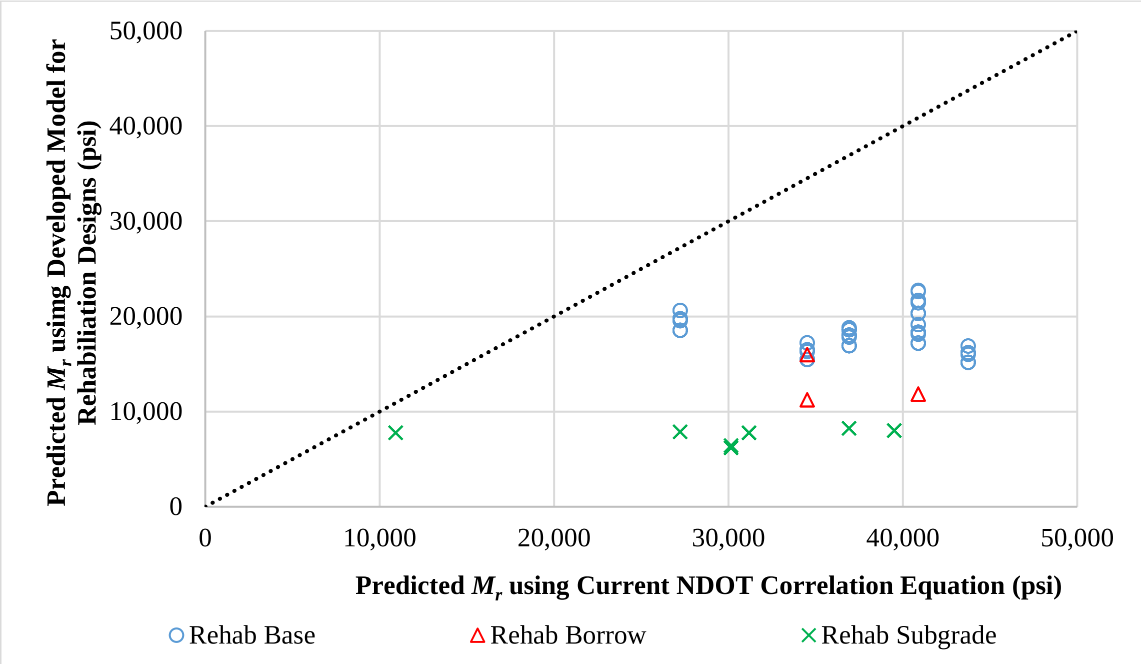

Figure 43. Comparison between current NDOT prediction model and developed M_r model for pavement rehabilitation design (District 1 materials).

The moduli that are predicted using the developed M_r models for pavement rehabilitation design in this study were consistently closer to the backcalculated moduli in comparison with the NDOT prediction equation for resilient modulus. The NDOT resilient modulus prediction equation predicted modulus values about two to five times higher than the backcalculated moduli. The moduli values predicted by the newly developed models are much closer to the backcalculated moduli. Therefore, the District 2 and District 3 material results helped verifying these newly developed resilient modulus prediction models for rehabilitated pavement design. These results are summarized in Table 47. The percent difference between backcalculated and predicted moduli using the developed model and the current NDOT correlation equation is shown in Table 48. A graphical comparison between the resilient modulus prediction of District 2 and District 3 materials using current NDOT equation and the model developed in this study is presented in Figure 44.

Table 47. Comparison of Backcalculated and Predicted Moduli.

Material	Average Backcalculated Modulus (psi)	Predicted Modulus Using Developed Model (psi)	Predicted Modulus Using Current NDOT Equation (psi)
Elko Base	15,350	16,131	34,512
Hunnewill Base	14,425	14,410	29,139
Lockwood Borrow	5,300	7,343	25,449
Jacks Valley Subgrade	5,350	7,607	18,766
SEM Soil	5,500	6,106	22,226

Table 48. Percent Difference Between Backcalculated and Predicted Moduli.

Material	Percent Difference	
	Based on Predicted Modulus Using Newly Developed Model	Based on Predicted Modulus Using Current NDOT Equation
Elko Base	5	125
Hunnewill Base	0	102
Lockwood Borrow	39	380
Jacks Valley Subgrade	42	251
SEM Soil	11	304

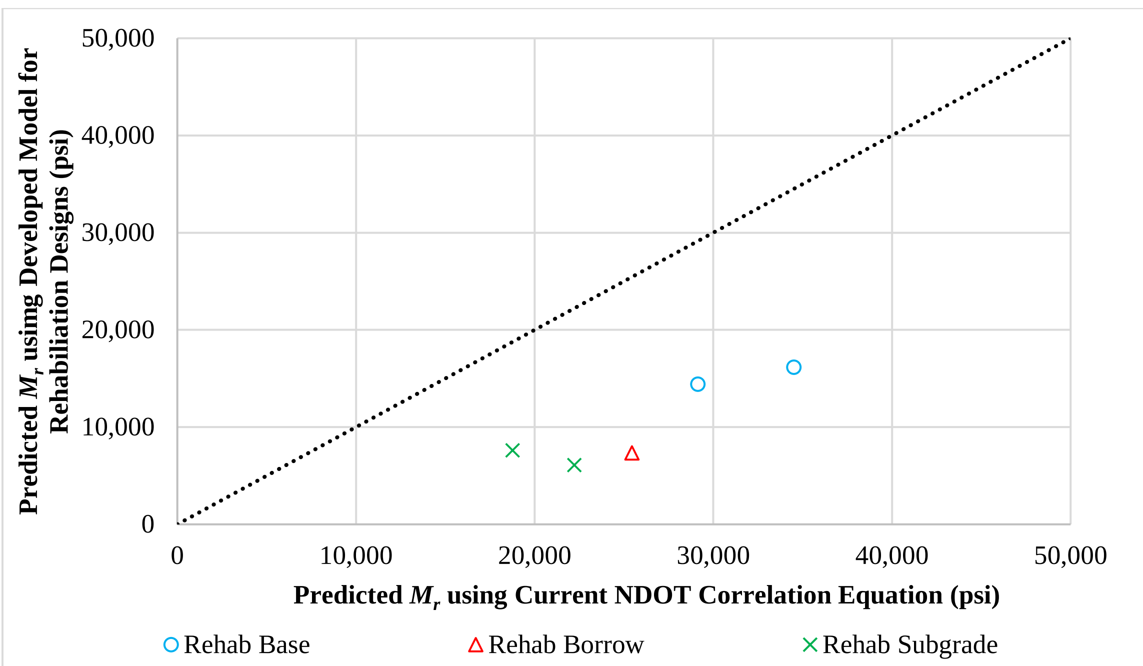

Figure 44. Comparison between current NDOT prediction model and developed M_r model for pavement rehabilitation design (Districts 2 and 3 materials).

CHAPTER 4 CONCLUSIONS

The main objective of this study was to develop a resilient modulus prediction model of unbound materials for pavement rehabilitation projects in Nevada. This objective was achieved by testing of different base, borrow, and subgrade materials sampled from all three Districts. The soil classification was conducted according to AASHTO and USCS systems. The maximum dry density and optimum moisture content were obtained by conducting the moisture density test. The resilient modulus test was conducted on the evaluated material at the optimum moisture content.

Based on the conducted analysis the following observations and conclusions can be made:

- The stress-dependent behavior of the resilient modulus for the base and borrow material fits very well the Theta model.
- The stress-dependent behavior of resilient modulus for the subgrade materials fits very well both the universal model and Uzan model.
- The resilient modulus of base and borrow materials is significantly influenced by the pavement structure.
- The rehabilitation design resilient modulus prediction model for the subgrade materials can be estimated from the following equations (refer to Table 49 for definition of model parameters).

$$\ln(Mr_{SG-Reh}) = 5.3982 + 0.0134 * \text{R-value} + 0.0125 * \text{P40} - 0.0032 * \text{P3/8} + 0.0168 * \gamma_{d-max} + 0.0177 * PI \qquad (25)$$

- The rehabilitation resilient modulus prediction model for the base materials can be estimated from the following equations (refer to Table 49 for definition of model parameters).

$$\ln(Mr_{CAB-Reh}) = 8.0140 + 0.0261 * \text{R-value} - 0.0485 * \text{P40} + 0.0161 * \text{P3/8} - 0.0659 * OMC - 0.0089 * H_{eq} \qquad (26)$$

- The rehabilitation resilient modulus prediction model for the borrow materials can be estimated from the following equations (refer to Table 49 for definition of model parameters).

$$\ln(Mr_{BOR-Reh}) = 9.2304 + 0.0136 * \text{R-value} - 0.0229 * \text{P40} + 0.0079 * \text{P3/8} - 0.0661 * OMC - 0.0127 * H_{eq} \qquad (27)$$

- The current NDOT correlation equation overestimates the resilient modulus. The equation predicts M_r from R-value only without taking into consideration any of the physical properties of the unbound materials.
- It is recommended for NDOT and local agencies to implement the developed models in this study for predicting resilient modulus of unbound materials in their

design of rehabilitated flexible pavements using AASHTO 93 or MEPDG (Level 2) approach.

- It is recommended to develop similar prediction models for estimating resilient modulus of unbound materials in Nevada for new flexible pavement design projects. Using the resilient modulus prediction models for rehabilitation designs developed in this study can over or under estimate the resilient modulus of unbound materials in new flexible pavement designs.

Table 50 to Table 52 summarizes representative inputs values for the model parameters of subgrade, base, and borrow materials. These representative values were determined based on evaluated unbound materials (i.e., subgrade, base, and borrow).

It should be noted that the developed equations will be applicable for the range of data that used to develop the models. District 1 unbound materials were used to develop the model, and District 2 and District 3 unbound materials were used to help verify the validity of this model. With more data, the model can be improved with advanced statistical analysis and the representative input values can also be updated.

Table 49. M_r Correlation Equations Parameters.

Parameter	Definition	Units	Test Procedure
R-value	Resistance R-Value	–	Nev. T115D
P40	Percent Passing No. 40 Sieve	Percent (%)	Nev. T206 ASTM D421 ASTM D422
P3/8	Percent Passing 3/8 inch	Percent (%)	Nev. T206 ASTM D421 ASTM D422
$\gamma_{d\text{-}max}$	Maximum Dry Density	pcf	Nev. T108B
OMC	Optimum Moisture Content	Percent (%)	Nev. T108B
PI	Plasticity Index	–	Nev. T212I
H_{eq}	Equivalent Thickness	Inch	–

–Not applicable.

Table 50. Representative Input Values for M_r Correlation Equations Parameters of Subgrade Materials.

Parameter	District 1	District 2	District 3
R-value	78	63	–
P40 (%)	28.0	96.8	–
P3/8 (%)	68.2	100.0	–
$\gamma_{d\text{-}max}$ (pcf)	133.6	129.2	–
OMC (%)	7.1	8.9	–
PI	2.2	3.0	–

–No data.

Table 51. Representative Input Values for M_r Correlation Equations Parameters of Base Materials.

Parameter	District 1	District 2	District 3
R-value	79	84	76
P40 (%)	16.5	14.8	17.3
P3/8 (%)	69.5	64.5	71.3
$\gamma_{d\text{-}max}$ (pcf)	139.5	134.5	140.3
OMC (%)	7.1	7.2	6.1
PI	3.4	3.7	4.7
H_{eq} (inch)	2.399**D* – 1.7468	2.399**D* – 1.7468	2.399**D* – 1.7468
D (inch)	Depth of critical location (at quarter depth of layer)	Depth of critical location (at quarter depth of layer)	Depth of critical location (at quarter depth of layer)

–No specification.

Table 52. Representative Input Values for M_r Correlation Equations Parameters of Borrow Materials.

Parameter	District 1	District 2	District 3
R-value	79	73	74
P40 (%)	38.4	26.6	13.8
P3/8 (%)	86.5	91.5	68.9
$\gamma_{d\text{-}max}$ (pcf)	135.3	122.8	129.4
OMC (%)	7.4	9.6	8.9
PI	2.5	14.6	–
H_{eq} (inch)	1.543**D* + 8.044	1.543**D* + 8.044	1.543**D* + 8.044
D (inch)	Depth of critical location (at quarter depth of layer)	Depth of critical location (at quarter depth of layer)	Depth of critical location (at quarter depth of layer)

–No data.

CHAPTER 5 REFERENCES

1. AASHTO. (2008). *Mechanistic-Empirical Pavement Design Guide: A Manual of Practice: Interim Edition*. American Association of State Highway and Transportation Officials.
2. Hajj, E.Y., P.E. Sebaaly, and P. Nabhan, *Manual for Designing Flexible Pavements in Nevada using the AASHTOWare Pavement ME*, Western Regional Superpave Center, University of Nevada, Reno, Draft Final Report to Nevada DOT, July 2015.
3. Schwartz, C. W., Li, R., Kim, S., Ceylan, H., and Gopalakrishnan, K. (2013). "Global Sensitivity Analysis of Mechanistic Empirical Pavement Design Guide for Flexible Pavements." *Transportation Research Record*, 2368, 12–23.
4. Von Quintus, H. L., Boudreau, R., and Cooley, A. (2015). *Precision and Bias of Resilient Modulus Test*. Washington D.C.
5. ARA, and ERES Consultants. (2004). *Guide for Mechanistic-Emperical Design of New and Rehabilitated Pavement Structures - Final Report Chapter 2: Design Inputs-Material Characterizations*. National Cooperative Highway Research Program, Washington DC.
6. AASHTOWare Pavement ME Design software. American Association of State Highway and Transportation Officials (AASHTO), http://me-design.com/MEDesign/.
7. Puppala, A. J. (2008). *Estimating Stiffness of Subgrades and Unbound Materials for Pavement Design*. Transportation Research Board, Washington DC.
8. Yau, A., and Von Quintus, H. (2002). *Study of LTPP Laboratory Resilient Modulus Test Data and Response Characteristics*. Federal Highway Administration, Washington, DC.
9. Ceylan, H., Kim, S., Gopalakrishnan, K., and Smadi, O. G. (2009). *MEPDG Work Plan Task No. 8 : Validation of Pavement Performance Curves for the Mechanistic-Empirical Pavement Design Guide MEPDG Work Plan Task No . 8 : Validation of Pavement Performance Curves for the Mechanistic-Empirical Pavement Design Guide Final R*. Iowa Department of Transportation, Ames, IA.
10. Mokwa, R., and Akin, M. (2009). *Measurement and Evaluation of Subgrade Soil Parameters: Phase I–Synthesis of Literature*. Montana Department of Transportation, Helena, MT.
11. Thompson, M. R., & Elliot, R. P. (1985). ILLI-PAVE based response algorithms for design of conventional flexible pavements. *Transportation Research Record*, *1043*, 50-57.
12. R Core Team (2017). R: A language and environment for statistical computing. R Foundation for Statistical Computing, Vienna, Austria.
13. D'Agostino, R. B. (1986). Tests for the normal distribution. *Goodness-of-fit techniques*, *68*, 576.
14. Fox, J., & Monette, G. (1992). Generalized collinearity diagnostics. *Journal of the American Statistical Association*, *87*(417), 178-183.

CHAPTER 6 APPENDIX A

Laboratory test results are shown in this appendix, including moisture-density relationships and resilient modulus tests.

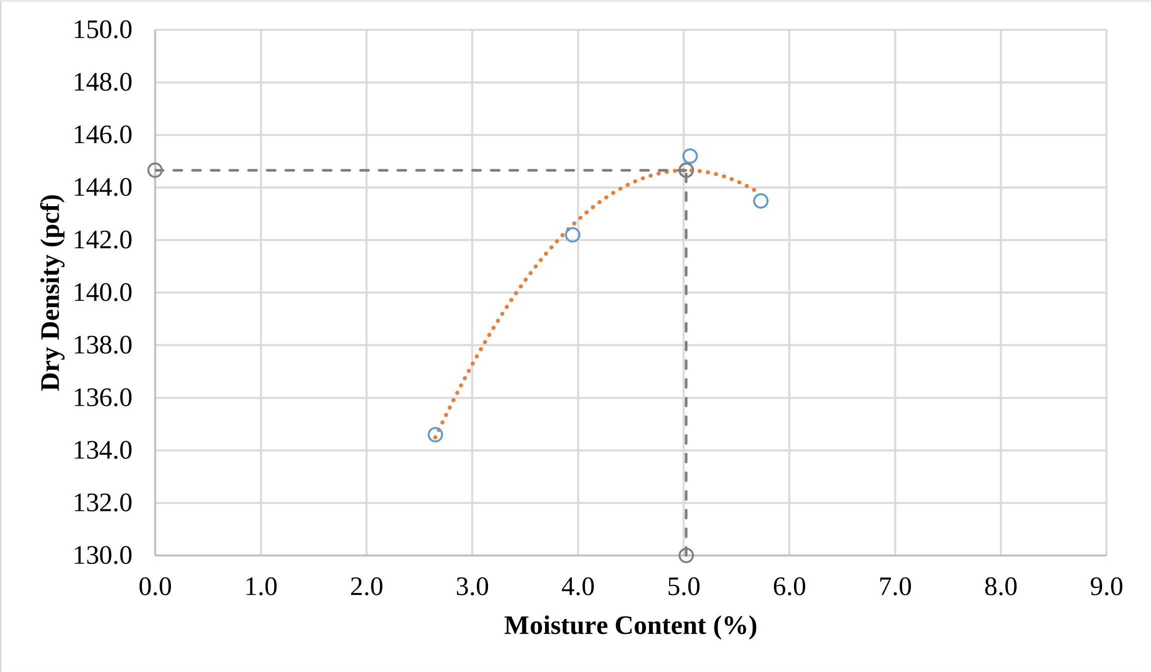

Figure 45. Moisture-density curve for base material (contract 3546).

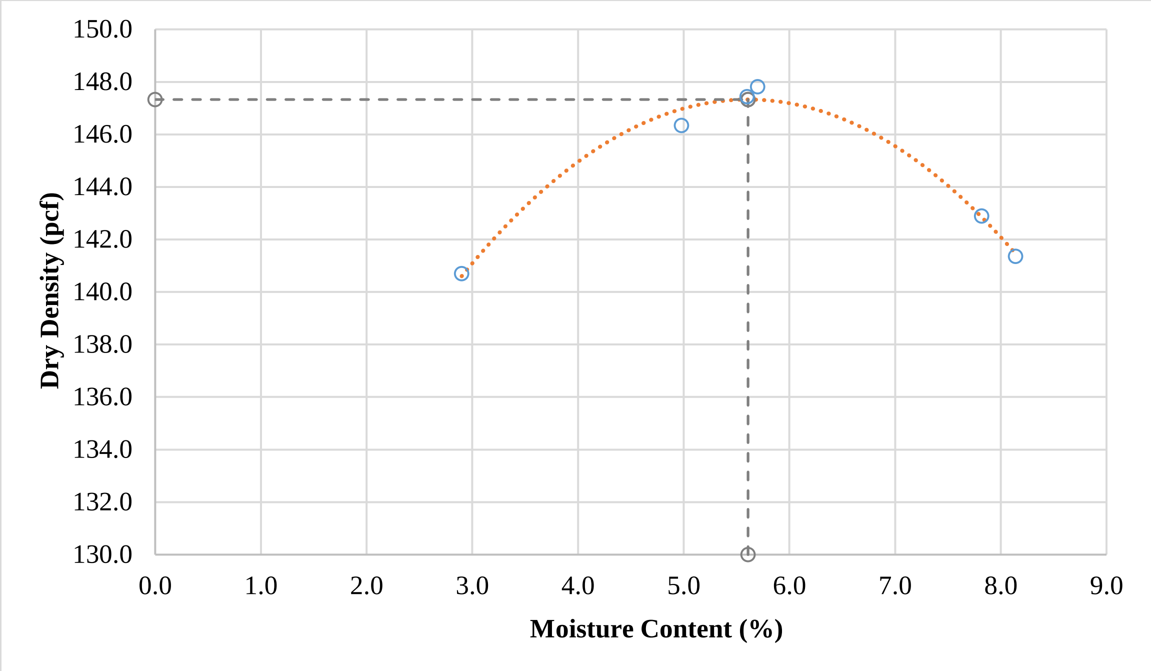

Figure 46. Moisture-density curve for base material (contract 3583).

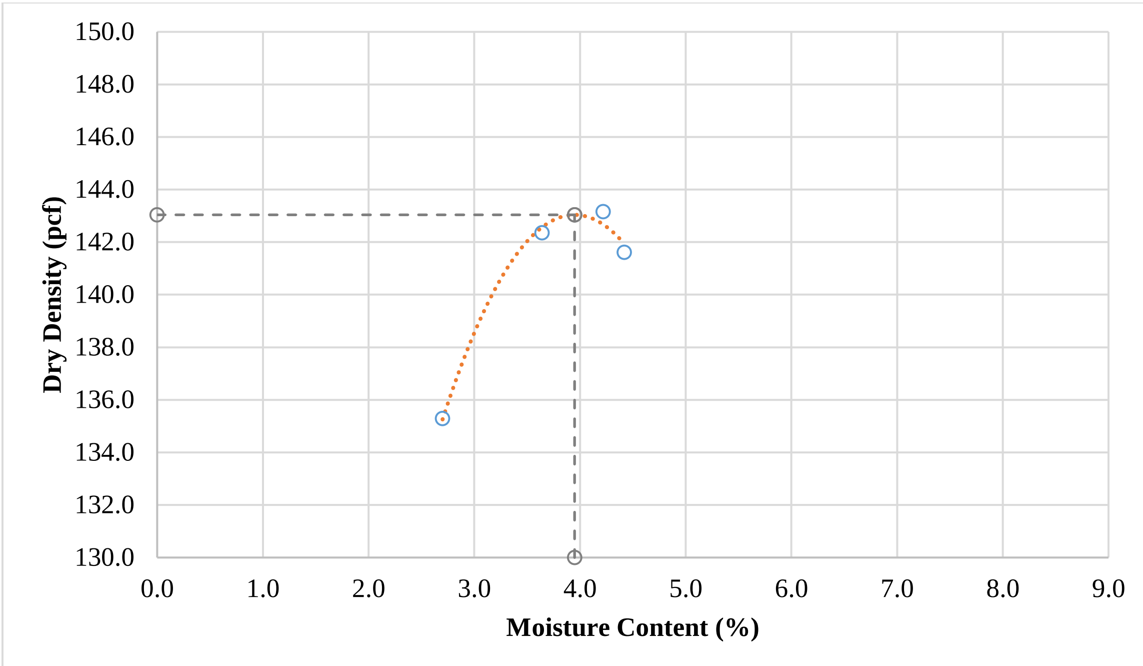

Figure 47. Moisture-density curve for base material (contract 3597).

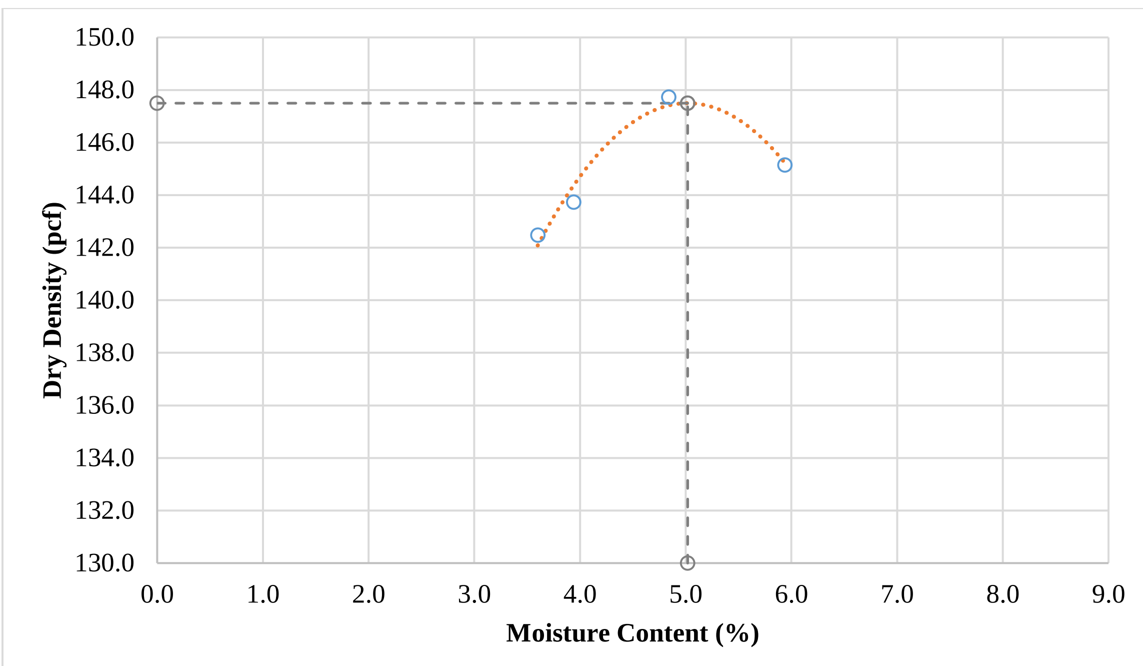

Figure 48. Moisture-density curve for base material (contract 3605).

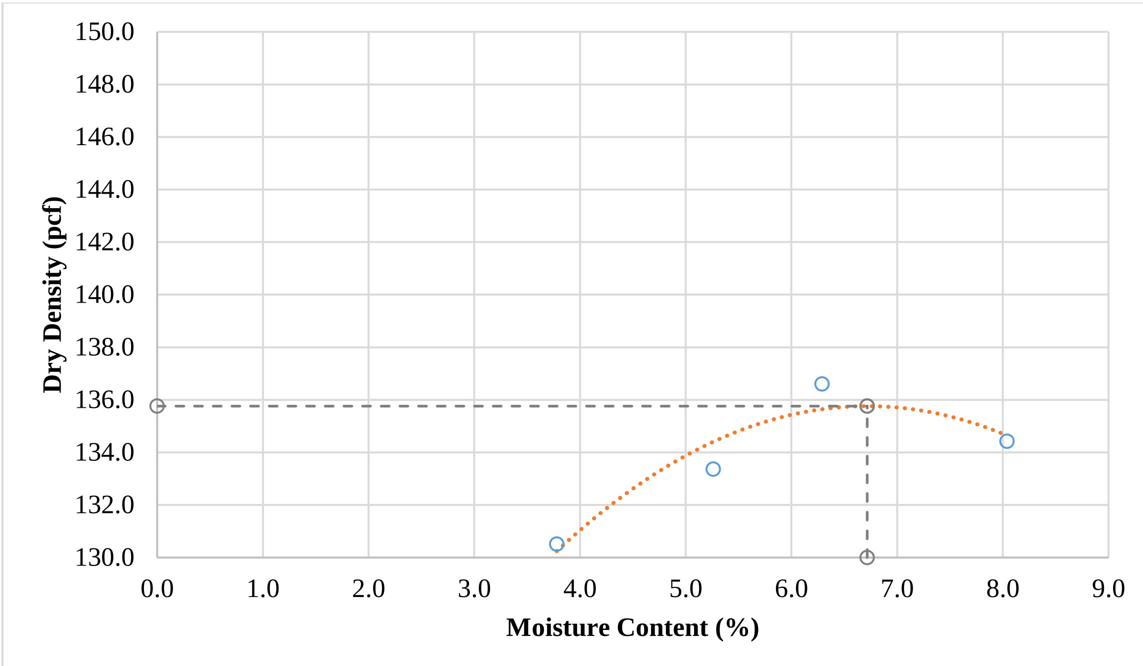

Figure 49. Moisture-density curve for base material (contract 3607).

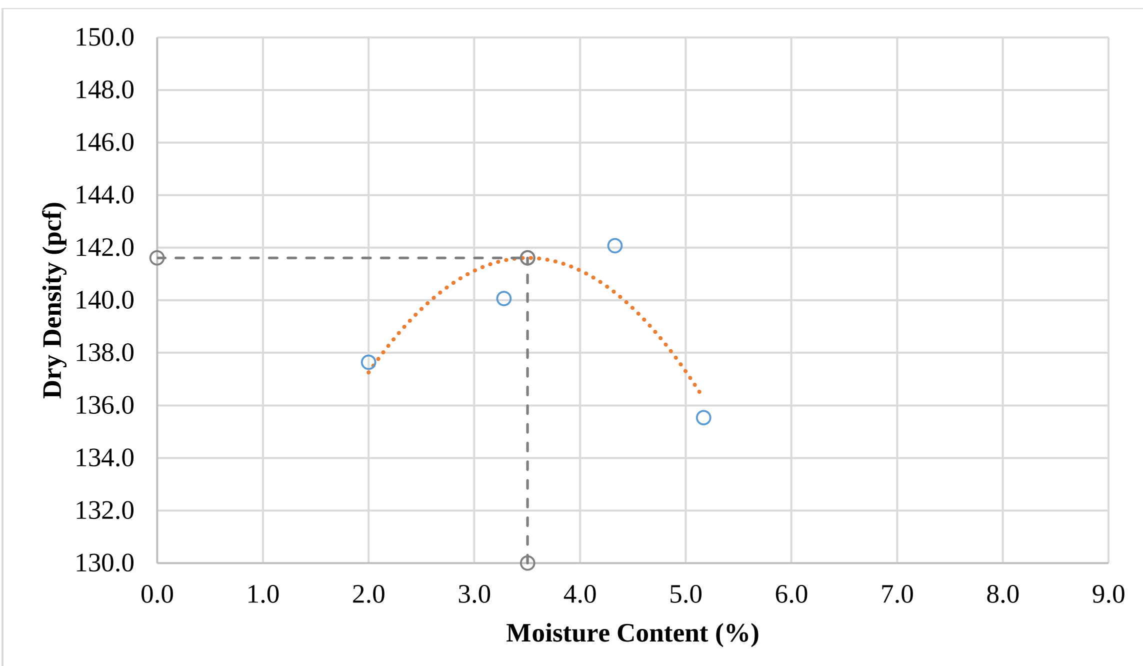

Figure 50. Moisture-density curve for base material (contract 3613).

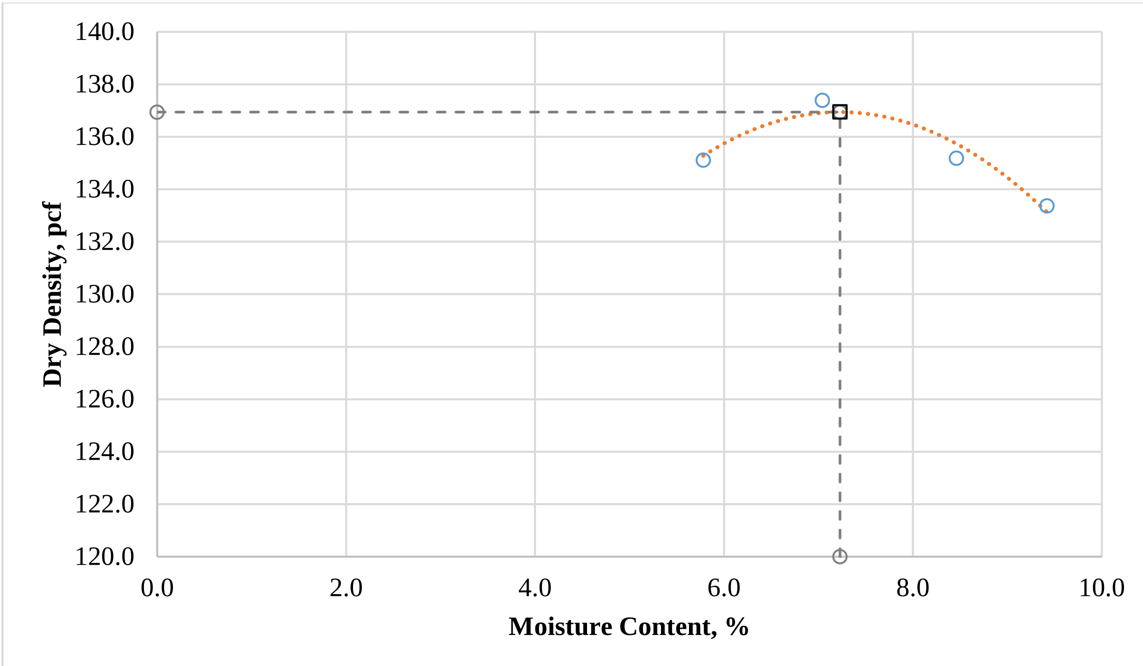

Figure 51. Moisture-density curve for borrow material (contract 3546).

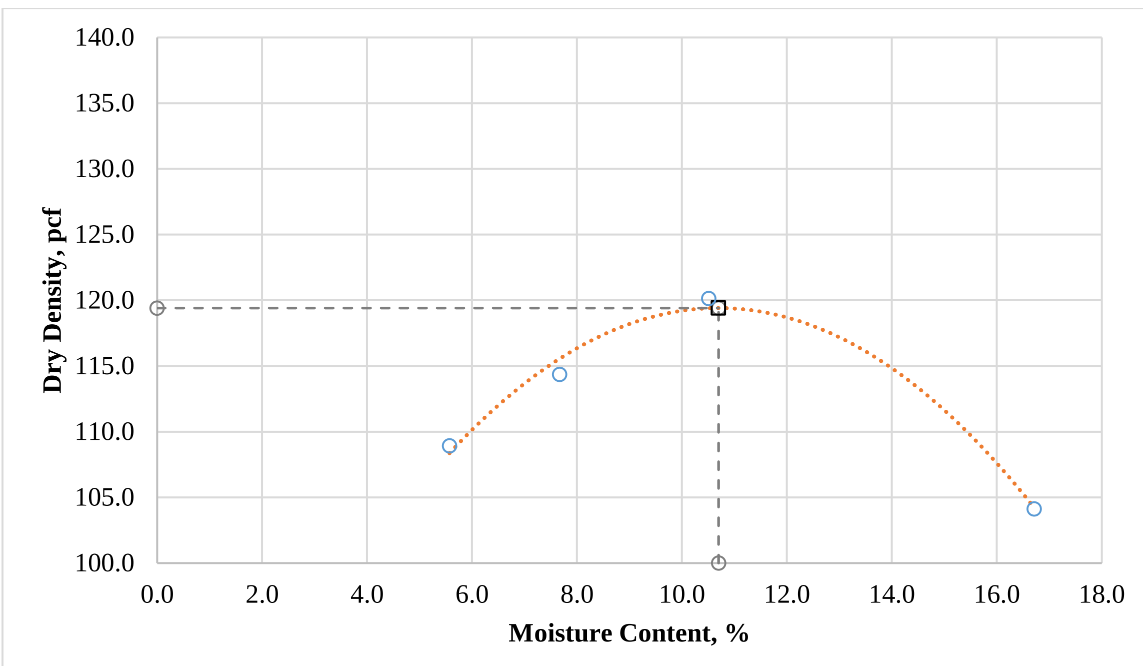

Figure 52. Moisture-density curve for borrow material (contract 3583).

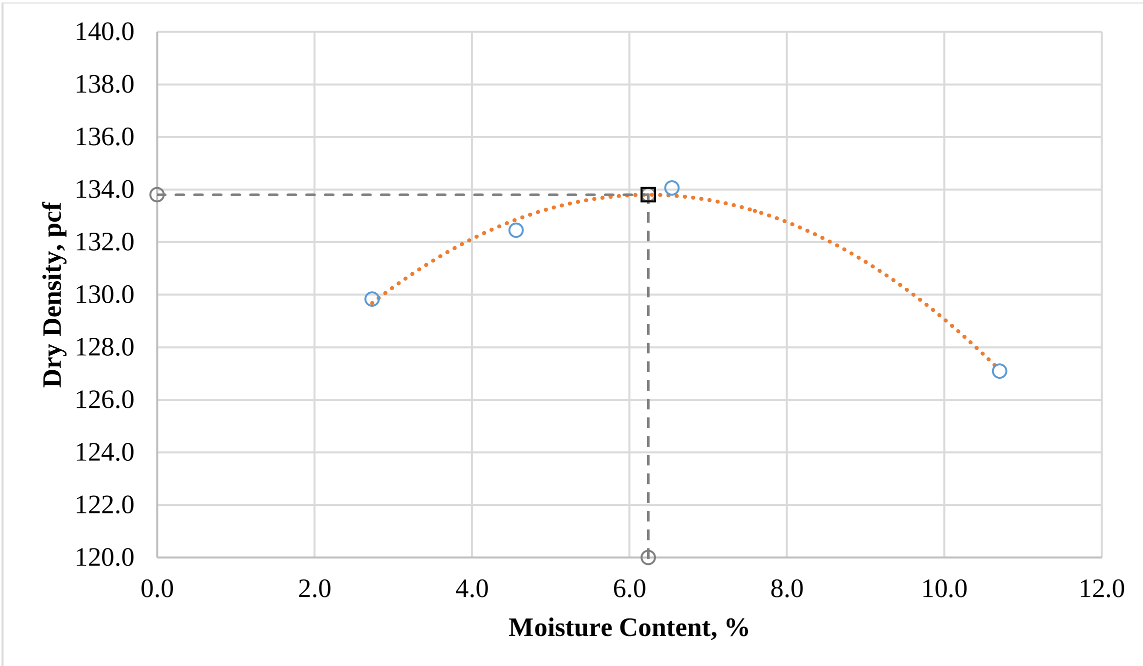

Figure 53. Moisture-density curve for borrow material (contract 3597).

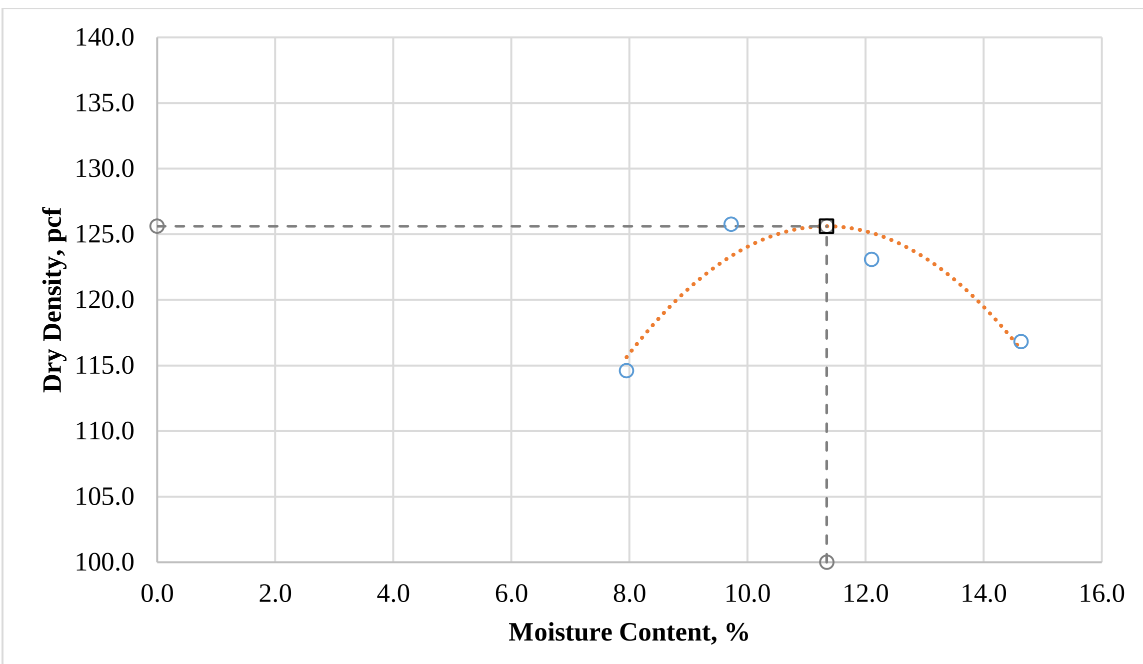

Figure 54. Moisture-density curve for borrow material (contract 3607).

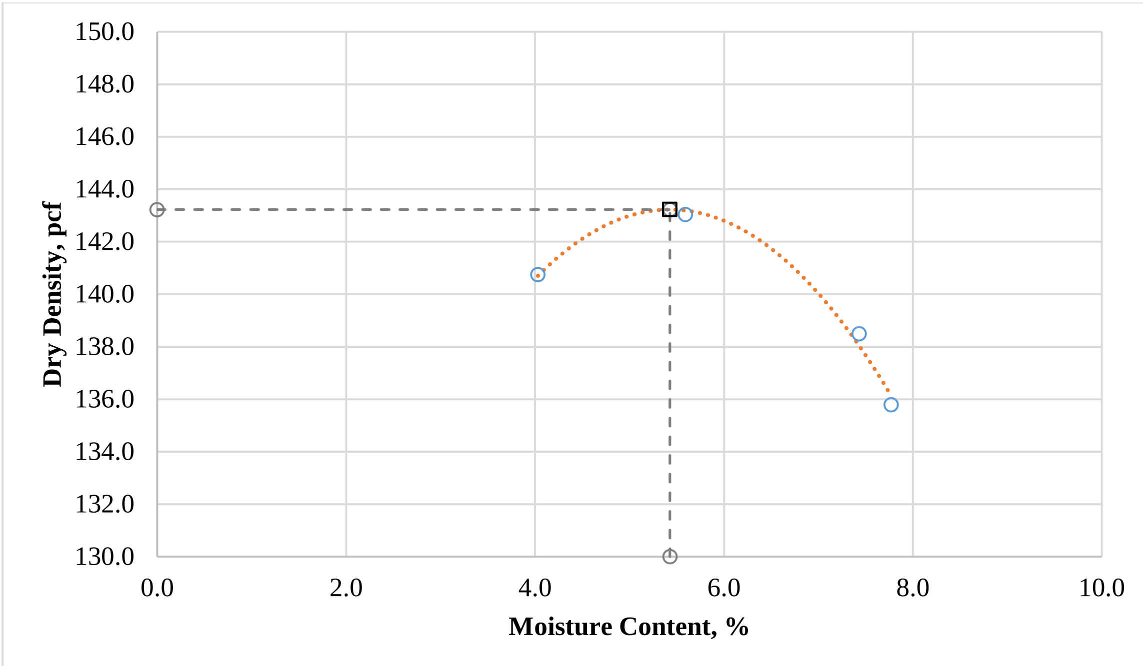

Figure 55. Moisture-density curve for borrow material (contract 3613).

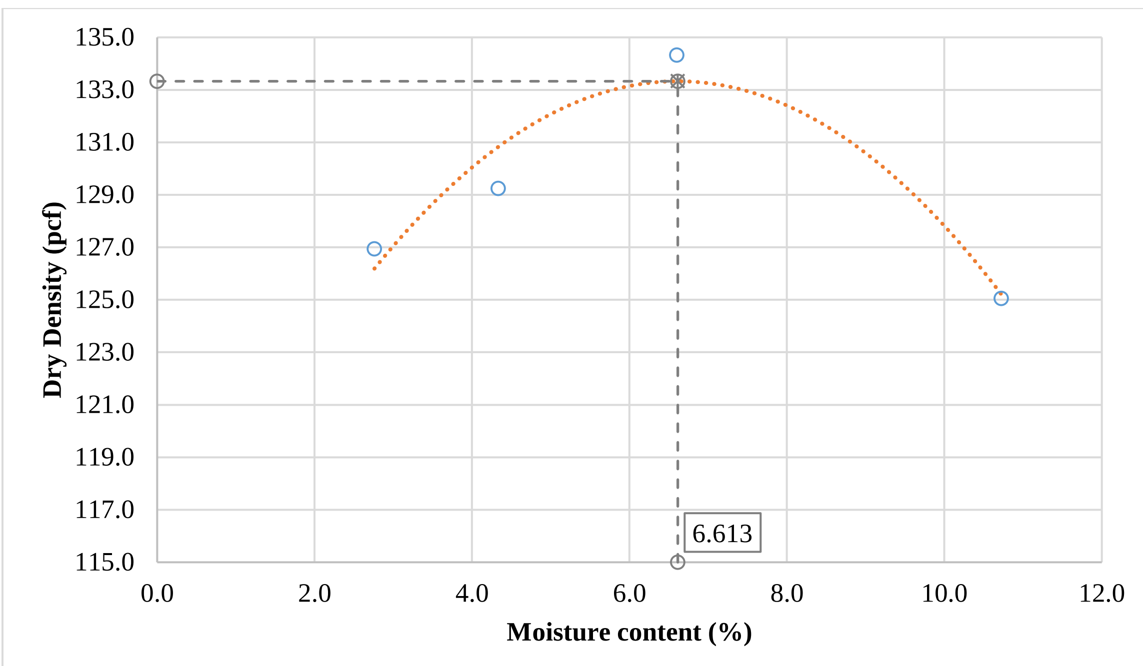

Figure 56. Moisture-density curve for subgrade material (US-95/Searchlight).

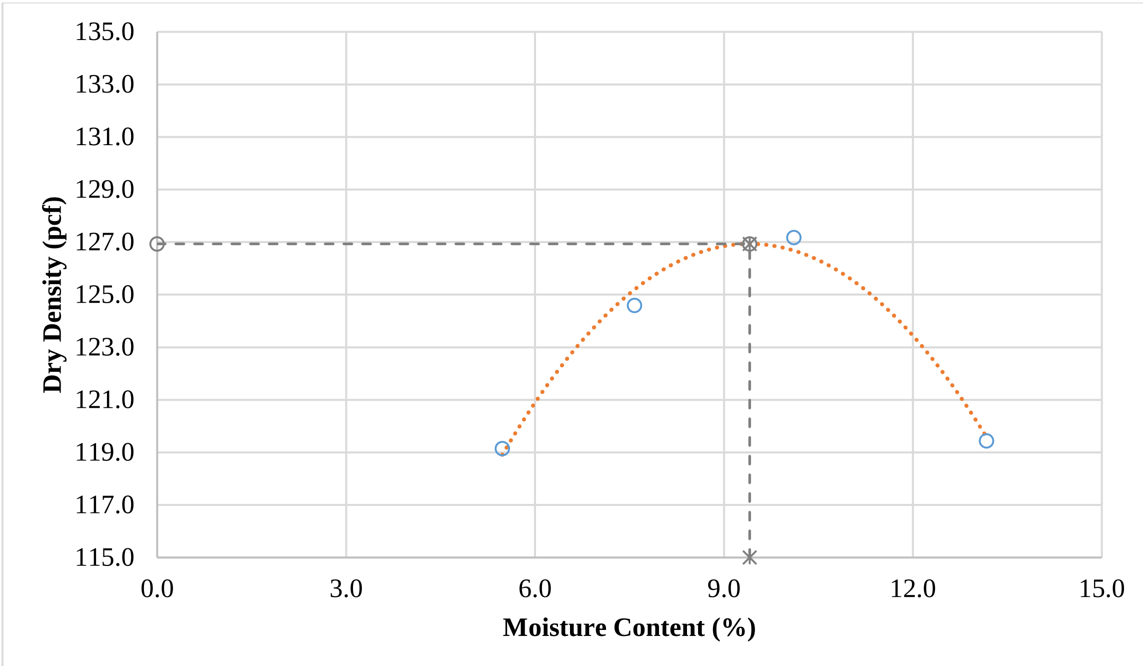

Figure 57. Moisture-density curve for subgrade material (US-95/Bonnie Claire).

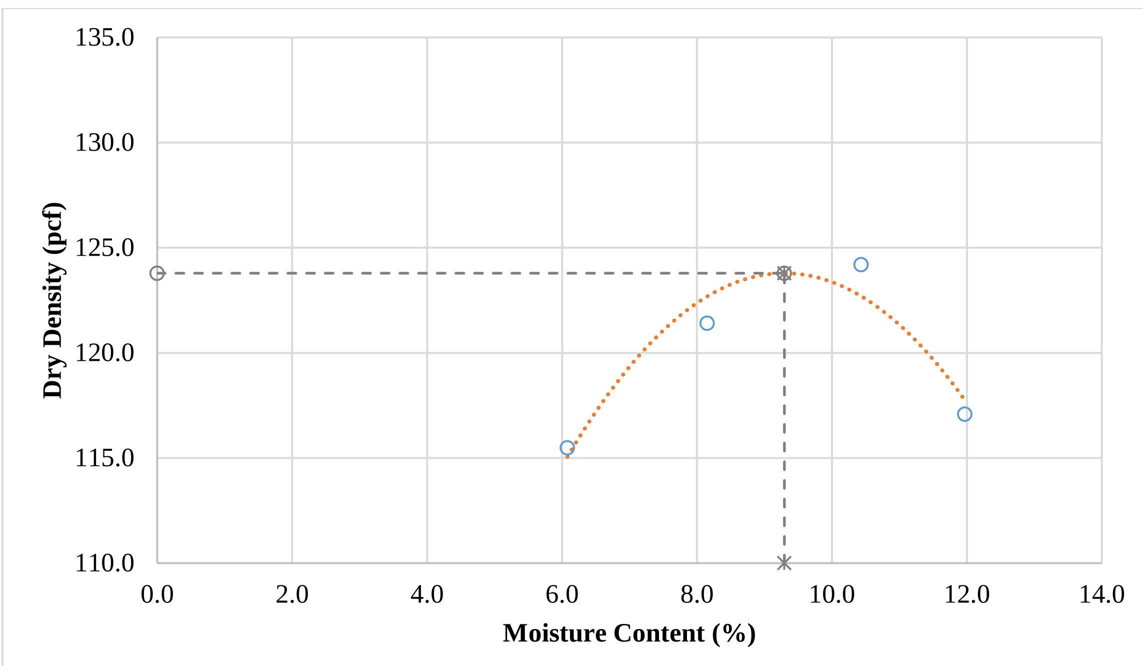

Figure 58. Moisture-density curve for subgrade material US-93/Crystal Spring MP67).

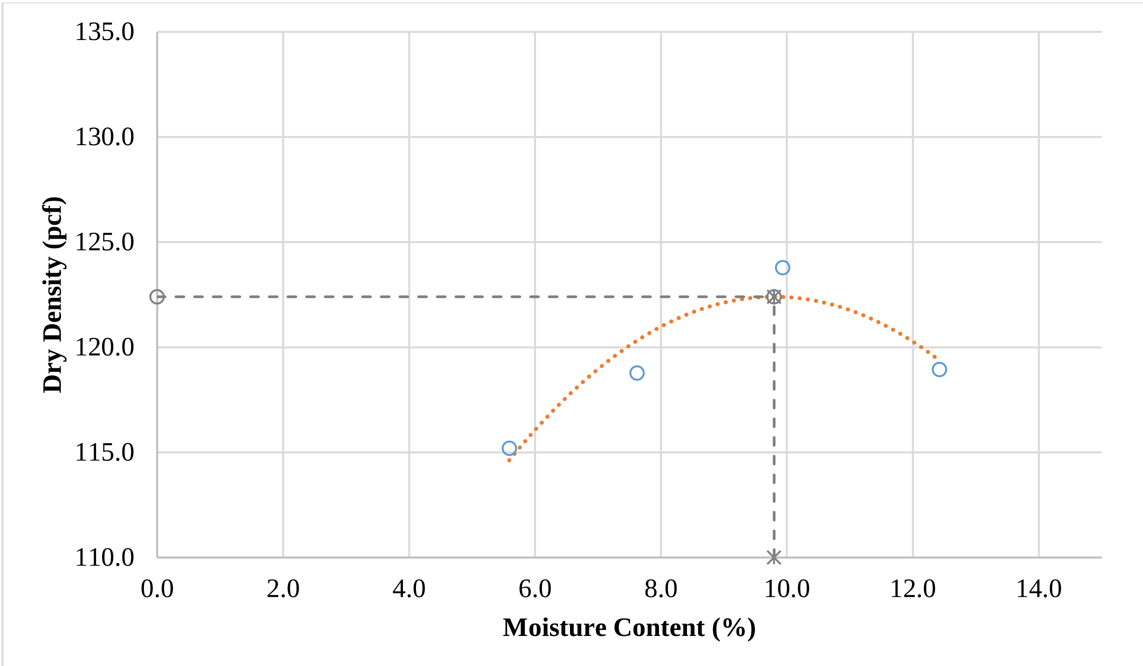

Figure 59. Moisture-density curve for subgrade material (US-93/Crystal Spring MP62).

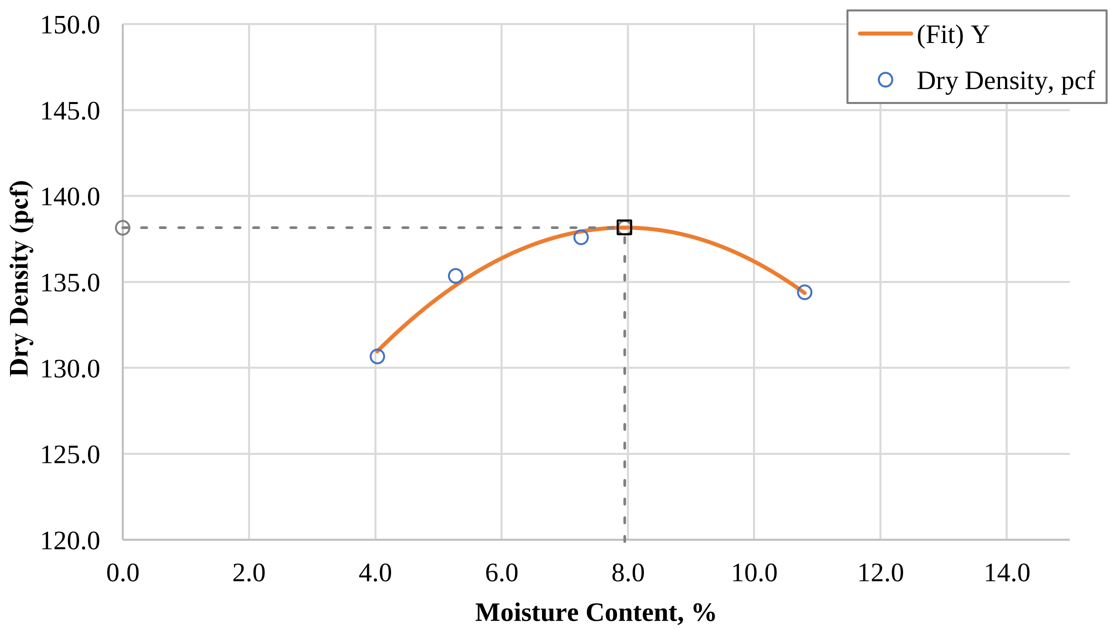

Figure 60. Moisture-density curve for Lockwood base.

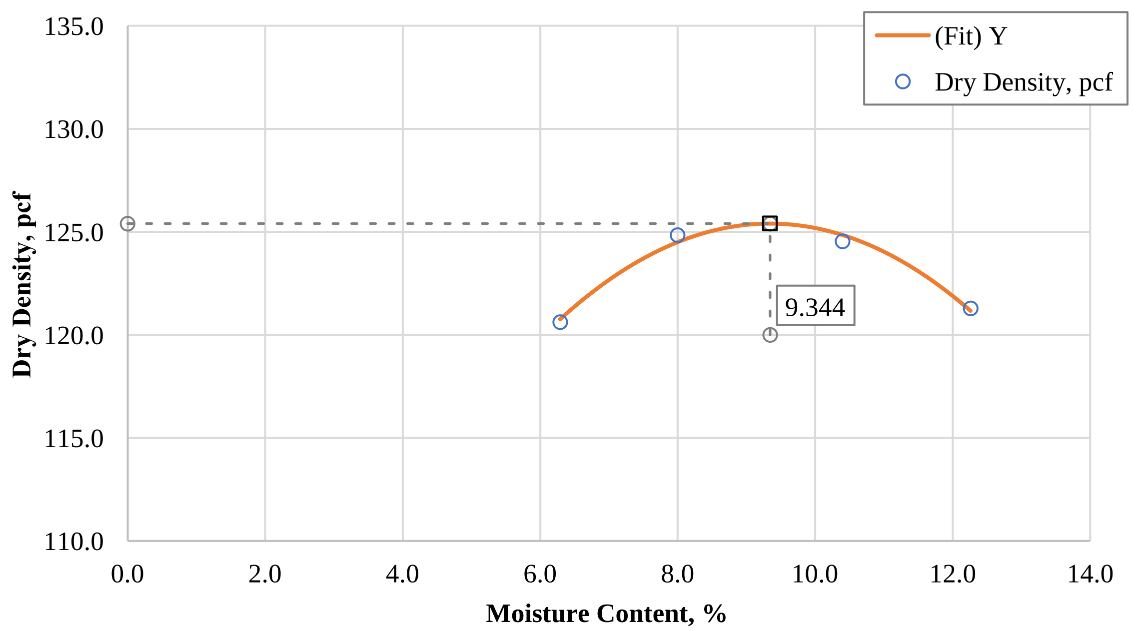

Figure 61. Moisture-density curve for Lockwood borrow.

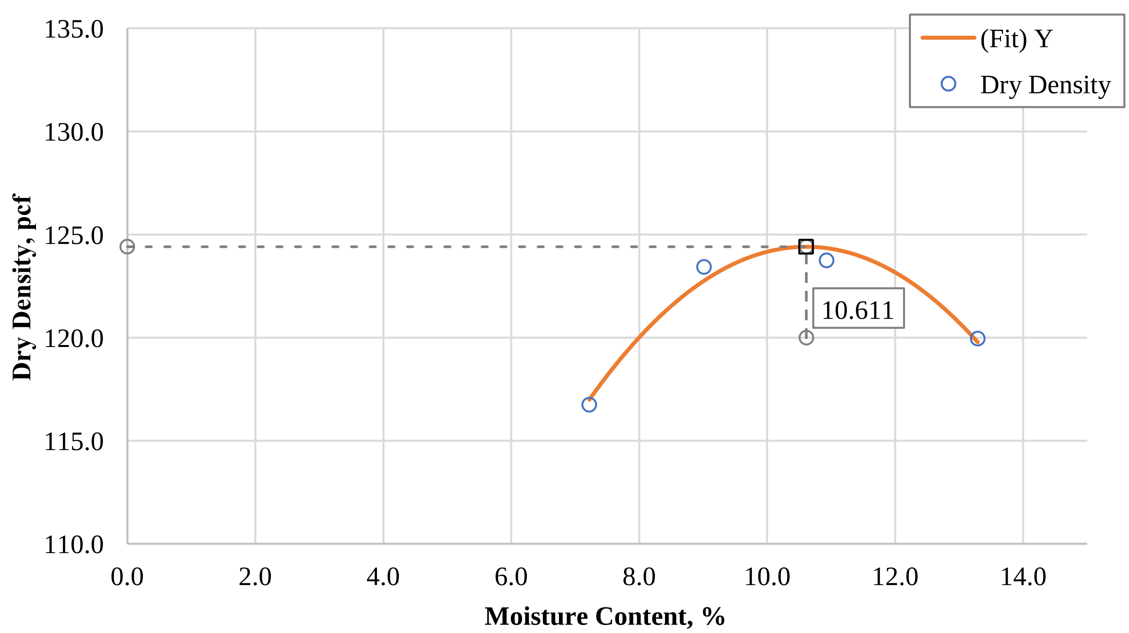

Figure 62. Moisture-density curve for SNC Primary borrow.

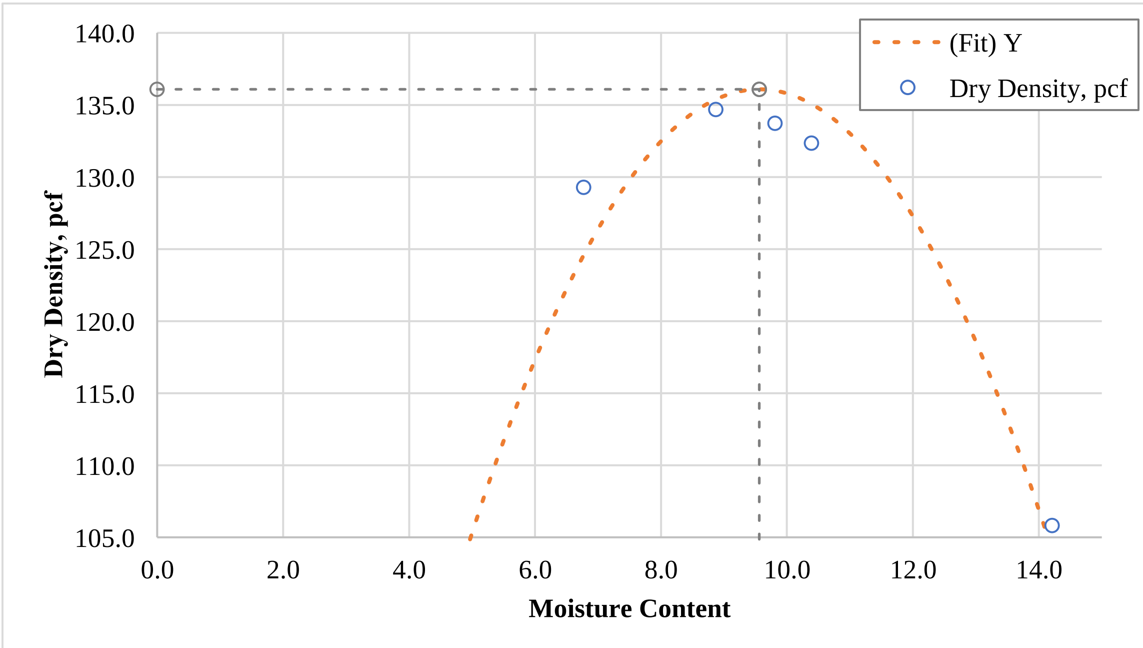

Figure 63. Moisture-density curve for SNC Secondary borrow.

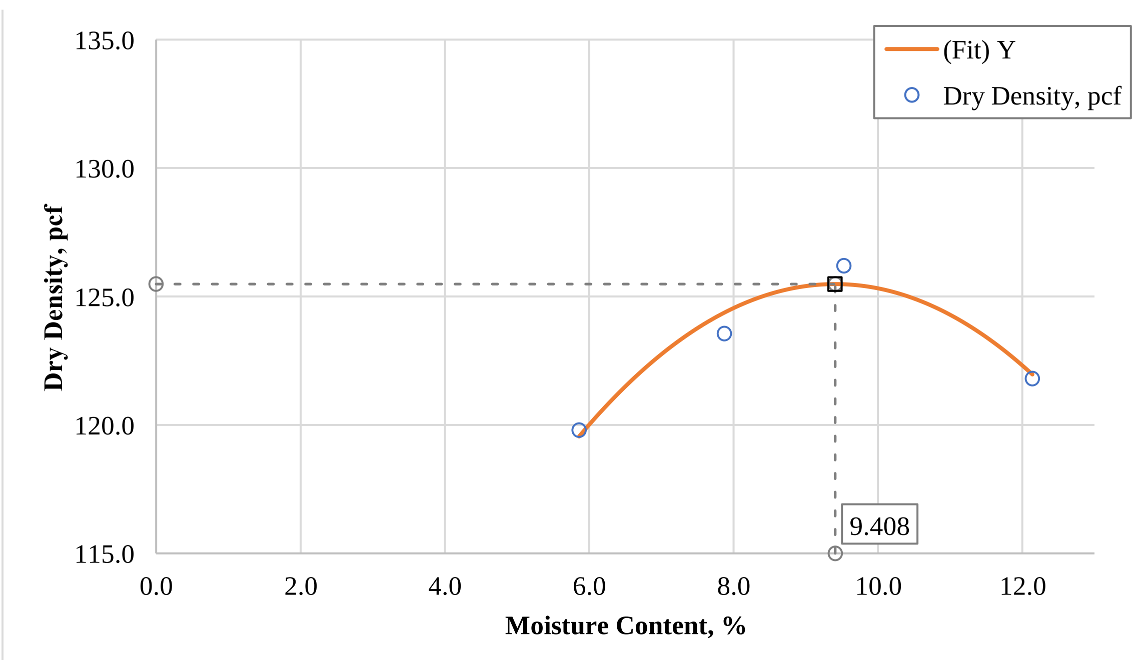

Figure 64. Moisture-density curve for Jacks Valley subgrade.

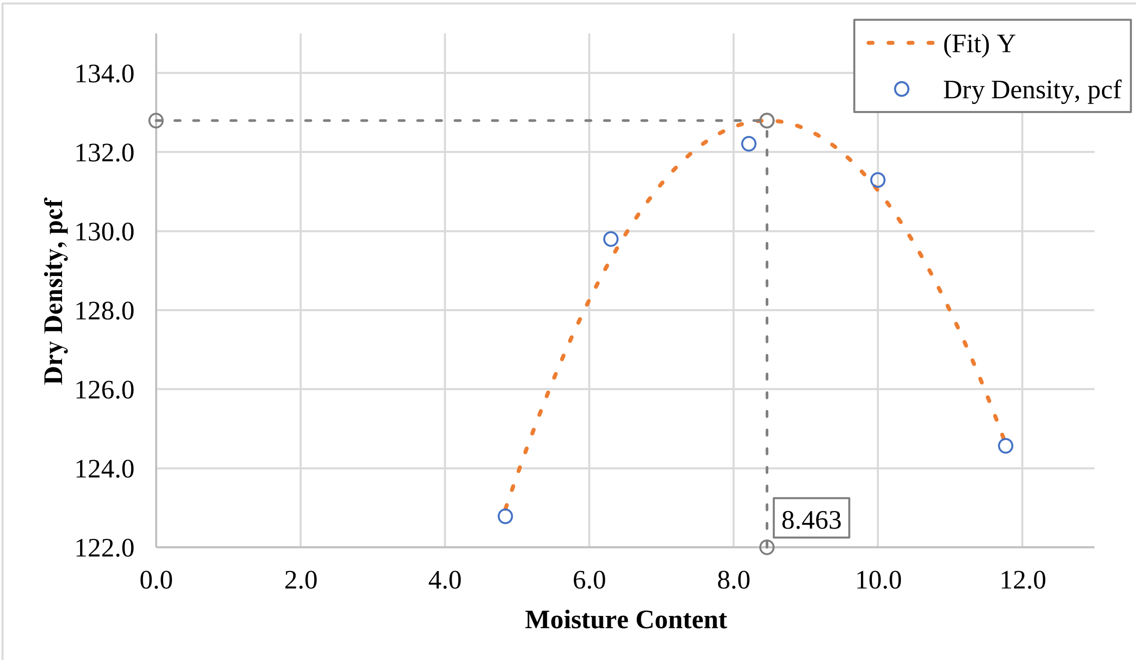

Figure 65. Moisture-density curve for SEM Soil at UNR.

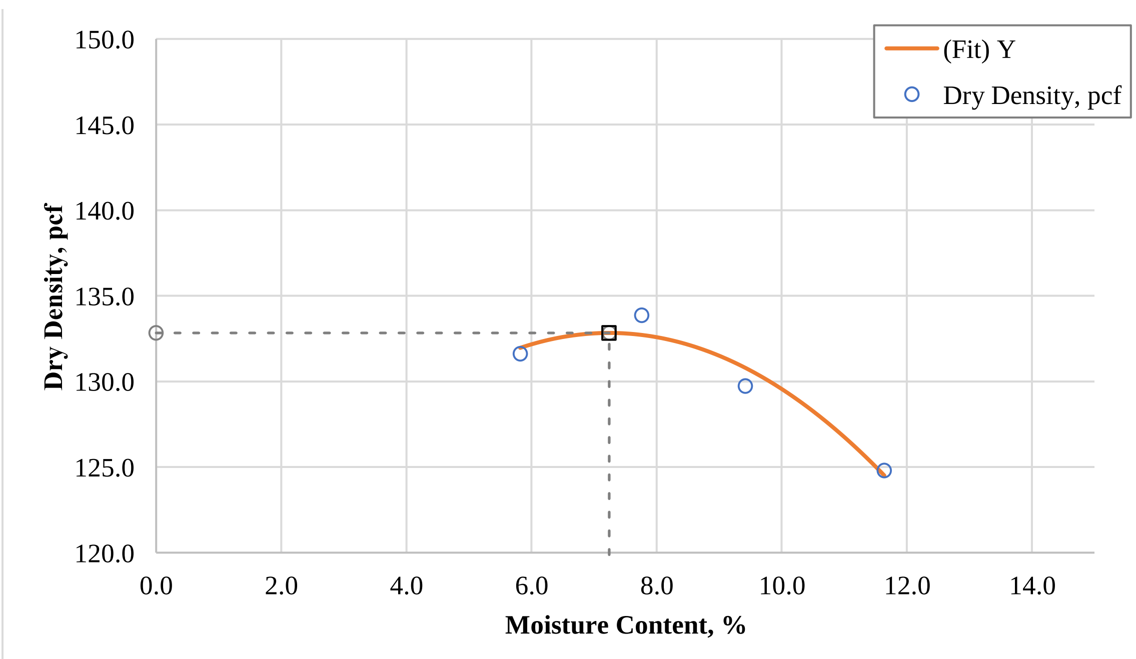

Figure 66. Moisture-density curve for Hunnewill base.

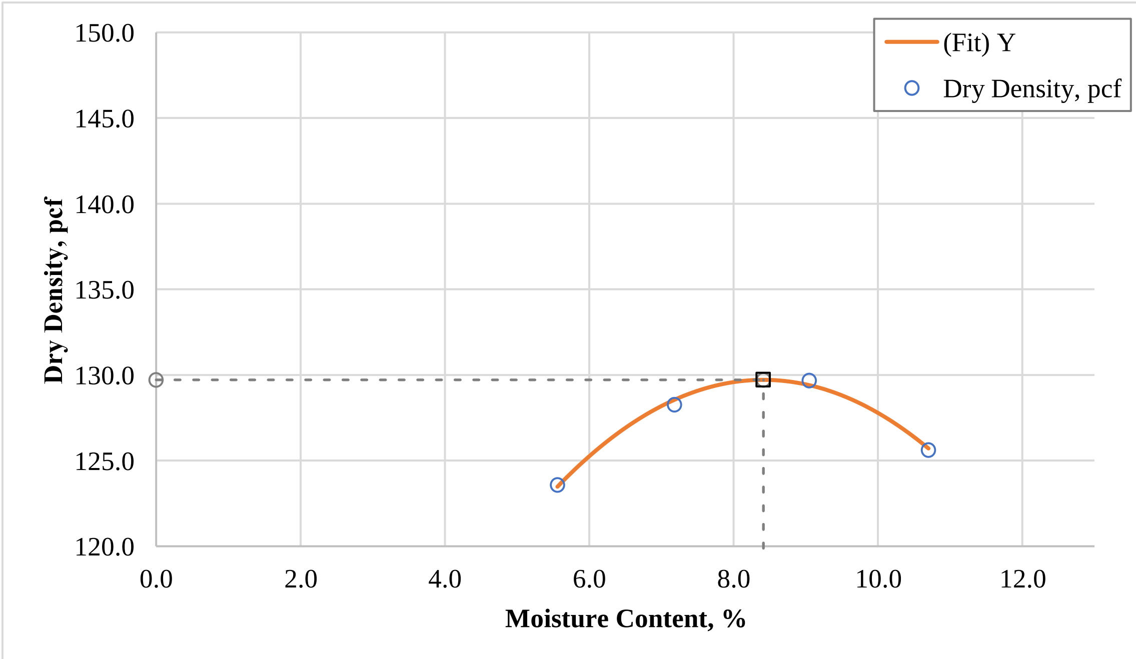

Figure 67. Moisture-density curve for Elko base.

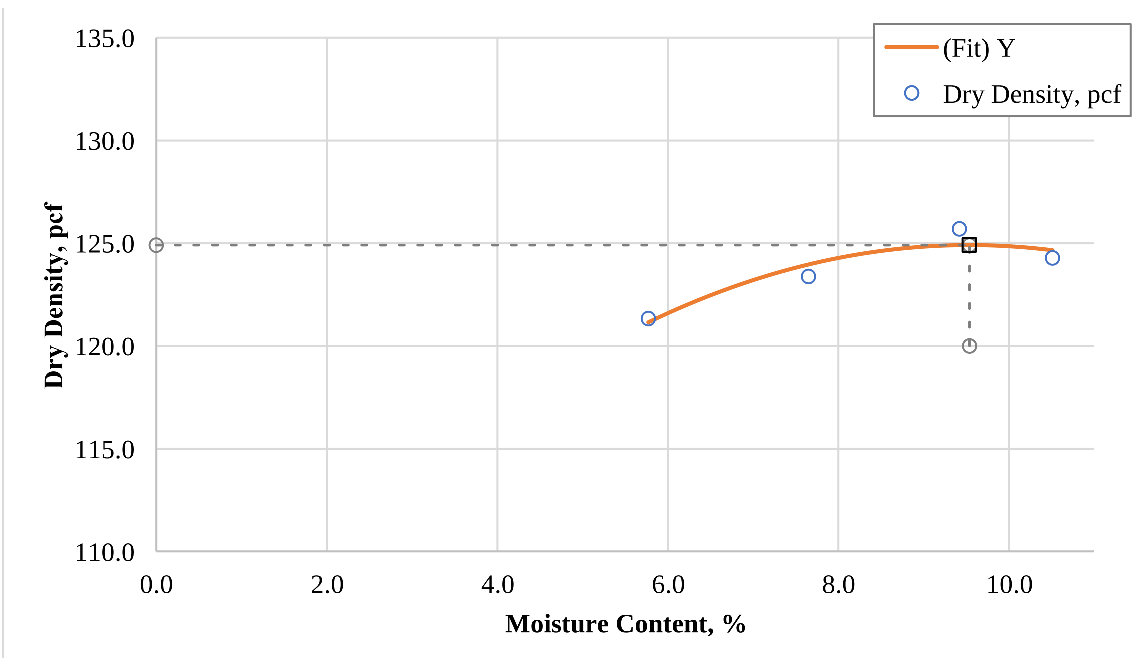

Figure 68. Moisture-density curve for Elko borrow.

Table 53. Resilient Modulus Test Results for Base Material (Contract 3546).

Sequence	Cyclic Axial Stress (psi)	Contact Stress (psi)	Confinement Stress (psi)	Axial Resilient Modulus (psi)	Deviator Stress, σ_d (psi)	Major Principal Stress, σ_1 (psi)	Minor Principal Stress, σ_3 (psi)	Bulk Stress, θ (psi)	Octahedral Shear Stress (psi)
1	13.5	1.5	14.8	46,385	15.0	29.8	14.8	59.5	7.1
2	2.7	0.3	2.8	22,854	3.0	5.8	2.8	11.4	1.4
3	5.3	0.6	2.8	23,661	5.9	8.8	2.8	14.4	2.8
4	8.1	0.9	2.8	25,371	9.0	11.8	2.8	17.5	4.2
5	4.5	0.5	4.8	25,231	5.0	9.9	4.8	19.5	2.4
6	9.0	1.0	4.8	28,698	10.0	14.8	4.8	24.4	4.7
7	13.5	1.5	4.8	30,357	15.0	19.9	4.8	29.5	7.1
8	9.0	1.0	9.8	35,372	10.0	19.8	9.8	39.4	4.7
9	18.0	2.0	9.8	41,542	20.0	29.8	9.8	49.5	9.4
10	26.8	3.0	9.8	43,812	29.8	39.7	9.8	59.3	14.1
11	9.0	1.0	14.8	39,750	10.0	24.8	14.8	54.5	4.7
12	13.5	1.5	14.8	43,625	15.0	29.8	14.8	59.4	7.1
13	26.8	3.0	14.8	49,674	29.8	44.6	14.8	74.3	14.0
14	13.7	1.5	19.8	49,374	15.2	35.0	19.8	74.6	7.1
15	18.1	2.0	19.8	53,101	20.1	39.9	19.8	79.6	9.5
16	34.6	4.0	19.8	59,304	38.6	58.4	19.8	98.0	18.2

Table 54. Resilient Modulus Test Results for Base Material (Contract 3583).

Sequence	Cyclic Axial Stress (psi)	Contact Stress (psi)	Confinement Stress (psi)	Axial Resilient Modulus (psi)	Deviator Stress, σ_d (psi)	Major Principal Stress, σ_1 (psi)	Minor Principal Stress, σ_3 (psi)	Bulk Stress, θ (psi)	Octahedral Shear Stress (psi)
1	13.4	1.5	14.9	37,900	14.9	29.9	14.9	59.8	7.0
2	2.7	0.3	2.9	17,271	3.0	5.9	2.9	11.8	1.4
3	5.4	0.6	2.9	19,119	6.0	8.9	2.9	14.8	2.8
4	8.0	0.9	3.0	20,614	8.9	11.9	3.0	17.8	4.2
5	4.5	0.5	4.9	21,228	5.0	10.0	4.9	19.9	2.4
6	9.0	1.0	4.9	24,154	10.0	15.0	4.9	24.9	4.7
7	13.4	1.5	5.0	26,025	14.9	19.9	5.0	29.8	7.0
8	9.0	1.0	10.0	30,687	10.0	19.9	10.0	39.9	4.7
9	18.0	2.0	9.9	33,837	20.0	29.9	9.9	49.8	9.4
10	27.0	3.0	9.9	35,517	30.0	40.0	9.9	59.9	14.2
11	9.0	1.0	14.9	32,838	10.0	24.9	14.9	54.8	4.7
12	13.5	1.5	15.0	35,322	15.0	30.0	15.0	59.9	7.1
13	26.9	3.0	15.0	40,462	29.9	44.8	15.0	74.8	14.1
14	13.7	1.5	19.9	39,028	15.2	35.1	19.9	75.0	7.2
15	18.1	2.0	19.9	41,872	20.1	40.0	19.9	79.9	9.5
16	17.4	4.0	19.9	38,051	21.4	41.4	19.9	81.3	10.1

Table 55. Resilient Modulus Test Results for Base Material (Contract 3597).

Sequence	Cyclic Axial Stress (psi)	Contact Stress (psi)	Confinement Stress (psi)	Axial Resilient Modulus (psi)	Deviator Stress, σ_d (psi)	Major Principal Stress, σ_1 (psi)	Minor Principal Stress, σ_3 (psi)	Bulk Stress, θ (psi)	Octahedral Shear Stress (psi)
1	13.5	1.5	14.7	43,837	15.0	29.7	14.7	59.2	7.1
2	2.7	0.3	2.7	18,985	3.0	5.7	2.7	11.2	1.4
3	5.4	0.6	2.7	21,208	6.0	8.8	2.7	14.2	2.8
4	8.0	0.9	2.7	22,543	8.9	11.6	2.7	17.1	4.2
5	4.5	0.5	4.7	23,140	5.1	9.8	4.7	19.3	2.4
6	9.0	1.0	4.7	26,244	10.0	14.7	4.7	24.2	4.7
7	13.5	1.5	4.7	28,732	15.0	19.7	4.7	29.2	7.1
8	9.1	1.0	9.7	32,788	10.1	19.9	9.7	39.4	4.8
9	18.0	2.0	9.7	38,023	20.1	29.8	9.7	49.3	9.5
10	26.9	3.0	9.7	40,903	29.9	39.7	9.7	59.1	14.1
11	9.0	1.0	14.7	36,665	10.0	24.8	14.7	54.2	4.7
12	13.5	1.5	14.7	39,178	15.0	29.7	14.7	59.2	7.1
13	26.9	3.0	14.7	47,096	29.9	44.6	14.7	74.1	14.1
14	13.6	1.5	19.7	43,398	15.1	34.8	19.7	74.3	7.1
15	18.2	2.0	19.7	49,003	20.3	40.0	19.7	79.5	9.5
16	34.5	4.0	19.7	56,815	38.5	58.3	19.7	97.7	18.2

Table 56. Resilient Modulus Test Results for Base Material (Contract 3605).

Sequence	Cyclic Axial Stress (psi)	Contact Stress (psi)	Confinement Stress (psi)	Axial Resilient Modulus (psi)	Deviator Stress, σ_d (psi)	Major Principal Stress, σ_1 (psi)	Minor Principal Stress, σ_3 (psi)	Bulk Stress, θ (psi)	Octahedral Shear Stress (psi)
1	13.5	1.5	15.0	38,800	15.0	29.9	15.0	59.8	7.1
2	2.7	0.3	3.0	15,056	3.0	6.0	3.0	11.9	1.4
3	5.3	0.6	3.0	16,734	5.9	8.9	3.0	14.8	2.8
4	8.1	0.9	2.9	18,600	9.0	12.0	2.9	17.9	4.3
5	4.4	0.5	5.0	19,680	5.0	9.9	5.0	19.8	2.3
6	9.1	1.0	4.9	22,302	10.1	15.0	4.9	24.9	4.7
7	13.5	1.5	5.0	24,051	15.0	19.9	5.0	29.8	7.1
8	9.0	1.0	10.0	29,860	10.0	20.0	10.0	39.9	4.7
9	18.0	2.0	10.0	33,595	20.0	29.9	10.0	49.9	9.4
10	26.8	3.0	10.0	34,616	29.8	39.8	10.0	59.7	14.1
11	9.1	1.0	15.0	33,620	10.1	25.0	15.0	55.0	4.8
12	13.6	1.5	14.9	36,136	15.1	30.0	14.9	59.9	7.1
13	27.0	3.0	15.0	40,879	30.0	44.9	15.0	74.8	14.1
14	13.6	1.5	20.0	40,414	15.1	35.0	20.0	75.0	7.1
15	18.0	2.0	20.0	42,512	20.0	40.0	20.0	79.9	9.4
16	35.4	4.0	19.9	49,098	39.4	59.3	19.9	99.2	18.6

Table 57. Resilient Modulus Test Results for Base Material (Contract 3607).

Sequence	Cyclic Axial Stress (psi)	Contact Stress (psi)	Confinement Stress (psi)	Axial Resilient Modulus (psi)	Deviator Stress, σ_d (psi)	Major Principal Stress, σ_1 (psi)	Minor Principal Stress, σ_3 (psi)	Bulk Stress, θ (psi)	Octahedral Shear Stress (psi)
1	13.5	1.5	14.3	37,768	15.0	29.3	14.3	57.9	7.1
2	2.7	0.3	2.3	14,357	3.0	5.3	2.3	9.9	1.4
3	5.4	0.6	2.3	15,807	6.0	8.3	2.3	12.9	2.8
4	8.1	0.9	2.3	17,012	9.0	11.3	2.3	15.9	4.2
5	4.5	0.5	4.3	17,810	5.0	9.3	4.3	17.9	2.4
6	8.9	1.0	4.3	20,323	9.9	14.2	4.3	22.8	4.7
7	13.6	1.5	4.3	22,873	15.1	19.4	4.3	28.0	7.1
8	9.0	1.0	9.3	27,093	10.0	19.3	9.3	37.9	4.7
9	18.0	2.0	9.3	32,894	20.0	29.3	9.3	47.9	9.4
10	27.0	3.0	9.3	35,618	30.0	39.3	9.3	57.9	14.1
11	9.1	1.0	14.3	32,890	10.1	24.4	14.3	53.0	4.8
12	13.4	1.5	14.3	36,272	14.9	29.2	14.3	57.8	7.0
13	27.0	3.0	14.3	42,799	30.0	44.3	14.3	72.9	14.1
14	14.0	1.5	19.3	41,969	15.5	34.8	19.3	73.4	7.3
15	18.2	2.0	19.3	44,864	20.2	39.5	19.3	78.1	9.5
16	35.2	4.0	19.3	51,748	39.2	58.5	19.3	97.1	18.5

Table 58. Resilient Modulus Test Results for Base Material (Contract 3613).

Sequence	Cyclic Axial Stress (psi)	Contact Stress (psi)	Confinement Stress (psi)	Axial Resilient Modulus (psi)	Deviator Stress, σ_d (psi)	Major Principal Stress, σ_1 (psi)	Minor Principal Stress, σ_3 (psi)	Bulk Stress, θ (psi)	Octahedral Shear Stress (psi)
1	13.7	1.5	15.0	38,859	15.1	30.1	15.0	60.1	7.1
2	2.7	0.3	3.0	17,223	3.0	6.0	3.0	11.9	1.4
3	5.3	0.6	3.0	18,871	5.9	8.8	3.0	14.8	2.8
4	8.5	0.9	3.0	21,026	9.4	12.4	3.0	18.3	4.4
5	4.4	0.5	5.0	21,262	4.9	9.9	5.0	19.8	2.3
6	8.9	1.0	5.0	23,960	9.9	14.9	5.0	24.8	4.7
7	13.4	1.5	5.0	25,751	14.9	19.9	5.0	29.9	7.0
8	8.9	1.0	10.0	30,775	9.9	19.9	10.0	39.9	4.7
9	17.9	2.0	10.0	33,889	19.9	29.9	10.0	49.8	9.4
10	27.0	3.0	10.0	35,301	30.0	39.9	10.0	59.9	14.1
11	9.0	1.0	15.0	32,603	10.0	25.0	15.0	55.0	4.7
12	13.5	1.5	15.0	35,350	15.0	30.0	15.0	59.9	7.1
13	27.0	3.0	15.0	40,558	30.0	45.0	15.0	75.0	14.2
14	13.6	1.5	20.0	39,540	15.1	35.1	20.0	75.0	7.1
15	18.2	2.0	20.0	42,611	20.2	40.1	20.0	80.1	9.5
16	35.2	4.0	20.0	48,969	39.2	59.1	20.0	99.1	18.5

Table 59. Resilient Modulus Test Results for Borrow Material (Contract 3546).

Sequence	Cyclic Axial Stress (psi)	Contact Stress (psi)	Confinement Stress (psi)	Axial Resilient Modulus (psi)	Deviator Stress, σ_d (psi)	Major Principal Stress, σ_1 (psi)	Minor Principal Stress, σ_3 (psi)	Bulk Stress, θ (psi)	Octahedral Shear Stress (psi)
1	13.5	1.5	14.8	36,969	15.0	29.8	14.8	59.3	7.1
2	2.7	0.3	2.8	15,355	3.0	5.8	2.8	11.4	1.4
3	5.5	0.6	2.8	17,586	6.1	8.9	2.8	14.5	2.9
4	8.2	0.9	2.8	18,860	9.1	11.8	2.8	17.4	4.3
5	4.4	0.5	4.8	19,484	4.9	9.7	4.8	19.3	2.3
6	8.9	1.0	4.8	22,107	9.9	14.7	4.8	24.2	4.7
7	13.4	1.5	4.8	23,425	14.9	19.7	4.8	29.2	7.0
8	9.0	1.0	9.8	28,556	10.0	19.8	9.8	39.3	4.7
9	18.0	2.0	9.8	32,585	20.0	29.8	9.8	49.4	9.4
10	27.0	3.0	9.8	34,008	30.0	39.7	9.8	59.3	14.1
11	9.1	1.0	14.8	32,001	10.1	24.9	14.8	54.4	4.8
12	13.5	1.5	14.8	33,651	15.0	29.7	14.8	59.3	7.1
13	27.0	3.0	14.8	38,956	30.0	44.8	14.8	74.3	14.1
14	13.8	1.5	19.8	37,861	15.3	35.0	19.8	74.5	7.2
15	18.1	2.0	19.8	40,689	20.1	39.8	19.8	79.4	9.5
16	35.1	4.0	19.8	46,956	39.1	58.9	19.8	98.4	18.4

Table 60. Resilient Modulus Test Results for Borrow Material (Contract 3583).

Sequence	Cyclic Axial Stress (psi)	Contact Stress (psi)	Confinement Stress (psi)	Axial Resilient Modulus (psi)	Deviator Stress, σ_d (psi)	Major Principal Stress, σ_1 (psi)	Minor Principal Stress, σ_3 (psi)	Bulk Stress, θ (psi)	Octahedral Shear Stress (psi)
1	13.4	1.5	14.7	16,244	14.9	29.6	14.7	59.1	7.0
2	2.7	0.3	2.7	11,167	3.0	5.7	2.7	11.1	1.4
3	5.3	0.6	2.7	10,489	5.9	8.6	2.7	14.0	2.8
4	8.1	0.9	2.7	10,012	9.0	11.7	2.7	17.1	4.2
5	4.5	0.5	4.7	12,149	5.0	9.8	4.7	19.2	2.4
6	9.0	1.0	4.7	11,267	10.0	14.7	4.7	24.1	4.7
7	13.5	1.5	4.7	10,847	15.0	19.7	4.7	29.2	7.1
8	8.9	1.0	9.7	14,029	9.9	19.6	9.7	39.1	4.7
9	17.9	2.0	9.7	12,915	19.9	29.6	9.7	49.1	9.4
10	26.5	3.0	9.7	11,246	29.5	39.2	9.7	58.6	13.9
11	9.0	1.0	14.7	16,039	10.0	24.7	14.7	54.2	4.7
12	13.5	1.5	14.7	15,442	15.0	29.7	14.7	59.2	7.1
13	26.9	3.0	14.7	14,653	29.9	44.6	14.7	74.0	14.1
14	13.7	1.5	19.7	18,521	15.2	34.9	19.7	74.4	7.2
15	18.1	2.0	19.7	18,488	20.1	39.9	19.7	79.3	9.5
16	34.0	4.0	19.7	16,316	38.0	57.7	19.7	97.1	17.9

Table 61. Resilient Modulus Test Results for Borrow Material (Contract 3597).

Sequence	Cyclic Axial Stress (psi)	Contact Stress (psi)	Confinement Stress (psi)	Axial Resilient Modulus (psi)	Deviator Stress, σ_d (psi)	Major Principal Stress, σ_1 (psi)	Minor Principal Stress, σ_3 (psi)	Bulk Stress, θ (psi)	Octahedral Shear Stress (psi)
1	13.5	1.5	14.6	35,264	15.0	29.6	14.6	58.8	7.1
2	2.7	0.3	2.6	16,966	3.0	5.6	2.6	10.9	1.4
3	5.4	0.6	2.6	17,628	6.0	8.6	2.6	13.9	2.8
4	8.1	0.9	2.6	18,718	9.0	11.6	2.6	16.8	4.2
5	4.5	0.5	4.6	19,896	5.1	9.7	4.6	18.9	2.4
6	9.1	1.0	4.6	21,766	10.1	14.7	4.6	23.9	4.8
7	13.5	1.5	4.6	23,047	15.0	19.6	4.6	28.8	7.1
8	8.9	1.0	9.6	27,102	9.9	19.5	9.6	38.8	4.7
9	18.0	2.0	9.6	30,128	20.0	29.6	9.6	48.8	9.4
10	26.9	3.0	9.6	31,053	29.9	39.5	9.6	58.7	14.1
11	9.1	1.0	14.6	29,872	10.1	24.7	14.6	53.9	4.8
12	13.6	1.5	14.6	32,406	15.1	29.8	14.6	59.0	7.1
13	27.2	3.0	14.6	37,144	30.2	44.8	14.6	74.0	14.2
14	13.7	1.5	19.6	37,280	15.2	34.8	19.6	74.0	7.2
15	18.0	2.0	19.6	39,087	20.0	39.6	19.6	78.9	9.4
16	35.0	4.0	19.6	44,426	39.0	58.6	19.6	97.8	18.4

Table 62. Resilient Modulus Test Results for Borrow Material (Contract 3613).

Sequence	Cyclic Axial Stress (psi)	Contact Stress (psi)	Confinement Stress (psi)	Axial Resilient Modulus (psi)	Deviator Stress, σ_d (psi)	Major Principal Stress, σ_1 (psi)	Minor Principal Stress, σ_3 (psi)	Bulk Stress, θ (psi)	Octahedral Shear Stress (psi)
1	13.5	1.5	14.7	37,085	15.0	29.7	14.7	59.1	7.1
2	2.8	0.3	2.7	15,729	3.1	5.7	2.7	11.0	1.4
3	5.4	0.6	2.7	17,481	6.0	8.6	2.7	14.0	2.8
4	8.0	0.9	2.7	18,980	8.9	11.6	2.7	16.9	4.2
5	4.5	0.5	4.7	19,925	5.0	9.7	4.7	19.0	2.4
6	8.7	1.0	4.7	21,992	9.7	14.3	4.7	23.7	4.6
7	13.5	1.5	4.7	24,546	15.0	19.7	4.7	29.0	7.1
8	8.8	1.0	9.7	27,691	9.8	19.5	9.7	38.8	4.6
9	17.9	2.0	9.7	32,462	19.9	29.6	9.7	48.9	9.4
10	27.1	3.0	9.7	34,900	30.1	39.7	9.7	59.1	14.2
11	9.0	1.0	14.7	30,752	10.0	24.6	14.7	53.9	4.7
12	13.6	1.5	14.7	33,837	15.1	29.8	14.7	59.1	7.1
13	27.2	3.0	14.7	40,414	30.2	44.8	14.7	74.2	14.2
14	13.8	1.5	19.7	38,433	15.2	34.9	19.7	74.3	7.2
15	18.1	2.0	19.7	41,491	20.1	39.7	19.7	79.0	9.5
16	35.4	4.0	19.7	49,656	39.4	59.1	19.7	98.4	18.6

Table 63. Resilient Modulus Test Results for Subgrade Material (I-15/Goodsprings).

Sequence	Cyclic Axial Stress (psi)	Contact Stress (psi)	Confinement Stress (psi)	Axial Resilient Modulus (psi)	Deviator Stress, σ_d (psi)	Major Principal Stress, σ_1 (psi)	Minor Principal Stress, σ_3 (psi)	Bulk Stress, θ (psi)	Octahedral Shear Stress (psi)
1	3.5	0.4	5.9	19,538	3.9	9.8	5.9	21.5	1.8
2	1.8	0.2	5.9	18,343	2.0	7.8	5.9	19.6	0.9
3	3.5	0.4	5.9	19,916	3.9	9.8	5.9	21.5	1.8
4	5.4	0.6	5.9	20,171	6.0	11.8	5.9	23.6	2.8
5	7.1	0.8	4.9	18,746	7.9	12.7	4.9	22.5	3.7
6	8.8	1.0	5.9	20,838	9.8	15.7	5.9	27.4	4.6
7	1.8	0.2	3.9	15,251	2.0	5.8	3.9	13.5	0.9
8	3.7	0.4	3.9	15,923	4.1	7.9	3.9	15.7	1.9
9	5.3	0.6	3.9	16,591	5.9	9.7	3.9	17.5	2.8
10	7.1	0.8	3.9	17,308	7.9	11.7	3.9	19.4	3.7
11	8.8	1.0	3.9	18,277	9.8	13.6	3.9	21.4	4.6
12	1.8	0.2	1.9	12,573	2.0	3.8	1.9	7.6	0.9
13	3.4	0.4	1.9	13,075	3.8	5.7	1.9	9.4	1.8
14	5.4	0.6	1.9	14,149	5.9	7.8	1.9	11.5	2.8
15	7.1	0.8	1.9	14,944	7.8	9.7	1.9	13.5	3.7
16	8.9	1.0	1.9	15,758	9.9	11.8	1.9	15.5	4.7

Table 64. Resilient Modulus Test Results for Subgrade Material (US-95/Searchlight).

Sequence	Cyclic Axial Stress (psi)	Contact Stress (psi)	Confinement Stress (psi)	Axial Resilient Modulus (psi)	Deviator Stress, σ_d (psi)	Major Principal Stress, σ_1 (psi)	Minor Principal Stress, σ_3 (psi)	Bulk Stress, θ (psi)	Octahedral Shear Stress (psi)
1	3.6	0.4	5.7	16,049	4.0	9.7	5.7	21.1	1.9
2	1.8	0.2	5.7	15,139	2.0	7.7	5.7	19.2	0.9
3	3.6	0.4	5.7	16,294	4.0	9.7	5.7	21.1	1.9
4	5.4	0.6	5.7	16,243	6.0	11.7	5.7	23.2	2.8
5	7.2	0.8	4.7	15,076	8.0	12.7	4.7	22.2	3.8
6	8.9	1.0	5.7	16,137	9.8	15.6	5.7	27.0	4.6
7	1.8	0.2	3.7	12,999	2.0	5.7	3.7	13.1	0.9
8	3.6	0.4	3.7	13,178	4.0	7.7	3.7	15.1	1.9
9	5.4	0.6	3.7	13,627	5.9	9.7	3.7	17.1	2.8
10	7.1	0.8	3.7	13,972	7.9	11.6	3.7	19.0	3.7
11	8.9	1.0	3.7	14,418	9.9	13.7	3.7	21.1	4.7
12	1.8	0.2	1.7	10,602	2.0	3.7	1.7	7.2	0.9
13	3.6	0.4	1.7	10,766	4.0	5.7	1.7	9.2	1.9
14	5.3	0.6	1.7	11,301	5.9	7.6	1.7	11.1	2.8
15	7.2	0.8	1.7	11,938	8.0	9.7	1.7	13.1	3.8
16	8.9	1.0	1.7	12,583	9.8	11.6	1.7	15.0	4.6

Table 65. Resilient Modulus Test Results for Subgrade Material (NV-375/Rachel).

Sequence	Cyclic Axial Stress (psi)	Contact Stress (psi)	Confinement Stress (psi)	Axial Resilient Modulus (psi)	Deviator Stress, σ_d (psi)	Major Principal Stress, σ_1 (psi)	Minor Principal Stress, σ_3 (psi)	Bulk Stress, θ (psi)	Octahedral Shear Stress (psi)
1	3.6	0.4	5.7	18,563	4.0	9.7	5.7	21.1	1.9
2	1.8	0.2	5.7	16,968	2.0	7.7	5.7	19.1	0.9
3	3.6	0.4	5.7	18,824	4.0	9.7	5.7	21.1	1.9
4	5.4	0.6	5.7	18,731	6.0	11.7	5.7	23.1	2.8
5	7.2	0.8	4.7	17,317	8.0	12.7	4.7	22.1	3.8
6	9.0	1.0	5.7	19,475	10.0	15.7	5.7	27.1	4.7
7	1.8	0.2	3.7	14,184	2.0	5.7	3.7	13.1	0.9
8	3.6	0.4	3.7	14,300	4.0	7.7	3.7	15.1	1.9
9	5.4	0.6	3.7	15,270	6.0	9.7	3.7	17.1	2.8
10	7.2	0.8	3.7	16,435	8.0	11.7	3.7	19.1	3.8
11	9.0	1.0	3.7	17,200	10.0	13.7	3.7	21.1	4.7
12	1.8	0.2	1.7	10,946	2.0	3.7	1.7	7.2	0.9
13	3.6	0.4	1.7	11,363	4.0	5.7	1.7	9.1	1.9
14	5.4	0.6	1.7	12,765	6.0	7.7	1.7	11.1	2.8
15	7.2	0.8	1.7	13,752	8.0	9.7	1.7	13.1	3.8
16	9.0	1.0	1.7	14,622	10.0	11.7	1.7	15.1	4.7

Table 66. Resilient Modulus Test Results for Subgrade Material (US-93/Crystal Spring MP62).

Sequence	Cyclic Axial Stress (psi)	Contact Stress (psi)	Confinement Stress (psi)	Axial Resilient Modulus (psi)	Deviator Stress, σ_d (psi)	Major Principal Stress, σ_1 (psi)	Minor Principal Stress, σ_3 (psi)	Bulk Stress, θ (psi)	Octahedral Shear Stress (psi)
1	3.6	0.4	5.8	13,028	4.0	9.8	5.8	21.3	1.9
2	1.8	0.2	5.8	12,184	2.0	7.8	5.8	19.3	0.9
3	3.6	0.4	5.8	13,115	4.0	9.8	5.8	21.3	1.9
4	5.6	0.6	5.8	13,025	6.2	12.0	5.8	23.5	2.9
5	7.2	0.8	4.8	12,302	8.0	12.8	4.8	22.3	3.8
6	9.0	1.0	5.8	13,420	10.0	15.7	5.8	27.3	4.7
7	1.8	0.2	3.8	9,997	2.0	5.8	3.8	13.3	0.9
8	3.6	0.4	3.8	10,223	4.0	7.8	3.8	15.3	1.9
9	5.4	0.6	3.8	10,567	6.0	9.8	3.8	17.3	2.8
10	7.3	0.8	3.8	11,363	8.1	11.8	3.8	19.4	3.8
11	9.0	1.0	3.8	11,685	10.0	13.8	3.8	21.3	4.7
12	1.8	0.2	1.8	7,710	2.0	3.8	1.8	7.3	0.9
13	3.6	0.4	1.8	8,095	4.0	5.7	1.8	9.3	1.9
14	5.4	0.6	1.8	8,822	6.0	7.7	1.8	11.3	2.8
15	7.2	0.8	1.8	9,648	8.0	9.8	1.8	13.4	3.8
16	8.9	1.0	1.8	9,982	9.9	11.7	1.8	15.2	4.7

Table 67. Resilient Modulus Test Results for Subgrade Material (US-93/Crystal Spring MP67).

Sequence	Cyclic Axial Stress (psi)	Contact Stress (psi)	Confinement Stress (psi)	Axial Resilient Modulus (psi)	Deviator Stress, σ_d (psi)	Major Principal Stress, σ_1 (psi)	Minor Principal Stress, σ_3 (psi)	Bulk Stress, θ (psi)	Octahedral Shear Stress (psi)
1	3.6	0.4	5.8	15,555	4.0	9.8	5.8	21.3	1.9
2	1.8	0.2	5.8	14,759	2.0	7.8	5.8	19.4	0.9
3	3.6	0.4	5.8	15,963	4.0	9.8	5.8	21.4	1.9
4	5.4	0.6	5.8	15,526	6.0	11.8	5.8	23.4	2.8
5	7.2	0.8	4.8	14,314	8.0	12.8	4.8	22.3	3.8
6	8.9	1.0	5.8	15,276	9.9	15.7	5.8	27.3	4.7
7	1.8	0.2	3.8	13,366	2.0	5.8	3.8	13.3	0.9
8	3.6	0.4	3.8	13,338	4.0	7.8	3.8	15.4	1.9
9	5.4	0.6	3.8	13,204	6.0	9.8	3.8	17.3	2.8
10	7.2	0.8	3.8	13,367	8.0	11.8	3.8	19.4	3.8
11	9.0	1.0	3.8	13,723	10.0	13.8	3.8	21.4	4.7
12	1.8	0.2	1.8	11,103	2.0	3.8	1.8	7.3	0.9
13	3.6	0.4	1.8	10,789	4.0	5.8	1.8	9.3	1.9
14	5.4	0.6	1.8	11,002	6.0	7.8	1.8	11.3	2.8
15	7.3	0.8	1.8	11,481	8.1	9.8	1.8	13.4	3.8
16	9.0	1.0	1.8	11,940	10.0	11.8	1.8	15.3	4.7

Table 68. Resilient Modulus Test Results for Elko Base.

Sequence	Cyclic Axial Stress (psi)	Contact Stress (psi)	Confinement Stress (psi)	Axial Resilient Modulus (psi)	Deviator Stress, σ_d (psi)	Major Principal Stress, σ_1 (psi)	Minor Principal Stress, σ_3 (psi)	Bulk Stress, θ (psi)	Octahedral Shear Stress (psi)
1	13.5	1.5	14.8	23,452	15.0	29.8	14.8	59.3	7.1
2	2.7	0.3	2.7	9,926	3.0	5.7	2.7	11.2	1.4
3	5.4	0.6	2.7	10,960	6.0	8.7	2.7	14.2	2.8
4	8.1	0.9	2.7	11,885	9.0	11.7	2.7	17.2	4.2
5	4.5	0.5	4.7	12,595	5.0	9.7	4.7	19.2	2.4
6	9.0	1.0	4.7	14,119	10.0	14.7	4.7	24.2	4.7
7	13.5	1.5	4.7	15,070	15.0	19.7	4.7	29.2	7.1
8	8.9	1.0	9.7	18,713	9.9	19.6	9.7	39.1	4.7
9	17.9	2.0	9.8	20,669	19.9	29.7	9.8	49.2	9.4
10	26.8	3.0	9.7	21,555	29.8	39.5	9.7	59.0	14.0
11	9.0	1.0	14.7	20,644	10.0	24.7	14.7	54.2	4.7
12	13.6	1.5	14.7	22,279	15.1	29.8	14.7	59.3	7.1
13	26.9	3.0	14.7	26,118	29.9	44.6	14.7	74.1	14.1
14	13.5	1.5	19.7	25,284	15.0	34.7	19.7	74.2	7.1
15	18.2	2.0	19.7	27,892	20.2	39.9	19.7	79.4	9.5
16	35.0	4.0	19.7	32,407	39.0	58.8	19.7	98.2	18.4

Table 69. Resilient Modulus Results for Hunnewill Base.

Sequence	Cyclic Axial Stress (psi)	Contact Stress (psi)	Confinement Stress (psi)	Axial Resilient Modulus (psi)	Deviator Stress, σ_d (psi)	Major Principal Stress, σ_1 (psi)	Minor Principal Stress, σ_3 (psi)	Bulk Stress, θ (psi)	Octahedral Shear Stress (psi)
1	13.5	1.5	14.7	21,217	15.0	29.6	14.7	59.0	7.1
2	2.7	0.3	2.7	9,255	3.0	5.6	2.7	10.9	1.4
3	5.4	0.6	2.7	10,314	6.0	8.7	2.7	14.0	2.8
4	8.1	0.9	2.7	10,805	9.0	11.6	2.7	17.0	4.2
5	4.5	0.5	4.7	9,810	5.0	9.7	4.7	19.0	2.4
6	9.2	1.0	4.7	12,257	10.2	14.9	4.7	24.2	4.8
7	13.5	1.5	4.7	13,895	15.0	19.7	4.7	29.0	7.1
8	8.9	1.0	9.7	16,438	9.9	19.6	9.7	38.9	4.7
9	18.0	2.0	9.7	18,487	20.0	29.7	9.7	49.0	9.4
10	26.9	3.0	9.7	20,294	29.9	39.6	9.7	58.9	14.1
11	9.1	1.0	14.7	19,013	10.1	24.8	14.7	54.1	4.8
12	13.7	1.5	14.7	19,971	15.2	29.9	14.7	59.2	7.2
13	27.0	3.0	14.7	23,804	30.0	44.6	14.7	73.9	14.1
14	13.6	1.5	19.7	22,934	15.1	34.8	19.7	74.1	7.1
15	18.1	2.0	19.7	24,763	20.1	39.8	19.7	79.1	9.5
16	35.3	4.0	19.7	31,023	39.3	59.0	19.7	98.3	18.5

Table 70. Resilient Modulus Test Results for Lockwood Borrow.

Sequence	Cyclic Axial Stress (psi)	Contact Stress (psi)	Confinement Stress (psi)	Axial Resilient Modulus (psi)	Deviator Stress, σ_d (psi)	Major Principal Stress, σ_1 (psi)	Minor Principal Stress, σ_3 (psi)	Bulk Stress, θ (psi)	Octahedral Shear Stress (psi)
1	13.5	1.5	14.6	18,493	15.0	29.6	14.6	58.8	7.0
2	2.7	0.3	2.6	11,861	3.0	5.6	2.6	10.9	1.4
3	5.4	0.6	2.6	11,879	6.0	8.6	2.6	13.9	2.8
4	8.0	0.9	2.6	11,468	8.9	11.5	2.6	16.8	4.2
5	4.5	0.5	4.6	12,862	5.0	9.6	4.6	18.9	2.4
6	9.0	1.0	4.6	12,695	10.0	14.6	4.6	23.9	4.7
7	13.5	1.5	4.6	12,611	15.0	19.6	4.6	28.9	7.1
8	9.1	1.0	9.6	15,400	10.1	19.7	9.6	39.0	4.8
9	18.0	2.0	9.6	15,673	20.0	29.6	9.6	48.9	9.4
10	26.3	3.0	9.6	17,677	29.3	38.9	9.6	58.1	13.8
11	9.1	1.0	14.6	18,057	10.1	24.7	14.6	54.0	4.8
12	13.7	1.5	14.6	18,258	15.2	29.8	14.6	59.1	7.2
13	26.7	3.0	14.6	21,996	29.7	44.3	14.6	73.6	14.0
14	13.6	1.5	19.6	22,106	15.1	34.7	19.6	74.0	7.1
15	18.1	2.0	19.6	24,259	20.1	39.7	19.6	79.0	9.5
16	33.7	4.0	19.6	56,471	37.7	57.4	19.6	96.6	17.8

Table 71. Resilient Modulus Test Results for SNC Primary Borrow (sequences 10-14 excluded in analysis).

Sequence	Cyclic Axial Stress (psi)	Contact Stress (psi)	Confinement Stress (psi)	Axial Resilient Modulus (psi)	Deviator Stress, σ_d (psi)	Major Principal Stress, σ_1 (psi)	Minor Principal Stress, σ_3 (psi)	Bulk Stress, θ (psi)	Octahedral Shear Stress (psi)
1	13.4	1.5	14.7	14,172	14.9	29.7	14.7	59.1	7.0
2	2.8	0.3	2.7	8,714	3.1	5.8	2.7	11.2	1.4
3	5.3	0.6	2.7	8,926	5.9	8.7	2.7	14.1	2.8
4	8.1	0.9	2.7	9,274	9.0	11.7	2.7	17.2	4.2
5	4.6	0.5	4.7	9,366	5.1	9.8	4.7	19.2	2.4
6	9.0	1.0	4.7	10,262	10.0	14.7	4.7	24.2	4.7
7	13.5	1.5	4.7	10,647	15.0	19.7	4.7	29.2	7.0
8	9.1	1.0	9.7	11,376	10.1	19.8	9.7	39.3	4.8
9	18.0	2.0	9.7	12,604	20.0	29.7	9.7	49.2	9.4
15	18.1	2.0	19.7	16,610	20.1	39.9	19.7	79.3	9.5
16	34.9	4.0	19.7	18,273	38.9	58.6	19.7	98.1	18.3

Table 72. Resilient Modulus Test Results for Jacks Valley Subgrade.

Sequence	Cyclic Axial Stress (psi)	Contact Stress (psi)	Confinement Stress (psi)	Axial Resilient Modulus (psi)	Deviator Stress, σ_d (psi)	Major Principal Stress, σ_1 (psi)	Minor Principal Stress, σ_3 (psi)	Bulk Stress, θ (psi)	Octahedral Shear Stress (psi)
1	3.6	0.4	5.7	9,729	4.0	9.7	5.7	21.0	1.9
2	1.8	0.2	5.7	9,863	2.0	7.7	5.7	19.1	1.0
3	3.6	0.4	5.7	10,078	4.0	9.7	5.7	21.0	1.9
4	5.4	0.6	5.7	9,653	6.0	11.7	5.7	23.0	2.8
5	7.2	0.8	4.7	8,892	8.0	12.6	4.7	22.0	3.8
6	9.0	1.0	5.7	9,501	10.0	15.7	5.7	27.0	4.7
7	1.8	0.2	3.7	9,714	2.0	5.7	3.7	13.0	0.9
8	3.6	0.4	3.7	9,027	4.0	7.7	3.7	15.0	1.9
9	5.4	0.6	3.7	8,759	6.0	9.7	3.7	17.0	2.8
10	7.2	0.8	3.7	8,741	8.0	11.7	3.7	19.0	3.8
11	9.0	1.0	3.7	8,616	10.0	13.7	3.7	21.0	4.7
12	1.8	0.2	1.7	8,638	2.0	3.7	1.7	7.0	0.9
13	3.6	0.4	1.7	7,895	4.0	5.6	1.7	9.0	1.9
14	5.4	0.6	1.7	7,777	6.0	7.7	1.7	11.0	2.8
15	7.2	0.8	1.7	7,872	8.0	9.7	1.7	13.1	3.8
16	8.9	1.0	1.7	7,667	9.9	11.6	1.7	15.0	4.7

Table 73. Resilient Modulus Test Results for SEM Soil.

Sequence	Cyclic Axial Stress (psi)	Contact Stress (psi)	Confinement Stress (psi)	Axial Resilient Modulus (psi)	Deviator Stress, σ_d (psi)	Major Principal Stress, σ_1 (psi)	Minor Principal Stress, σ_3 (psi)	Bulk Stress, θ (psi)	Octahedral Shear Stress (psi)
1	3.5	0.4	6.0	14,640	3.5	9.9	6.0	21.9	1.9
2	1.6	0.3	6.0	13,950	1.6	7.8	6.0	19.8	0.9
3	3.5	0.3	6.0	12,612	3.5	9.8	6.0	21.7	1.8
4	5.5	0.6	6.0	13,285	5.5	12.0	6.0	24.0	2.9
5	7.1	0.8	5.0	12,292	7.1	12.9	5.0	22.9	3.7
6	8.9	1.0	6.0	13,251	8.9	15.9	6.0	27.8	4.7
7	1.8	0.2	4.0	10,690	1.8	6.0	4.0	14.0	0.9
8	3.5	0.4	4.0	10,668	3.5	7.9	4.0	15.9	1.9
9	5.4	0.6	4.0	10,714	5.4	9.9	4.0	17.9	2.8
10	7.1	0.8	4.0	10,979	7.1	11.9	4.0	19.8	3.7
11	8.9	1.0	4.0	10,867	8.9	13.9	4.0	21.8	4.7
12	1.8	0.2	2.0	8,121	1.8	3.9	2.0	7.9	0.9
13	3.5	0.4	2.0	8,476	3.5	5.9	2.0	9.9	1.9
14	5.4	0.6	2.0	8,905	5.4	7.9	2.0	11.9	2.8
15	7.2	0.8	2.0	9,461	7.2	10.0	2.0	14.0	3.8
16	8.9	1.0	2.0	9,643	8.9	11.8	2.0	15.8	4.7

Nevada Department of Transportation
Rudy Malfabon, P.E. Director
Ken Chambers, Research Division Chief
(775) 888-7220
kchambers@dot.nv.gov
1263 South Stewart Street
Carson City, Nevada 89712